



Adaptations métaboliques des organismes dans la zone de balancement des marées. Implications sur la biodiversité locale dans un contexte de changement climatique.

Morgana Tagliarolo

► To cite this version:

Morgana Tagliarolo. Adaptations métaboliques des organismes dans la zone de balancement des marées. Implications sur la biodiversité locale dans un contexte de changement climatique.. Biodiversité et Ecologie. Université de Bretagne occidentale - Brest, 2012. Français. NNT: . tel-00816887v1

HAL Id: tel-00816887

<https://theses.hal.science/tel-00816887v1>

Submitted on 23 Apr 2013 (v1), last revised 27 Nov 2014 (v2)

HAL is a multi-disciplinary open access archive for the deposit and dissemination of scientific research documents, whether they are published or not. The documents may come from teaching and research institutions in France or abroad, or from public or private research centers.

L'archive ouverte pluridisciplinaire **HAL**, est destinée au dépôt et à la diffusion de documents scientifiques de niveau recherche, publiés ou non, émanant des établissements d'enseignement et de recherche français ou étrangers, des laboratoires publics ou privés.



université de bretagne
occidentale



THÈSE / UNIVERSITÉ DE BRETAGNE OCCIDENTALE

sous le sceau de l'Université européenne de Bretagne

présentée par

Morgana Tagliarolo

Préparée à l'Unité Mixte de Recherche LEMAR

UMR 6539 CNRS/IRD/UBO

Laboratoire des Sciences de l'environnement Marin

DOCTEUR DE L'UNIVERSITÉ DE BRETAGNE OCCIDENTALE

Mention : Biologie Marine

École Doctorale des Sciences de la Mer

Thèse soutenue le 14 décembre 2012

devant le jury composé de :

Guy Bachelet

Directeur de recherche CNRS, Station Marine d'Arcachon, Université Bordeaux 1 / Rapporteur

Dominique Davout

Professeur, Station Biologique de Roscoff, Université Pierre et Marie Curie Paris 6 / Rapporteur

Gérard Thouzeau

Directeur de recherche CNRS, IUEM, LEMAR / Examinateur

Sophie Martin

Chargée de recherche CNRS, Station Biologique de Roscoff / Examinateur

Jacques Clavier

Professeur, IUEM, LEMAR, l'Université de Bretagne Occidentale / Directeur de thèse

Laurent Chauvaud

Directeur de recherche CNRS, IUEM, LEMAR / co-directeur de thèse



Remerciements

Après ces trois ans de thèse et huit mois de stage passés dans le pays de la crêpe et du caramel au beurre salé je tiens à remercier une longue liste de personnes qui m'ont aidée et soutenue :

Merci à Guy Bachelet et Dominique Davoult pour avoir accepté d'être les rapporteurs de ce travail de thèse.

Merci à Jacques Clavier pour son encadrement, toujours disponible quand j'en avais besoin et prêt à ouvrir sa maison pour me permettre de faire les analyses de terrain. Il m'a appris à affronter toutes les difficultés avec un sourire et m'a toujours poussée à m'améliorer.

Merci à Jacques Grall pour ses enseignements et son support depuis mon arrivée à Brest. Il a toujours été prêt à sauter dans ses bottes pour m'accompagner sur l'estran à la recherche de petites bestioles.

Merci à Laurent Chauvaud pour son aide en plongée comme en surface, grâce à lui j'ai appris le lexique de base pour le bricolage du biologiste marin.

Merci à Sophie Martin d'avoir accepté de juger mon travail à la fois à mi-parcours et à la fin du périple.

Merci à Gérard Thouzeau d'avoir accepté d'être examinateur de cette thèse et de m'avoir accompagné dans le magnifique monde sous-marin de la plongée scientifique.

Merci à Erwan Amice, Isabelle Bihannic et Robert Marc pour leur aide fondamental sur le bateau comme sous l'eau, sans eux le travail sur le terrain n'aurait pas pu être possible.

Merci à Anne Donval et Aude Leynaert pour les analyses de pigments, merci à Marion Maguer pour avoir compté toutes les petites balanes sur les photos, merci à Mathias Rouan pour les données de température en un temps record, merci à Sorin Moga et Philippe Lenca de Télécom Bretagne de m'avoir aidé avec « data miner ». Merci également à Sébastien Hervé pour les explications des fonctions cachées et mystérieuses d'Adobe.

Merci à Gauthier pour ses conseils...grâce à lui je pourrai partir pour de nouvelles aventures scientifiques sous le soleil de l'Afrique du Sud.

Merci à Mélanie de m'avoir choisi pour le stage de master et de m'avoir permis de venir à Brest pour la première fois : les heures à tamiser la boue ont été plus sympas à deux.

Merci à Vincent de m'avoir appris les bases du français et de m'avoir donné les bons conseils pour trouver un stage et une thèse en France.

Merci à mes enseignants de la formation sur la macrofaune benthique de Roscoff de m'avoir passionnée à la biologie des espèces benthiques.

Merci à Vincent, Nolwenn et tous mes stagiaires intrépides (Olivier, Meriem, Alicia, Camilla, Mélanie et Lucie) de m'avoir accompagné sur le terrain, sous le soleil come sous la pluie et de m'avoir aidé avec les manips en laboratoire.

Merci à mes collègues de « sport » et de soirée, merci à mon prof de danse et à tous mes collègues et merci à mes copains sous-marins ...le sport a été fondamental pour déconnecter du travail et passer de bons moments.

Merci à tous mes amis et collègues : Tony, Jp, Chloé, Romain, Aude, Camille, Seb, Bichon, Malwenn, Marc, Adeline, Mélanie, Mathias, Violette, Valérie, Manon, Mickael, Jonas...d'avoir été à mes côtés dans les bonnes comme les mauvaises périodes, d'avoir corrigé mon français, de m'avoir fait découvrir les us et coutumes des soirées bretonnes et surtout de m'avoir fait rire!

Merci à Cédric, qui a demandé une dédicace spéciale et finalement il la mérite bien; merci de m'avoir motivé au footing naturaliste, pour les soirées apéros, pour les dimanches télé et pour les corrections de mails, rapports...thèse.

Merci à ma famille d'adoption brestoise de m'avoir toujours supporté et de m'avoir accueilli quand je n'avais pas de maison.

Merci à Marcaurelio d'avoir partagé sa vie avec moi pendant cette thèse et pour continuer à le faire, merci de ta patience.

Maintenant, petits remerciements pour le non francophones :

Grazie al Professor Bressan d'aver creduto in me e avermi incoraggiato a partire e cominciare questa avventura.

Grazie ai miei amici che ho abbandonato in Italia ma che non si sono dimenticati di me, grazie a Lorenzo, Annalisa, Marco, Francesca, Marco, Federica, Pierfrancesco, Rubina, Nicolo, Alan...

Grazie ad Elisa, per le lunghe discussioni telefoniche, per le vacanze passate assieme e per essere venuta due volte fino à Brest per vedermi.

Grazie ad Arianna e Rossana, per aver condiviso con me la scoperta della Bretagna.

Grazie alla mia famiglia e soprattutto ai miei genitori per avermi aiutato, incoraggiato, per essere stati sempre presenti quando ne ho avuto bisogno. Anche se le Alpi ci separano vi ho sempre sentiti vicini.

Table des matières

Introduction générale	5
1. <i>La zone côtière</i>	5
2. <i>Le milieu rocheux intertidal</i>	6
3. <i>La diversité des organismes intertidaux</i>	8
4. <i>Le métabolisme et les flux de carbone</i>	11
5. <i>Le rôle de la zone côtière dans le contexte du changement climatique</i>	13
Objectifs de l'étude	14
Partie I	17
Respiration et calcification à l'air et sous l'eau des animaux intertidaux selon leur position sur l'estran.	
<i>Chapitre 1 : Comparaison du métabolisme de moules vivant en milieu intertidal et subtidal.</i>	19
1. <i>Contexte général et résumé</i>	20
2. <i>Introduction</i>	22
3. <i>Material and methods</i>	23
<i>Sampling</i>	23
<i>Genomic DNA analysis</i>	24
<i>Aerial respiration</i>	25
<i>Ammonium excretion</i>	26
<i>Calcification</i>	26
<i>Underwater respiration</i>	27
<i>Calcium carbonate content</i>	28
<i>Data treatment</i>	28
4. <i>Results</i>	29
<i>Environmental parameters</i>	29
<i>Genomic DNA analysis</i>	29
<i>Aerial respiration</i>	30
<i>Ammonium excretion</i>	33
<i>Calcification</i>	34
<i>Underwater respiration</i>	34
<i>CO₂ contribution</i>	35
5. <i>Discussion</i>	36
<i>Genomic DNA analysis</i>	36
<i>Aerial respiration</i>	36
<i>Underwater respiration</i>	38
<i>Aerial/Underwater comparison</i>	39
<i>Ammonium excretion</i>	40
<i>Calcification and calcium carbonate content</i>	40
<i>CO₂ contribution</i>	42
<i>Chapitre 2 : Étude du métabolisme en émersion et en immersion de Patella vulgata, selon la position sur l'estran.</i>	43
1. <i>Contexte général et résumé</i>	44
2. <i>Introduction</i>	46
3. <i>Materials and methods</i>	47
<i>Sampling</i>	47
<i>Environmental parameters</i>	48
<i>Underwater respiration</i>	48

<i>Calcification</i>	49
<i>Ammonium excretion</i>	50
<i>Aerial respiration</i>	50
<i>Data analysis</i>	51
4. Results	52
<i>Environmental parameters</i>	52
<i>Ammonium excretion</i>	52
<i>Calcification</i>	53
<i>Underwater respiration</i>	54
<i>Aerial respiration</i>	55
<i>Annual carbon budget</i>	57
5. Discussion	58
<i>Calcification and ammonium excretion</i>	58
<i>Underwater and aerial respiration</i>	60
<i>Carbon budget</i>	61
Chapitre 3 : Respiration et calcification comparées de neuf espèces de gastéropodes intertidaux.	63
1. Contexte général et résumé	64
2. Introduction	67
3. Materials and methods	68
<i>Sampling</i>	68
<i>Aerial respiration</i>	69
<i>Underwater respiration and calcification</i>	70
<i>Underwater ammonium excretion</i>	71
<i>Calcium carbonate content</i>	72
<i>Data analysis</i>	72
4. Results	74
<i>Aerial and underwater respiration</i>	74
<i>Ammonium excretion</i>	77
<i>Annual carbon budget</i>	79
5. Discussion	80
<i>Aerial and underwater respiration</i>	80
<i>Calcification and ammonium excretion</i>	82
<i>Annual carbon budget</i>	83
Partie II	85
Production primaire, respiration et calcification des communautés intertidales de substrat rocheux.	
Chapitre 4 : Variation saisonnière du métabolisme des communautés intertidales de substrat rocheux semi-exposé.	87
1. Contexte général et résumé	88
2. Introduction	91
3. Material and methods	92
<i>Study site</i>	92
<i>Environmental parameters</i>	93
<i>Carbon flux measurements</i>	93
<i>Community description</i>	96
<i>Data analysis</i>	97
4. Results	99
<i>Environmental parameters</i>	99
<i>Community respiration</i>	99
<i>Underwater community production</i>	100

<i>Underwater community calcification</i>	101
<i>Community description</i>	105
5. <i>Discussion</i>	107
<i>Community respiration</i>	107
<i>Underwater community calcification</i>	108
<i>Net community production</i>	109
<i>Community description</i>	111
<i>Chapitre 5 : Contribution de la macrofaune de substrat rocheux exposé aux flux de carbone sur une échelle régionale. Évaluation de l'effet du réchauffement climatique sur les flux respiratoires.</i>	113
1. <i>Contexte général et résumé</i>	114
2. <i>Introduction</i>	116
3. <i>Material and methods</i>	117
4. <i>Results</i>	121
<i>Environmental parameters</i>	121
<i>Spatial and temporal natural variation of carbon fluxes</i>	121
<i>Effect of temperature variation on carbon fluxes</i>	123
5. <i>Discussion</i>	124
<i>Spatial and temporal natural variation of carbon fluxes</i>	124
<i>Effect of temperature variation on carbon fluxes</i>	125
Synthèse générale et perspectives	129
<i>Comparaison des flux de carbone des différentes espèces macrozoobenthiques intertidales</i>	129
<i>Contribution de la faune benthique aux flux de carbone en milieu rocheux intertidal</i>	132
References	137
Liste des figures	148
Liste des tableaux	151
Annexes	161

Introduction générale

1. La zone côtière

La zone côtière, interface entre terre et mer, est un milieu riche et diversifié qui s'étend depuis le plateau continental jusqu'à une profondeur d'environ 200 m (Catanzano & Thébaud 1995). Dans cette zone, la lumière peut atteindre le benthos lorsque les conditions le permettent et les interactions avec le domaine terrestre sont très importantes ; pour ces raisons les zones côtières jouent un rôle considérable dans les cycles biogéochimiques.

Plus de 10% de la population mondiale vit dans la partie terrestre du littoral (McGranahan et al. 2007) et exploite les écosystèmes côtiers peu profonds qui produisent la majeure partie des captures de la pêche mondiale (Cicin-Sain et al. 2002). La pêche, le tourisme et l'aquaculture sont des exemples d'activités humaines qui participent à la perturbation des habitats côtiers. La pollution via les apports fluviaux et les rejets industriels ou domestiques peut modifier significativement la composition des communautés côtières. L'augmentation des apports de matière organique peut induire des phénomènes d'anoxie et les polluants chimiques comme les métaux lourds, peuvent causer des mortalités ou difformités pour certaines espèces (Southward & Southward 1978, Gibbs et al. 1988, Little et al. 2009).

Au cours des dernières années, la zone côtière a fait l'objet d'une attention particulière pour son rôle clef dans le cycle du carbone et elle est considérée comme très active en termes de respiration et de production primaire (Gazeau et al. 2004). Bien que les zones côtières ne représentent que 7% de la surface totale des océans, elles sont un réservoir de biodiversité bénéficiant d'une multiplicité d'habitats. L'hétérogénéité et la complexité des systèmes côtiers induisent aussi une grande diversité en termes d'écophysiologie et de métabolisme, avec des communautés hétérotrophes déficitaires en énergie et d'autres autotrophes susceptibles d'exporter de l'énergie. Divers travaux ont permis d'établir que les communautés estuariennes, de maërl et des estrans sableux sont hétérotrophes (Martin et al. 2007, Spilmont et al. 2007, Migne et al. 2009). En revanche, les communautés dominées par les macrophytes,

les mangroves et les récifs coralliens sont considérées comme autotrophes (Bensoussan & Gattuso 2007, Duarte et al. 2010).

2. *Le milieu rocheux intertidal*

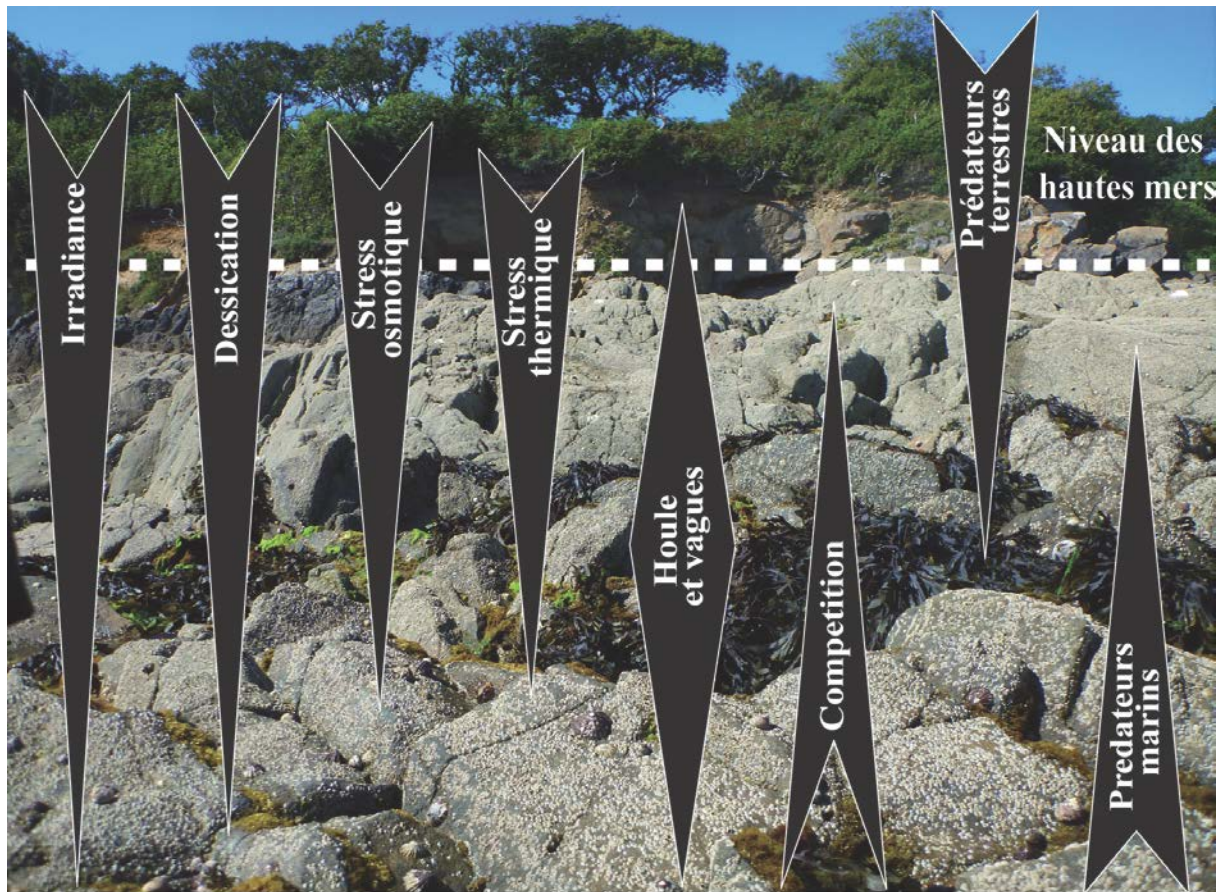


Fig. 1. Représentation schématique de l'influence relative des différents stress physiques et biologiques subis par les communautés intertidales en haut de l'estran (d'après Raffaelli & Hawkins 1999, Little et al. 2009).

Les estrans rocheux sont présents dans le monde entier. Leurs caractéristiques sont très variables dans l'espace en fonction des différents types de structures géologiques, mais aussi dans le temps sous l'influence des changements de la salinité, de la température de l'eau et de l'hydrodynamisme (Little et al. 2009). Malgré cette grande diversité de conditions environnementales, les facteurs climatiques et le cycle de la marée sont les principaux déterminants de la distribution des espèces habitant l'estran rocheux (Lewis 1964, Connell 1972). Sur les côtes NE de l'Atlantique, la zone intertidale émerge deux fois par jour lors des marées basses. Le marnage (différence entre le niveau de l'eau à pleine mer et celui à basse

mer) peut être très différent d'un secteur à l'autre selon la configuration de la côte. Si le marnage est faible au centre des océans, il s'amplifie à proximité des côtes permettant une résonance de l'onde de marée, comme en Manche (8-15 m) (Amat et al. 2008).

Le milieu rocheux intertidal est donc soumis à une alternance d'émergence et d'immersion sous l'effet de la marée. Dans cette zone, les facteurs physico-chimiques associés à la marée comme la température, l'irradiance et la salinité varient très rapidement et vont créer un gradient de stress pour les organismes du bas vers le haut de l'estran (Fig. 1) (Vermeij 1972). L'association des ces facteurs physiques avec les interactions biologiques (compétition, préation et ressources) affecte donc la distribution verticale des espèces (Little & Kitching 1996). La majorité des animaux et des plantes présents sur ces estrans rocheux ont une origine marine plutôt que terrestre (excepté les lichens, insectes et oiseaux) (Little & Kitching 1996). Pendant la marée basse, la dessiccation, les fortes irradiances et les variations de température peuvent influencer le métabolisme et augmenter significativement les coûts énergétiques des organismes (Sokolova & Portner 2001, Somero 2002).

Pour pouvoir vivre et coloniser les plus hauts niveaux de l'estran, les espèces ont développé différentes adaptations au niveau morphologique, comportemental, physiologique et métabolique. Certaines d'entre elles contrôlent les pertes en eau lors de l'émergence en limitant les mouvements et les échanges avec l'air. Les réponses comportementales les plus communes sont une rétention d'eau par application de la coquille contre le substrat ou sa fermeture par un opercule, ou bien le refuge dans les fissures et sous les algues (Truchot 1990). D'autres taxons comme les crabes, les chitons et certains gastéropodes réduisent les risques de dessiccation par des migrations verticales synchronisées avec le cycle de marée (Chelazzi et al. 1988, Warman et al. 1993, Gibson 2003). La présence d'une carapace externe, notamment chez les crustacés, peut aider à la conservation de l'eau mais les structures les plus efficaces restent la coquille des mollusques et les plaques calcifiées des balanes (Little & Kitching 1996). La forme, la couleur et l'épaisseur de la coquille sont des paramètres très importants pour assurer la survie des animaux sur les plus hauts niveaux de l'estran (Alyakrinskaya 2004). L'adaptation physiologique la plus commune en milieu intertidal est la modification du système respiratoire pour utiliser l'oxygène contenu dans l'air ; les branchies sont ainsi réduites et remplacées par de l'épithélium vasculaire (Fretter & Graham 1962). Le

Le système excréteur peut aussi subir des modifications pour permettre la réabsorption de l'eau avec une production d'acide urique à la place de l'ammoniaque (Little 1981). La tolérance à la dessiccation peut enfin être améliorée par des adaptations biochimiques comme l'augmentation du contenu en aminoacides libres dans les cellules (Hoyaux et al. 1976).

La distribution et la composition en espèces du milieu intertidal peut varier significativement entre les sites en raison de l'exposition aux vagues. Les milieux exposés bénéficient d'une meilleure oxygénation et d'une plus grande disponibilité en nutriments, mais l'hydrodynamisme provoque un stress par les variations de pression et par l'abrasion liée au mouvement des particules en suspension. Ces effets mécaniques vont affecter les possibilités de mouvement des animaux vagiles et décrocher les organismes sessiles les plus fragiles (McQuaid & Branch 1984). Les réponses adaptatives des organismes aux milieux exposés correspondent à une amélioration des systèmes d'ancre sur le substrat, la réduction de la hauteur du corps pour obtenir une forme plus compacte et hydrodynamique, et la vie en groupe pour mieux se protéger contre le choc des vagues (Little & Kitching 1996).

3. La diversité des organismes intertidaux

L'estran rocheux est, lorsque l'hydrodynamisme n'est pas trop fort, caractérisé par une forte abondance des producteurs et consommateur primaires. Les liens et les interactions entre le milieu benthique et les zones terrestre et océanique contribuent à la complexité fonctionnelle de ce type d'habitat.



Fig. 2. Exemples de producteurs primaires présents sur l'estran rocheux : A- *Fucus vesiculosus*, B- *Xanthoria* sp., C- *Laminaria digitata*.

La communauté des producteurs primaires de l'estran rocheux peut être très diversifiée avec des macroalgues, des lichens, des microalgues et des cyanobactéries (Fig. 2). Sur les plus hauts niveaux, les lichens sont prédominants et assurent la transition entre le milieu marin et le milieu terrestre. Les lichens sont des associations symbiotiques entre un champignon hétérotrophe et une algue photosynthétique. Ces organismes sont capables de résister à de très fortes dessiccations et de coloniser le haut de l'estran grâce à leur bonne tolérance au stress osmotique (Grube & Blaha 2005). Les microalgues sont abondantes sur les estrans les plus exposés où les macroalgues se développent surtout en niveau bas. Une partie des producteurs primaires appartient au microphytobenthos qui contribue au biofilm recouvrant tous les substrats. Le biofilm intertidal est une association de bactéries, cyanobactéries, protozoaires, propagules de macroalgues, diatomées et autres microalgues (Anderson 1995). Il forme un élément important de l'écosystème; il est source d'énergie et fait office d'assemblage pionnier pour les successions des communautés benthiques (Leite et al. 2012). La diversité algale augmente dans les zones abritées où elle peut recouvrir tout le substrat (Little & Kitching 1996). Les macroalgues peuvent avoir des morphologies et des physiologies très différentes. La majorité des espèces intertidales a un taux de reproduction élevé et est considérée comme pionnière (Little et al. 2009). Les caractéristiques de la zone de marée, notamment l'hydrodynamisme, contraignent les macroalgues à des tailles réduites et des taux de croissance élevés. Ainsi, différents types de thalles (fusiformes, encroûtants, etc.) permettant de minimiser la résistance à l'arrachement et d'assurer une protection contre les vagues (Cubit 1984, Underwood & Jernakoff 1984). La distribution verticale des espèces de macroalgues est liée à l'irradiance reçue par les différents niveaux de l'estran, à travers la capacité photosynthétique, de compensation et de saturation de chaque espèce (Lüning 1980).



Fig. 3 Exemples de consommateurs primaires : A- *Patella* sp., B- *Osilinus lineatus*, C- *Littorina saxatilis*.

Les consommateurs primaires benthiques sont très diversifiés et largement répandus sur l'estran avec principalement des gastéropodes (Fig. 3). Les patelles sont des consommateurs importants du biofilm épilithique grâce à leur radula qui leur permet de racler le substrat (Jenkins & Hartnoll 2001). Ces gastéropodes sont largement distribués sur toute la zone intertidale et présentent une augmentation interspécifique significative de la hauteur de la coquille du bas vers le haut de l'estran (Vermeij 1973). Cette adaptation morphologique permet aux patelles de coloniser les plus hauts niveaux intertidaux et de se protéger contre le stress thermique en réduisant leur surface de contact relative avec le substrat (Harley et al. 2009). D'autres consommateurs de macroalgues et de biofilm épiphytique (sur la surface des végétaux) sont les gastéropodes tels que les gibbules et les littorines (Little & Kitching 1996). Les littorines sont des gastéropodes universellement présents sur les estrans rocheux. Ce groupe présente une grande plasticité qui lui permet de résister aux stress environnementaux. Les stratégies reproductive vont depuis des œufs planctoniques jusqu'à l'ovoviviparité (Little 1990) et les morphologies sont très variables du bas vers le haut de l'estran, avec différentes hauteurs et structures externes des coquilles (Vermeij 1973).

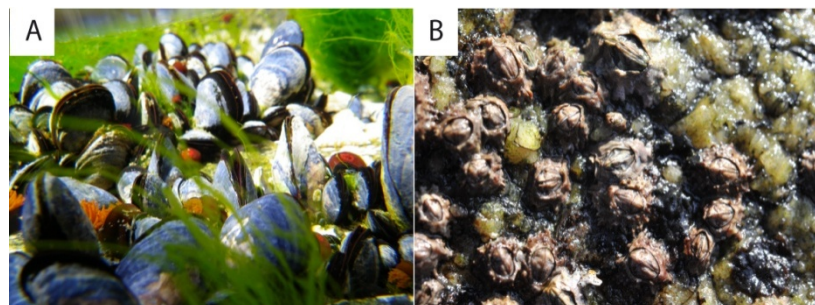


Fig. 4. Exemples de filtreurs :A- *Mytilus* spp., B-balanes.

Un autre groupe fonctionnel très commun dans la zone de balancement des marées est celui des filtreurs tels que les moules et les balanes (Fig. 4), qui peuvent développer des populations importantes sur l'estran rocheux (Lewis 1964). Les balanes forment généralement des populations très denses sur les sites exposés où l'abondance des prédateurs et la couverture de macroalgues sont limités par l'action des vagues (Little & Kitching 1996). Sur ces estrans exposés, les balanes sont souvent en compétition pour l'espace avec les moules. L'abondance de leurs populations respectives dépend des différentes conditions de recrutement et de prédation (Navarrete & Castilla 1990).



Fig. 5. Exemples de prédateurs : A- *Carcinus meanas*, B- *Haematopus ostralegus*, C- *Nucella lapillus*.

Moins nombreux mais très importants pour l'équilibre des réseaux trophiques, les prédateurs sont aussi présents sur les estrans rocheux. Les gastéropodes du genre *Nucella* sont très fréquents sur les côtes rocheuses et peuvent se nourrir des balanes et des moules (West 1986). L'estran est aussi habité par des prédateurs plus grands tels que les étoiles de mer ou plus rapides comme les crabes, qui peuvent exploiter une large gamme de proies (Little & Kitching 1996). En plus des prédateurs aquatiques, les oiseaux peuvent se nourrir de mollusques présents sur la zone intertidale (Marsh 1986). L'effet de prédateurs mobiles (oiseaux, poissons et crabes) sur la distribution des espèces sur l'estran est souvent variable avec la morphologie du substrat car les proies peuvent se cacher dans les fissures et les anfractuosités (Menge & Lubchenco 1981). En revanche, l'effet des prédateurs benthiques (*Nucella* sp. et étoiles de mer) est presque toujours majeur sur la structuration des communautés (Edwards et al. 1982).

4. Le métabolisme et les flux de carbone

Des méthodes très différentes ont été employées en laboratoire et *in situ* pour étudier le métabolisme des organismes et des communautés benthiques intertidales. Le métabolisme des animaux a principalement été étudié en laboratoire à travers la mesure des flux d' O_2 (Bayne & Scullard 1978, Branch 1978, Houlihan & Innes 1982, McMahon 1988, Babarro et al. 2000) ou celle des rythmes cardiaques (Newell 1973, Santini et al. 2000, Marshall et al. 2011). Très peu

d'études ont utilisé la méthode des incubations en laboratoire pour évaluer les flux de carbone en immersion et en émersion (Clavier et al. 2009, Lejart et al. 2012).

L'accepteur terminal d'électrons utilisé au cours du métabolisme respiratoire aérobie est l'oxygène moléculaire. Cependant, les accepteurs terminaux peuvent également être des molécules oxydées provenant de composés inorganiques (nitrates, sulfates, carbonates...) dans le cas du métabolisme anaérobie. Les mesures des flux d'oxygène peuvent entraîner une sous-estimation de la respiration totale si un temps de latence existe entre la production des composés réduits et leur réoxydation ; ces mesures sont donc considérées comme peu adéquates pour l'estimation du métabolisme total (Boucher et al. 1994).

L'estimation des flux respiratoires sur de petits organismes comme certains mollusques est plus simple et précise lorsqu'elle est obtenue par des mesures de variations de CO₂ que par celles d'O₂ (Lighton & Halsey 2011). En effet, les concentrations en oxygène sont très élevées dans l'air par rapport à celles de CO₂, aussi il est plus compliqué de mesurer de faibles variations d'O₂ que de CO₂. Les organismes marins peuvent modifier les concentrations de CO₂ principalement à travers les processus de photosynthèse et de respiration mais aussi grâce aux réactions de précipitation et de dissolution du carbonate de calcium (Frankignoulle et al. 1994). Les mesures de flux de CO₂ à l'air et de carbone inorganique dissous (DIC) sous l'eau, permettent de mesurer les deux processus respiratoires aérobies et anaérobies et d'évaluer les flux nets de calcification en immersion par la méthode de l'anomalie d'alcalinité (Smith & Key 1975). Ces méthodes ont déjà été validées par des études sur des organismes isolés sur de courtes périodes d'incubation (Martin et al. 2006, Clavier et al. 2009, Lejart et al. 2012).

La mesure du métabolisme à l'échelle communautaire permet d'estimer à la fois l'activité respiratoire et photosynthétique des organismes autotrophes et hétérotrophes présents. Différentes études se sont focalisées sur ce type de mesure, en particulier sur la zone côtière. Les analyses conjointes des flux d'oxygène et de carbone sont ainsi les plus utilisées pour établir des bilans de matière lors d'incubations *in situ* (Spilmont et al. 2007, Golley et al. 2008, Davoult et al. 2009, Migne et al. 2009, Ouisse et al. 2010). Les mesures effectuées à la lumière permettent de mesurer la somme des processus de photosynthèse et de respiration (production nette) et les mesures à l'obscurité permettent d'estimer la respiration. Le calcul des bilans annuels de carbone des différentes communautés passe par une extrapolation des

données acquises *in situ* et permet de définir les systèmes comme autotrophes ou hétérotrophes.

Dans les systèmes hétérotrophes la respiration de la communauté est plus importante que la photosynthèse, par conséquent il y a une consommation nette de carbone organique provenant de sources externes. Au contraire, dans un système autotrophe la photosynthèse dépasse la respiration et il y a une production nette de carbone organique.

La littérature a classé parmi les systèmes autotrophes les herbiers tempérés ($138 \text{ g C m}^{-2} \text{ année}^{-1}$), l'écosystème des mangroves ($226 \text{ g C m}^{-2} \text{ année}^{-1}$) et les marais salants ($218 \text{ g C m}^{-2} \text{ année}^{-1}$) (Duarte et al. 2005, Duarte et al. 2010, Sanders et al. 2010). Au contraire, d'autres systèmes côtiers tels que les estrans vaseux tempérés ($-78 \text{ g C m}^{-2} \text{ année}^{-1}$), les lagons coralliens ($-19 \text{ g C m}^{-2} \text{ année}^{-1}$) et les estrans sableux subtropicaux ($-91 \text{ g C m}^{-2} \text{ année}^{-1}$) ont été classé comme hétérotrophes (Clavier & Garrigue 1999, Migne et al. 2009, Lee et al. 2011). En effet, les écosystèmes côtiers sont très diversifiés, ce qui rend les flux de carbone très hétérogènes (Chen & Borges 2009). Les échanges de CO₂ en zone côtière sont de plus en plus étudiés en particulier dans les zones estuariennes (Duarte & Ferreira 1997, Santos et al. 2004, Laruelle et al. 2010), mais très peu d'études se sont focalisées sur le milieu intertidale rocheux (Golley et al. 2008).

5. Le rôle de la zone côtière dans le contexte du changement climatique

Le dioxyde de carbone d'origine anthropique est le gaz effet serre qui participe le plus à l'augmentation de l'effet de serre (Borges 2011). La capacité d'assimilation et séquestration du CO₂ atmosphérique par l'océan a été longtemps surévaluée en raison d'une connaissance encore imparfaite des facteurs physiques, chimiques et biologiques, surtout en zone côtière (Wollast 1991). La quantité de carbone inorganique dissous dans l'océan est plus de 60 fois supérieure à celle qui est contenue dans le CO₂ atmosphérique. Le cycle du carbone dans la zone côtière est principalement influencé par les activités biologiques (photosynthèse, respiration, décomposition) et les apports d'origine terrestre (Suzuki & Tanoue 1991). La

zone côtière assure 15 à 30% de la production primaire océanique et environ 80% de la séquestration de la matière organique océanique ; les taux de fixation biologique du carbonate de calcium (CaCO_3) sont également importants (Gattuso et al. 1998). Par conséquent, les flux de carbone sont élevés dans la zone côtière et les échanges avec l'atmosphère peuvent significativement affecter les budgets de CO_2 à l'échelle régionale et mondiale (Borges 2011).

Dans le contexte du changement global et de l'augmentation des concentrations atmosphériques en CO_2 , la quantification des processus de respiration et de production primaire est fondamentale pour établir des bilans de carbone et évaluer le rôle des différents écosystèmes. Actuellement, la contribution des zones côtières aux flux de carbone océanique est encore mal connue en raison de la grande diversité des communautés et de la difficulté de la mesure des flux de CO_2 .

Le changement climatique peut, entre autres, provoquer des changements dans l'environnement physique et chimique de la zone côtière, et induire des modifications des flux de CO_2 et des échanges entre la mer et l'atmosphère. On admet généralement qu'une augmentation de la température et des apports de nutriments d'origine terrestre peut provoquer une élévation des émissions de CO_2 (Borges 2011).

Objectifs de l'étude

L'objectif général de ce travail est de contribuer à la connaissance du métabolisme du carbone dans les communautés intertidales d'estran rocheux (Fig. 6).

Nous proposons pour cela:

- d'évaluer les différentes adaptations métaboliques des animaux intertidaux en immersion et en émersion ;
- de quantifier au laboratoire les flux de carbone liés aux processus de respiration (immersion et émersion) et de calcification (immersion) ;

- d'établir *in situ* les bilans de carbone (production primaire, respiration, calcification) pour des communautés rocheuses de mode semi-exposé et de comparer les résultats avec ceux qui ont été obtenus en laboratoire ;
- d'extraire les bilans de carbone des estrans rocheux à une échelle régionale.

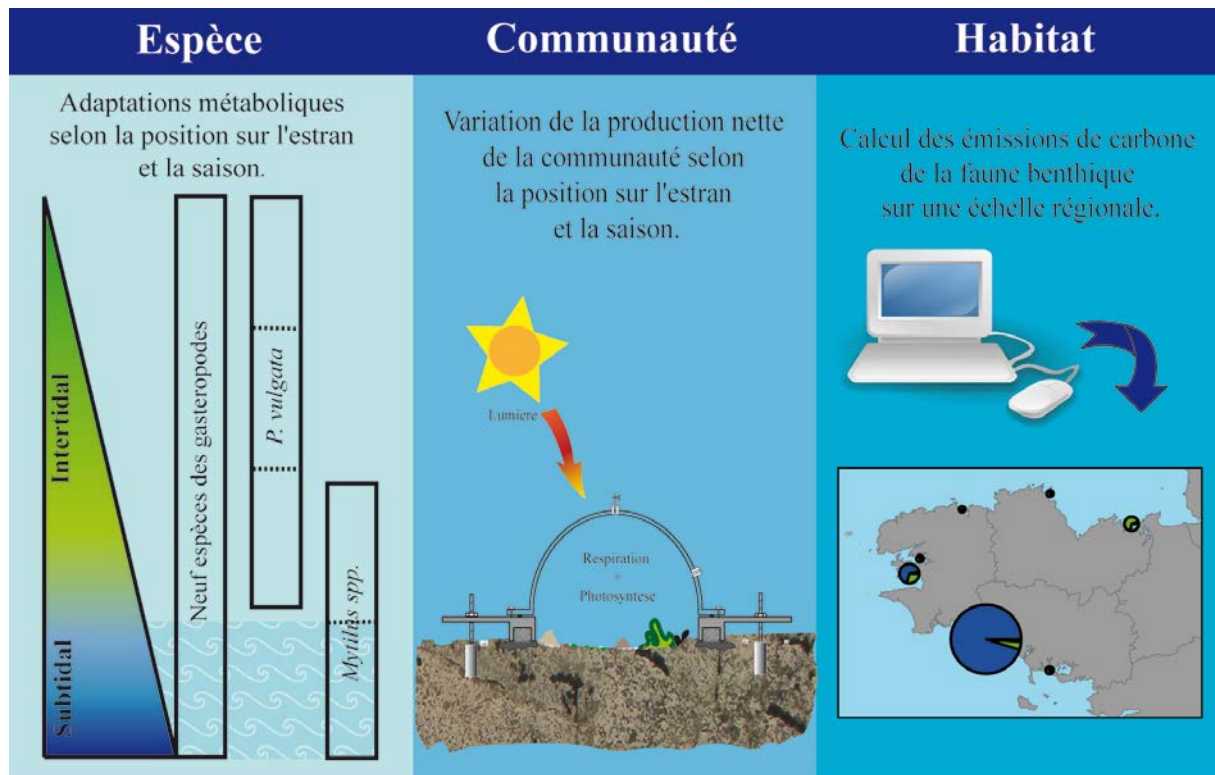


Fig. 6. Présentation schématique des phénomènes étudiés à trois échelles.

Chaque chapitre comprend le texte d'un article en anglais qui a été ou sera soumis pour publication, précédé d'un court résumé en français, qui présente le contexte, les objectifs et les principaux résultats de l'étude.

Le texte est organisé en trois parties. La première est articulée en trois chapitres et porte sur les mesures métaboliques effectuées en laboratoire sur les moules intertidales et subtidales, les patelles et neuf espèces de gastéropodes. La seconde partie présente les résultats obtenus *in situ* sur les communautés d'un estran rocheux semi-exposé et tente une extrapolation des résultats à l'échelle régionale. La dernière partie contient une synthèse des principaux résultats et propose des perspectives pour compléter ce travail.

Partie I

**Respiration et calcification à l'air et
sous l'eau des animaux intertidaux
selon leur position sur l'estran.**

Chapitre 1

Comparaison du métabolisme de moules vivant en milieu intertidal et subtidal.



Fig. 7. Photo de la moulière intertidale étudiée (Plage des blancs sablons, Le Conquet).

1. Contexte général et résumé

L'objectif de ce chapitre est de comparer deux populations naturelles de moules intertidales et subtidales, pour comprendre leurs adaptations métaboliques à l'émergence et l'immersion. Les côtes occidentales françaises sont un lieu de recouvrement de la distribution de deux espèces de moule, *Mytilus galloprovincialis* et *Mytilus edulis*, qui forment une structure complexe avec des populations monospécifiques ou mixtes (Bierne et al. 2003). Les conditions environnementales influencent le recrutement et déterminent la présence des deux espèces et de leurs hybrides (Gosling & Wilkins 1981). De précédentes études ont ainsi montré un tel mélange de *M. galloprovincialis* et de *M. edulis* en Bretagne et plus précisément dans la région de Brest (Daguin et al. 2001, Bierne et al. 2003). Après avoir caractérisé les deux espèces et leurs hybrides sur les zones d'étude par des tests génétiques, nous avons considéré que les deux populations avaient une composition similaire et comparable.

Mytilus spp. est un mollusque bivalve filtreur de la classe des Lamellibranches. La moule est protégée par deux valves de tailles égales produites par l'épithélium externe du manteau. Les deux valves sont reliées par un ligament externe au niveau d'une charnière et maintenues par deux muscles adducteurs de différente taille (Haris 1990). Les moules sont des organismes sessiles qui se fixent au substrat avec un byssus régénérable qui leur permet de se détacher en cas de besoin (Alyakrinskaya 2002). En immersion, ces animaux utilisent leurs branchies à la fois pour respirer et pour se nourrir. L'activité de ces branchies est facilitée par une grande surface d'échange; cependant le coût énergétique pour maintenir une forte circulation d'eau peuvent être limitant (Bayne 1976). Les moules qui vivent dans la zone de balancement des marées sont périodiquement exposées à l'air (Fig. 7). Pendant la marée basse, le comportement de «gaping» permet une respiration partiellement aérobie. Le comportement de «gaping» consiste en une légère ouverture intermittente des valves pour assurer l'oxygénéation de l'eau retenue dans la cavité palléale en contact avec les branchies (McMahon 1988).

La distribution bathymétrique de *Mytilus* spp. est très large et va du milieu de la zone intertidale à la zone subtidale, ce qui permet de comparer les capacités d'adaptation des moules aux conditions de ces deux habitats. De précédentes études ont comparé des moules

intertidales du milieu naturel à des moules subtidales provenant de l'aquaculture. Les résultats montrent que les animaux intertidaux ont la meilleure tolérance à l'exposition aérienne mais que les moules subtidales peuvent acquérir cette tolérance après acclimatation en milieu intertidal (Demers & Guderley 1994, Sukhotin & Pörtner 1999).

Afin d'évaluer l'effet du changement saisonnier de la température sur le métabolisme des moules, des mesures de respiration et de calcification ont été effectuées à différents moments de l'année. Les premiers échantillonnages ont révélé une différence significative dans la taille maximale des coquilles avec des longueurs plus importantes pour les moules subtidales. Pour cette raison, deux classes d'âge ont été choisies pour pouvoir comparer les deux populations. Les petites moules intertidales et subtidales (2-3 ans) ont des tailles similaires avec une moyenne de 25 mm, contrairement aux grandes moules (5-7 ans) qui mesurent en moyenne 66 mm en subtidal et 43 mm en intertidal.

Les résultats montrent que les petites moules ont des taux de respiration similaires à l'air et sous l'eau. A l'inverse, les grandes moules intertidales sont mieux adaptées à la respiration aérienne que les moules subtidales. Le flux de calcification suit un cycle saisonnier avec des valeurs plus élevées par unité de biomasse pour les petites moules.

L'ensemble des résultats suggère que les petites moules ont des réponses similaires aux stress, indépendamment du site de prélèvement, avec des taux métaboliques élevés et une résistance inférieure aux hautes températures. Les grandes moules ont élaboré des stratégies adaptatives différentes selon les conditions environnementales du site.

Les calculs de bilan de carbone démontrent que les populations de *Mytilus* spp. peuvent contribuer significativement aux émissions de CO₂ dans leur environnement.

Metabolism in blue mussel: Intertidal and subtidal beds compared.

Morgana Tagliarolo, Jacques Clavier, Laurent Chauvaud, Marcel Koken, Jacques Grall

2. Introduction

The intertidal zone supports a rich and unique biota consisting almost entirely of marine organisms that are dependent on water cover or at least a very wet environment for most of their activities (Little & Kitching 1996). Intertidal organisms are regularly exposed to large variations in environmental factors such as temperature, food availability, humidity and salinity. This exposure is particularly true for sessile and sedentary organisms that cannot move to escape from environmental stresses imposed during low tide exposure to air (Nicastro et al. 2010). Intertidal mollusks display a number of specialized adaptations to periodic emersion, correlated with level of exposure. The different adaptive strategies may include resistance mechanisms to elevated temperature and/or desiccation, tissue freeze, and hypoxia and anoxia tolerance (McMahon & Russel-Hunter 1977, McMahon 1988).

Mussels are common in coastal water, and they are important species in aquaculture (FAO 2010). The French mussel industry produces around 60,000 metric tons year⁻¹ and the “Bouchots” technique, used in intertidal areas, accounts for the bulk of production in Brittany (Prou & Gouletquer 2002). In the Mediterranean zone, deep-water longlines and suspended culture techniques are more commonly used. Bivalves such as mussels and oysters, especially if grown intertidally, tolerate desiccation and are capable of journey times of several days for commercial purposes (Laing & Spencer 2006).

Environmental differences between the intertidal and subtidal zones provide an excellent opportunity to study the adaptation of species to different habitats. To illustrate adaptive variations independently of phylogeny effect (Stillman & Somero 2000), we chose to

investigate adaptation to intertidal and subtidal conditions of mussels living in the same area. Previous studies have shown that acclimatization to intertidal conditions can modify both tolerance to emersion and metabolic rates in *Mytilus edulis* (L.) (Demers & Guderley 1994). The importance of temperature variations on respiration has been investigated in several studies that all agree that temperature is among the most important factors affecting oxygen consumption in mussels (Bayne 1976, Marsden & Weatherhead 1998, Jansen et al. 2009). Respiratory adaptation to emersion has mainly been assessed through oxygen flux measurements (Griffiths 1981, Marsden & Weatherhead 1998, Babarro et al. 2000, Jansen et al. 2009), but intertidal carbon metabolism related to both aerobic and anaerobic respiration and to calcification remains poorly known. Some recent studies on rocky-shore species living in the coastal zone have shown that benthic animals could be a significant source of CO₂ for their surrounding environment (Clavier et al. 2009, Lejart et al. 2012). To complement these data, we here investigate the importance of *Mytilus* spp. in coastal carbon fluxes.

In this study, we investigated seasonal variations of aquatic and aerial metabolism rates of *Mytilus* spp. populations, addressing the following questions: Are there respiratory differences between aerial and aquatic CO₂ rates? Are metabolic rates different for intertidal and subtidal mussels? Are intertidal animals better adapted to aerial exposure?

3. Material and methods

Sampling

Mussels were sampled in a coastal macrotidal ecosystem (maximum tidal amplitude: 8 m; tidal periodicity: 12 h 15 min) from Brittany, France (Fig. 8). Intertidal mussels were collected from the rocky shore at low tide, and subtidal

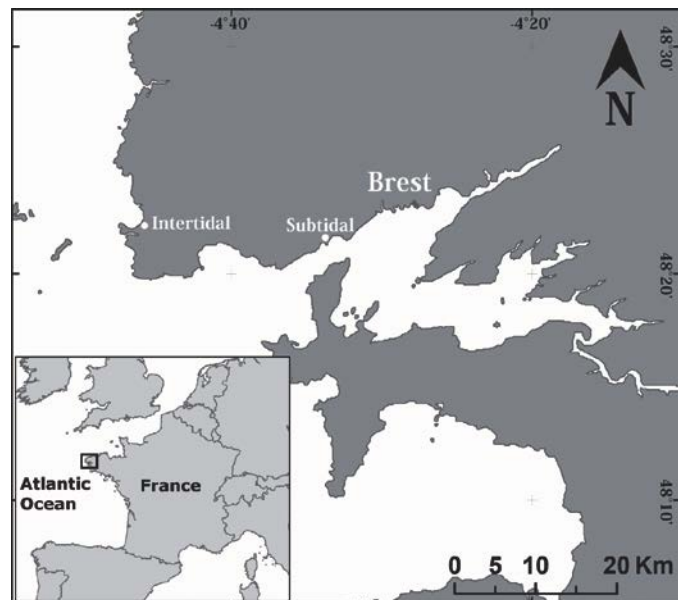


Fig. 8. Sampling sites for intertidal and subtidal mussel respiration measurements in western Brittany (France).

mussels were collected from a mooring in the vicinity of Brest. Intertidal mussels were collected around mean tide level (aerial exposure time rate was 55%) and subtidal mussels at a depth of ca. 3 m below chart datum.

Mussels were collected the day before metabolic measurements were made. They were cleaned of epibionts. In the laboratory, subtidal mussels were kept in running sea water, whereas intertidal mussels were exposed to air during low tide in tanks that simulated the natural tidal cycle. Fifty-five specimens were selected from each site. Mussels were sorted by size and age; their age was determined by counting the rings of winter growth delays on the shells (Millstein & O'Clair 2001, Sukhotin et al. 2003). Intertidal and subtidal small (2-3 yr old) mussels had a similar average shell length (24 and 26 mm, respectively), while subtidal large (5-7 yr old) mussels were larger than intertidal large mussels (66 mm and 43 mm respectively). The biomass of the specimens was determined by drying at 60°C for 24 h and burning at 450°C for 4 h in a muffle furnace. The ash mass was then subtracted from the dry mass to obtain the “ash-free dry weight” (AFDW). All biomass results were expressed as g AFDW.

Genomic DNA analysis

The blue mussel, *Mytilus edulis*, and the Mediterranean mussel, *Mytilus galloprovincialis* Lmk., occur widely on the coasts of northern Europe, and wherever they are sympatric, they hybridize (Gosling et al. 2008). The hybrid zone is large, ranging from the Atlantic coasts of France to northern Scotland, and is spatially complex, containing a mixture of pure, hybrid and introgressed individuals (Daguin et al. 2001, Gosling et al. 2008). Despite some differences in shell morphology, distinguishing between *M. galloprovincialis* and *M. edulis* based solely on morphological characters is difficult and highly uncertain due to interbreeding and adaptations to environmental conditions (Gosling 1992).

To identify *Mytilus* taxa, 10 mussels each from intertidal and subtidal studied zones were sampled for DNA analysis. Mussel foot tissue was powdered in a mortar in liquid nitrogen, and genomic DNA was isolated using a commercial DNA extraction kit (DNeasy blood & tissue kit, Qiagen) and quantified by UV absorbance spectroscopy (OD). PCR was performed

with standard methods (Sambrook et al. 1989) using the following amplification regime : 1 cycle, 5 min/94°C; 40 cycles, 30 s/94°C, 30 s/56°C, 1 min 30 s/72°C; 1 cycle, 10 min/72°C; 1 cycle, overnight/4°C. The primers were designed in the non-repetitive region of the “Foot Protein 1” gene, coding for one of the adhesive proteins of the Mytilidae which contained inserts or deletions that are species-specific (Inoue et al. 1995).

Amplification with primers Me15 (5'-CCA.GTA.TAC.AAA.CCT.GTG.AAG.A-3') and Me16 (5'-TGT.TGT.CTT.AAT.AGG.TTT.GTA.AGA-3') gave species-specific fragments of, respectively, 180 (*M. edulis*) 168 (*M. trunculus*) and 126 bp (*M. galloprovincialis*) (Inoue et al. 1995). Fragments were separated on 5% NUSieve GTG agarose (FMC Bioproducts, Rockland, Maine) gels.

Aerial respiration

For metabolic measurements, we used 10 samples with number of individuals increasing from 1 to 10 and a reference. Aerial CO₂ metabolism was measured during short-time incubations in an airtight chamber, using an infrared gas analyzer (Migné et al. 2002). At low tide time i.e. when natural population were emerged, animals were placed on a glass table in a climatic room. The indoor air in the climatic room was controlled by an aeration system directly connected with the exterior. Since laboratory is located near coastal zone the air temperature and humidity in the climatic chamber was similar to what is found in natural environment.

Samples were covered with an opaque chamber with an airtight rubber seal, connected via a closed circuit to the infrared gas analyzer (Li-Cor, LI 820). An adjustable pump maintained an air flow of 0.8/0.9 l min⁻¹ into the circuit. To dehumidify the air, a desiccation column filled with anhydrous calcium sulfate (Drierite, USA) was placed at the analyzer gas inlet. The CO₂ partial pressure (pCO₂; in parts per million, ppm = μmol CO₂ mol air⁻¹) was displayed on a laptop computer and recorded at 5-s intervals for about 3 min. Aerial carbon respiration was measured for the 10 samples and a control without mussel, every hour for 6 h to mimic the low tide condition for a natural population. Air temperature and relative humidity (RH) were measured every hour (T200 thermo-hygrometer, Trotec). Since the air of

the room was directly pumped from the outside, the air humidity naturally varied with temperature such as in the natural environment. Aerial fluxes correspond to the linear slope of the change in CO₂ concentration over time during the incubation period, corrected from the net volume of the enclosure and the incubation time.

Ammonium excretion

Ammonium ions (NH₄⁺) are the major nitrogenous waste product of aquatic mollusks (Bishop et al. 1983). Excretion of ammonium resulting from the catabolism of organic nitrogen potentially causes an increase in total alkalinity (TA) by 1 equivalent per mole. The rate of ammonia excretion was determined for intertidal and subtidal mussels (large and small individuals) in summer and winter. Samples of water were taken at the beginning and at the end of respiration incubations and stored in 100 ml bottles. Ammonium concentration was determined according to the phenol-hypochlorite method (Solorzano 1969). Reagents were added to the water samples immediately after sampling. After 24 h, sample coloration was measured at 630 nm (UV-1700 PharmaSpec, UV-VIS spectrophotometer, Shimadzu, Japan) using Milli-Q water as the blank. Ammonium excretion rates are expressed as μmol NH₄⁺ g AFDW⁻¹ h⁻¹.

Calcification

Net calcification was estimated during immersion only, using the alkalinity anomaly technique (Smith & Key 1975) based on the fact that TA decreases by 2 equivalents for each mole of CaCO₃ precipitated. Net calcification rates in a bottle (μmol CaCO₃ h⁻¹) were estimated using the following equation:

$$G = \frac{\Delta TA \times v}{2 \times \Delta t}$$

where ΔTA is the variation of total alkalinity during incubation (μmol l⁻¹), v is net bottle volume (l), and Δt is incubation time (h). Variations in nutrient concentrations may bias

estimation of calcification from alkalinity changes. We assumed that in our short-time incubation, nitrification process variation could be considered insignificant with regard to the total alkalinity variation observed in the present study, and we considered only ammonium production by an excretion process.

Underwater respiration

During natural high tide, animals were placed in opaque plastic bottles filled with natural filtered seawater directly pumped from the Bay of Brest. Underwater respiration fluxes were assessed during 1–1.5-h incubations. Bottles were kept in the dark and immersed in running sea water pumped from the Bay of Brest to maintain constant temperature matching natural conditions. Water was sampled from each bottle at the beginning and end of incubation. The pH (total scale) was measured immediately, using a pH meter (Radiometer PH240) standardized with Tris-HCl (2-amino-2-hydroxymethyl-1,3-propanediol) and 2-aminopyridine/HCl buffer solutions in synthetic sea water with a salinity of 35. TA samples were filtered through 0.7-µm Whatman GF/F filters, stored in 250-ml bottles in the dark. Analyses were carried out within 1 wk. TA (mmol kg^{-1}) was determined on 20-ml subsamples by Gran automatic potentiometric titration (Radiometer, Titrilab TIM 865) using 0.01 mol l^{-1} HCl. Water temperature was measured at the beginning and end of the incubations. Salinity, phosphate and silicate concentrations were determined using the automated Marel Iroise Station (IUEM-UBO, Observatoire du Domaine Côtier), located near the pumping station providing the water for these experiments. The concentration of dissolved inorganic carbon (DIC) was calculated from the pH, TA, temperature, salinity, phosphate and silicate concentrations (Pierrot et al. 2006). The CO_2 dissociation constants K1 and K2 (Roy et al. 1993) were used in the computation. Underwater respiration (R , mmol DIC h^{-1}) in each bottle was calculated according to

$$R = \frac{\Delta \text{DIC} \times v}{\Delta t \times 10^3} - G$$

where, G is the net CaCO_3 flux in a bottle ($\text{mmol CaCO}_3 \text{ h}^{-1}$), v is the bottle volume (l), Δt is the incubation time (h), and ΔDIC is the change in the total inorganic carbon concentration (mmol DIC l^{-1}).

Calcium carbonate content

Intertidal and subtidal individuals show different shell thickness and roughness. To help clarify calcification rates, differences between shells were tested with calcium carbonate measures. Calcium carbonate is predominantly found in the shell as outer calcite and the inner aragonite layer associated with the organic matrix (Soído et al. 2009). Five individuals of each intertidal and subtidal studied population were sampled. Soft tissues were removed, and dried shell was pestled to obtain fine powder. The mass of shell treated was 0.35 g, dry weight, for all samples. The calcium carbonate of the sample was treated with an excess of hydrochloric acid, and the volume of carbon dioxide gas released was measured using a Bernard apparatus (Hulseman 1966). Results were compared with the volume of CO_2 released by pure CaCO_3 . The carbonate content is expressed in weight percentage.

Data treatment

Relationships were established between carbon fluxes during emersion and immersion and mussel AFDW biomass using a functional regression because both fluxes and biomass are affected by natural variability. To analyze the effect of temperature on respiration rates of mussels in emersion and immersion, an Arrhenius plot was established after logarithmic transformation as an inverse function of temperature:

$$\ln Flux = \ln a - \frac{E_a}{k} \times \frac{1}{T}$$

where $Flux$ is mussel respiration rate (ΔDIC underwater or ΔCO_2 in the air, $\mu\text{mol g}^{-1} \text{ h}^{-1}$), a is a normalization constant, E_a is the activation energy (J mole^{-1}), k is Boltzmann's constant ($8.31 \text{ J K}^{-1} \text{ mol}^{-1}$), and T is the absolute temperature (K). An ANOVA test was used to

compare Arrhenius linear regression (Sokal & Rohlf 1995). When samples were too small or not normally distributed, the Kruskal–Wallis and Mann–Whitney non-parametric tests were performed.

To estimate CO₂ fluxes on an annual scale, average contributions were calculated for aerial and underwater mean annual temperature. The CO₂ contribution was calculated considering that subtidal mussels are constantly immersed and that intertidal mussels are exposed to air for about 12 h per day.

4. Results

Environmental parameters

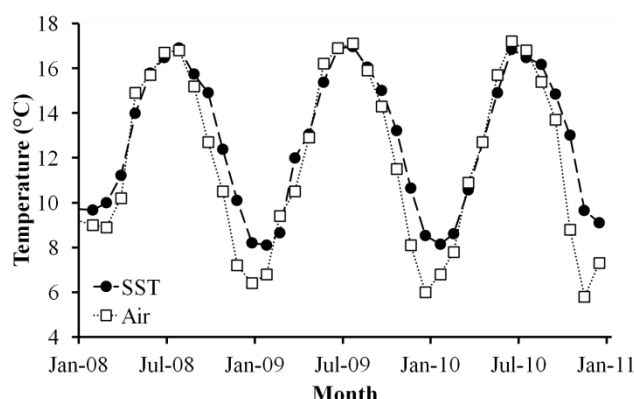


Fig. 9. Monthly variation of mean sea surface (Marel Iroise Station) and air temperature (Météo France, Camaret station) from 2008 to 2011.

Air and sea surface temperatures were respectively recorded in the bay of Brest at Camaret station (Météo France) and from the Marel Iroise Station, from January 2008 to April 2011 (Fig. 9). Temperature ranged from 5.8 to 17.2°C in air and from 8.1 to 17.0°C in sea surface. Average temperature for the studied period was 12.5°C for sea water and 12.1°C in the air.

Genomic DNA analysis

Of the 10 intertidal mussels examined, five exhibited two bands of 126 (*M. galloprovincialis* specific) and 180 bp (*M. edulis* specific), whereas the other five mussels were homozygous for the 126-bp band (Fig. 10, upper panel). One of the subtidal mussels (N°12) was a heterozygote and mussel N°15 was homozygous for the *M. edulis* allele. All

other animals were homozygous for the *M. galloprovincialis* type allele (Fig. 10, lower panel).

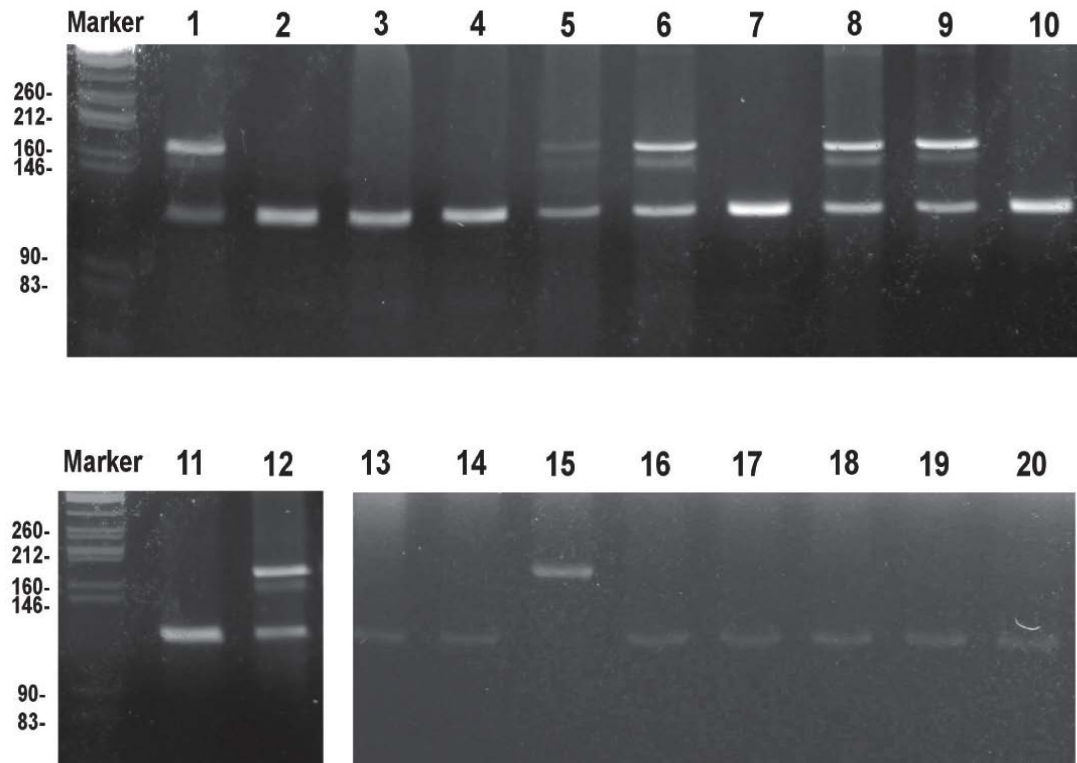


Fig. 10. Agarose gel of the PCR products of the “Foot protein 1” gene of mussels. Lanes 1 to 10, intertidal mussels; lanes 11 to 20, subtidal mussels.

Aerial respiration

Carbon dioxide release during emersion differed between large and small mussels (Fig. 11). Aerial respiration of large *Mytilus* remained stable during the 6-h aerial exposure, and slopes did not differ significantly between the temperatures tested (large intertidal ANOVA, $p = 0.55$; large subtidal ANOVA, $p = 0.12$) (Fig. 11 A, B). Respiration of small mussels was highly variable during the 6-h emersion. Slopes differed significantly between the temperature tested (small intertidal ANOVA, $p = 0.00$; small subtidal ANOVA, $p = 0.03$) (Fig. 11 C, D). Large intertidal mussel respiration increased with temperature from 7 to 18°C and decreased

for higher temperatures. For hot and dry conditions (28°C, 45% RH), fluxes were always low from the first hour after emersion. Comparatively, large subtidal aerial respiration remained very low during emersion at any tested temperature (Fig. 11 B). The lower respiration was observed at the higher temperature (29°C) and lower humidity (40%). Temperature and atmospheric humidity were significantly related during our experiments ($R^2=0.45$, $p = 0.00$); thus our experimental procedure did not allow to separately study the effects of these two parameters.

Tab. 1. Parameters of Arrhenius plots relating the logarithm of hourly underwater and aerial respiration per g AFDW to the inverse of absolute temperature.

	Underwater				Air			
	Intertidal		Subtidal		Intertidal		Subtidal	
	Small	Large	Small	Large	Small	Large	Small	Large
Ln a	15.59	-0.13	15.83	24.03	54.95	49.15	48.68	-8.95
Ea/k	5.49	0.97	3.47	6.02	14.99	13.77	13.35	2.64
R²	0.25	0.03	0.15	0.37	0.97	0.83	0.98	0.35

The relationship between temperature and aerial respiration rate was compared for intertidal and subtidal populations (Fig. 12 A, B). Intertidal and subtidal large mussels showed different aerial respiration patterns (Fig. 12 A), and Arrhenius plots (Tab. 1) differed significantly for slopes (ANOVA, $p = 0.00$). Subtidal large mussels always exhibited low CO₂ fluxes (between 0.6 and 1.8 µmol CO₂ g AFDW⁻¹ h⁻¹). Intertidal *Mytilus* respiration rates increased exponentially with temperature from 7 to 18°C. Rates measured outside this temperature range did not fit the exponential curve and were found below critical limits for aerobic metabolism. The Arrhenius break temperature (ABT) was between 21 and 24°C.

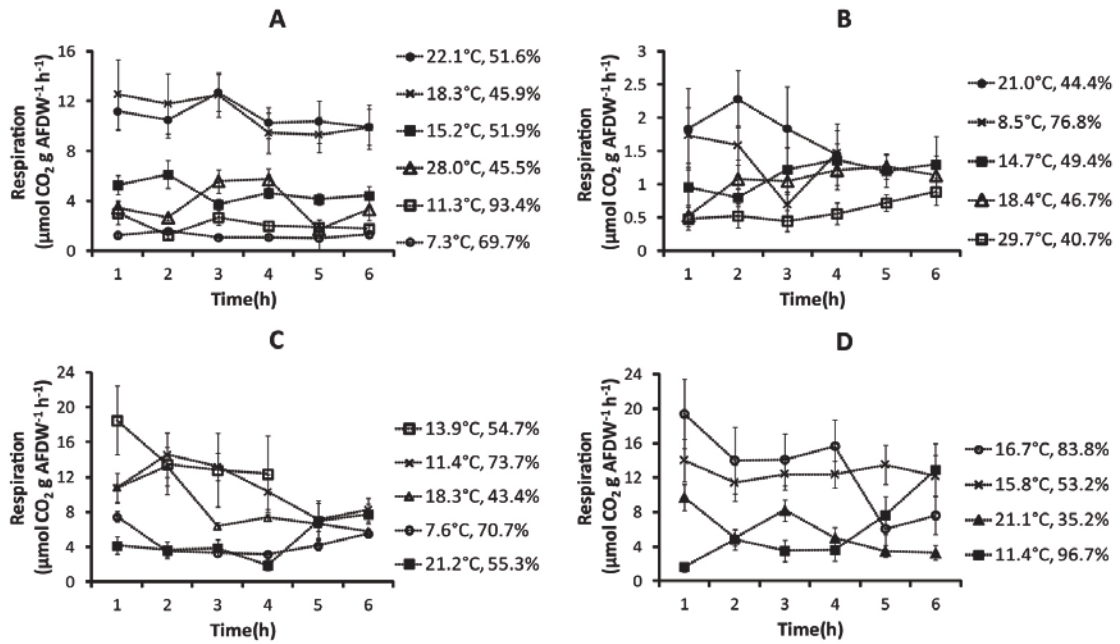


Fig. 11. Variation in aerial respiration of mussels during the low-tide period at different temperatures ($^{\circ}\text{C}$) and relative humidity levels (%), estimated from the variation of CO_2 concentration in incubation chambers. **A:** large intertidal, **B:** large subtidal, **C:** small intertidal, **D:** small subtidal mussels.

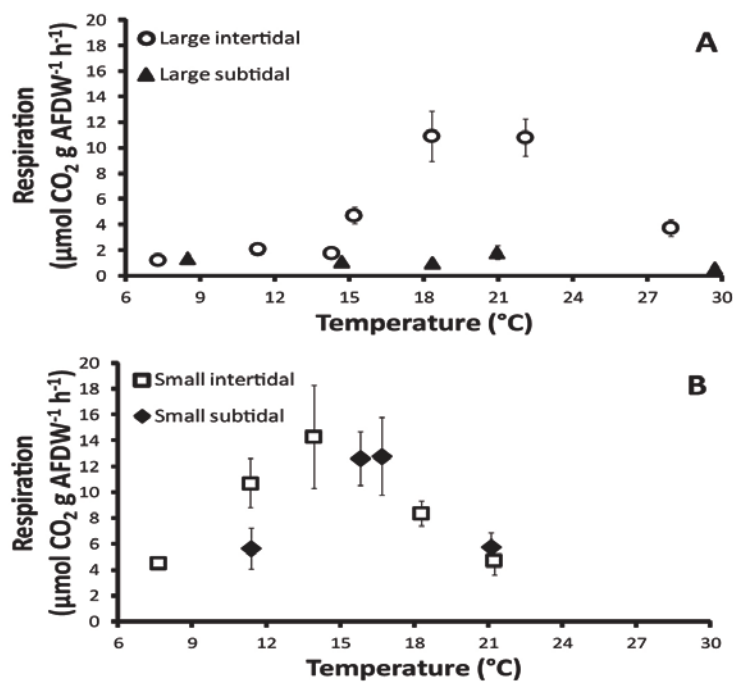


Fig. 12. Relationships between intertidal and subtidal hourly aerial respiration rates per g AFDW, and temperature (mean \pm SD). **A:** large mussels, **B:** small mussels.

Intertidal and subtidal small mussels showed similar fluxes for the same temperature and humidity (RH) ranges, and Arrhenius plots (Tab. 1) did not differ significantly for slopes (ANOVA, $p=0.66$) (Fig. 12 B). For both mussel beds, small animal aerial respiration increased exponentially with temperature; the Arrhenius plot fit CO_2 fluxes from 7 to 16 $^{\circ}\text{C}$ (Tab. 1). Fluxes decreased for temperatures higher than ABT with minimal values at 21 $^{\circ}\text{C}$.

Maximal respiration rates were slightly higher for small ($14.3 \mu\text{mol CO}_2 \text{ g AFDW}^{-1} \text{ h}^{-1}$) than for large intertidal mussels ($10.9 \mu\text{mol CO}_2 \text{ g AFDW}^{-1} \text{ h}^{-1}$). Maximal aerial CO_2 flux was 7-fold higher for small than for large subtidal mussels.

Ammonium excretion

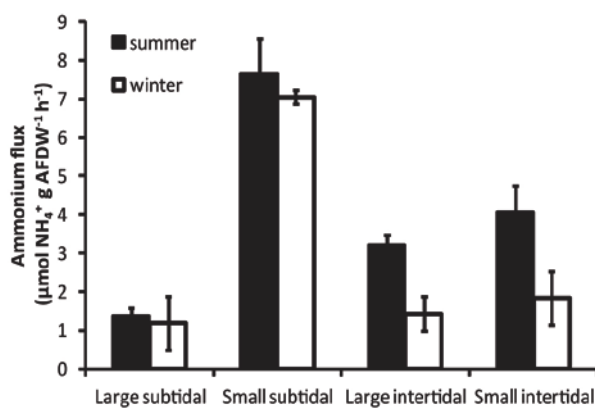


Fig. 13. Variation in ammonium excretion rates of mussels during summer and winter.

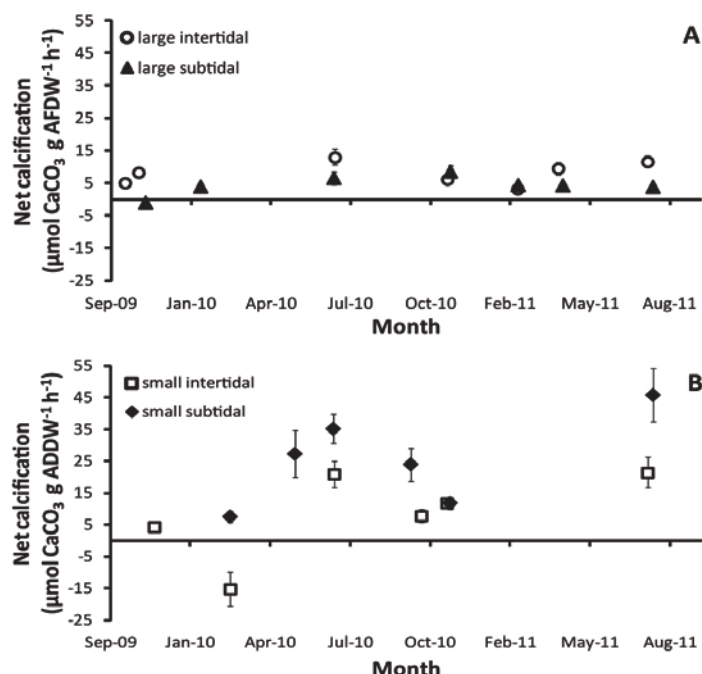


Fig. 14. Seasonal variation of net calcification rate (mean \pm SD) estimated from total alkalinity variation during incubation. Positive values correspond to calcification. A: large mussels, B: small mussels.

Ammonium fluxes varied from 1.4 to $7.6 \mu\text{mol NH}_4 \text{ g AFDW}^{-1} \text{ h}^{-1}$ in summer and from 1.2 to $7.0 \mu\text{mol NH}_4 \text{ g AFDW}^{-1} \text{ h}^{-1}$ in winter (Fig. 13). Small mussels showed stronger fluxes than large individuals. Winter and summer ammonium fluxes were significantly different for large and small intertidal mussels (ANOVA, $p < 0.01$) with higher values during summer. Conversely, large and small subtidal mussels showed similar fluxes during summer and winter. Average NH_4^+ rate was used to correct TA for subtidal mussels. For intertidal mussels, calcification fluxes were corrected with summer and winter ammonium values; spring and autumn analyses were corrected with average NH_4^+ rates.

Calcification

Net calcification was positive for all mussels tested (Fig. 14 A, B). Average uptake was $4.3 \mu\text{mol CaCO}_3 \text{ g AFDW}^{-1} \text{ h}^{-1}$ and $15.7 \mu\text{mol CaCO}_3 \text{ g AFDW}^{-1} \text{ h}^{-1}$, for large and small mussels, respectively. Net calcification showed a clear seasonal pattern with minimum values in winter and maximum in summer. Intertidal and subtidal beds did not show significant differences (large $p = 0.47$, small $p = 0.07$, Mann–Whitney test). Considering that subtidal animals are always immersed and that intertidal mussels are in water for 12 h per day, net calcification fluxes would be slightly lower for large intertidal mussels ($0.05 \text{ mmol CaCO}_3 \text{ g}^{-1} \text{ d}^{-1}$) than for subtidal ($0.11 \text{ mmol CaCO}_3 \text{ g}^{-1} \text{ d}^{-1}$).

Underwater respiration

Relationship between temperature and underwater respiration rate was compared for intertidal and subtidal populations (Fig. 15 A, B). Arrhenius plots show that underwater respiration was not directly correlated with temperature (large mussel $R^2 = 0.10$; small mussel

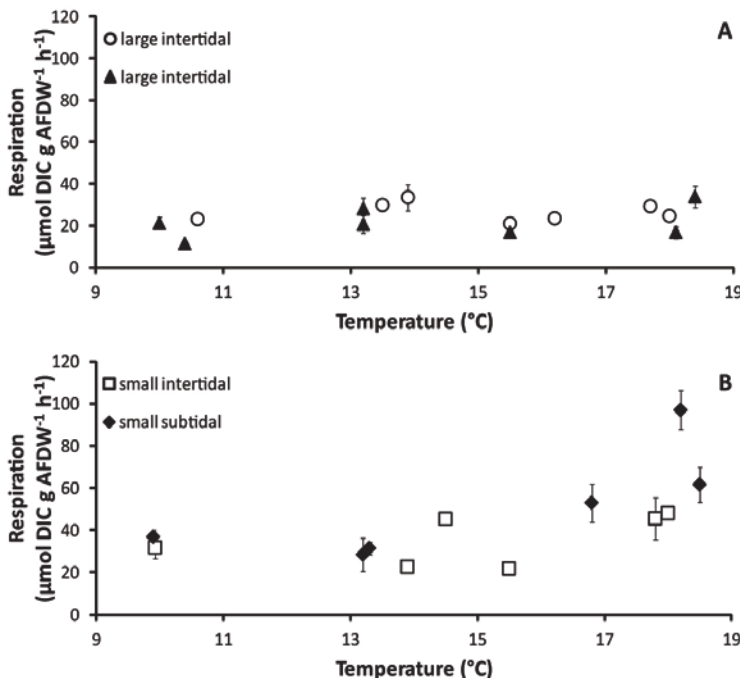


Fig. 15. Relationship between intertidal and subtidal hourly underwater respiration (dissolved inorganic carbon, DIC) rates per g biomass (AFDW) and temperature (mean \pm SD). A: large mussels, B: small mussels.

$R^2 = 0.00$). Average respiration rates were higher in small (intertidal $35.9 \mu\text{mol DIC g}^{-1} \text{ h}^{-1}$, subtidal $51.4 \mu\text{mol DIC g}^{-1} \text{ h}^{-1}$) than in large mussels (intertidal $26.4 \mu\text{mol DIC g}^{-1} \text{ h}^{-1}$, subtidal $21.3 \mu\text{mol DIC g}^{-1} \text{ h}^{-1}$). Respiration rates differed significantly among the four mussels groups (Kruskall–Wallis, $p < 0.05$). Comparing mussel groups two-by-two, significant differences existed between large intertidal and small intertidal and between large subtidal and small intertidal and

subtidal mussels (Mann–Whitney, $p < 0.05$).

Considering that subtidal animals are always immersed and intertidal animals are in water for 12 h per day, average underwater respiration fluxes for large *Mytilus* would be slightly lower for the intertidal ($0.32 \text{ mmol DIC g AFDW}^{-1} \text{ d}^{-1}$) than for the subtidal population ($0.51 \text{ mmol DIC g AFDW}^{-1} \text{ d}^{-1}$).

Intertidal mussel respiration was higher during submersion than during emersion for all samples (Fig. 16). The aerial/aquatic respiration ratio of 0.2 was the same for large and small intertidal, as well as for small subtidal mussels, whereas aerial respiration was less efficient for large subtidal mussels (ratio of 0.06). The Arrhenius plots (Tab. 1) for underwater and air respiration differed significantly for large intertidal (ANOVA, $p = 0.02$) but not for the other mussels tested (ANOVA, large subtidal $p = 0.19$; small subtidal $p = 0.24$; small intertidal $p = 0.20$).

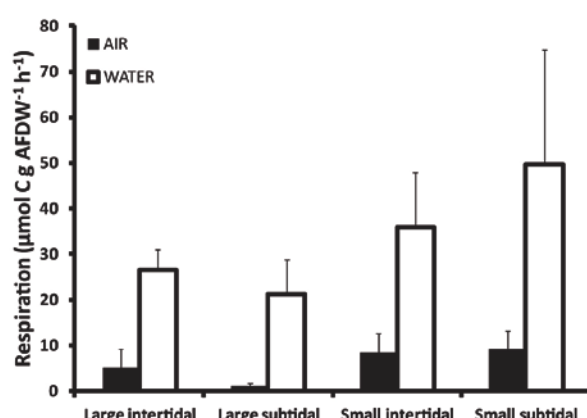


Fig. 16. Average hourly underwater and aerial carbon respiration of mussels per g AFDW (\pm SD).

Calcium carbonate content

Mean percentage of calcium carbonate content in subtidal shells was lower ($82.46 \pm 2.73\% \text{ CaCO}_3$) than in intertidal shells ($89.45 \pm 2.52\% \text{ CaCO}_3$) ($p = 0.01$, Mann–Whitney test).

CO₂ contribution

The mean total daily CO₂ emission by large intertidal and subtidal mussels was estimated respectively at 0.4 and 0.8 mmol CO₂ g AFDW⁻¹ d⁻¹. Mean annual carbon production by large intertidal mussels was 16 g C g⁻¹ yr⁻¹ and 29 g C g AFDW⁻¹ yr⁻¹ for large subtidal. For intertidal mussels the relative contribution of annual carbon sources varied between, 28-8% for aerial respiration, 50-81% for underwater respiration, and 22-11% for calcification, for small and large animals, respectively. The

relative contributions for subtidal mussels were 57-85 % for underwater respiration and 43-14% for calcification, for small and large animals, respectively.

5. Discussion

Genomic DNA analysis

In the present study, a total of 20 individuals were genotyped for Foot-Protein-1 alleles through amplification with PCR primers Me15 and Me16. Despite this relatively small sample, our results demonstrate that homozygotes and hybrids are present in both the intertidal and subtidal mussel beds. In the studied area, the *M. galloprovincialis* clearly dominates, as already described by Bierne et al. (2003). In European Atlantic coasts, the spatial distribution of mussel species shows a mosaic structure correlated with environmental factors such as salinity, wave exposure and tidal height at a local scale (Gosling & Wilkins 1981, Gosling & McGrath 1990, Bierne et al. 2002, Bierne et al. 2003). The different allele compositions between intertidal and subtidal mussels beds has been studied in the Wadden Sea (Luttikhuizen et al. 2002), and no significant differences were detected. Previous studies in mussel metabolism did not tested if individuals belonged to a single species. The genomic analysis permitted testing for the presence of two mussel species and their hybrids in the studied zone. Our results suggest that intertidal and subtidal populations had similar species and hybrids compositions.

Aerial respiration

In this study, respiration rates were measured in the laboratory where mussels were exposed to ecologically realistic conditions of temperature, humidity and tidal cycle. Body temperature and desiccation rates can significantly affect metabolism and survival of intertidal invertebrates. To clarify the responses of mussels to intertidal conditions, we compared intertidal and subtidal population metabolisms. Intertidal large mussel aerial respiration rates

showed clear seasonal variation related to temperature, contrary to subtidal animals that always exhibited low CO₂ fluxes during emersion time for all temperatures tested. Large intertidal mussels seemed better adapted to aerial conditions than large subtidal animals. Mussels from higher tidal levels, exposed to periodic emersion acquire adaptation to air exposure and desiccation with intermittent air breathing “gaping” behavior and improved water conservation ability (McMahon 1988, McMahon 1990, Demers & Guderley 1994, Sokolova et al. 2000, Sokolova & Portner 2001). Even if intertidal *Mytilus* can use atmospheric oxygen through the slight valve gape (gaping) (McMahon 1988), oxygen consumption is 4 to 15% lower during emersion than during immersion (Widdows et al. 1979, Widdows & Shick 1985). The ability to retain water in the mantle cavity can provide a most suitable condition for respiratory exchanges and a better ionic regulation. As reported for different mollusks and crustaceans, water stores are progressively depleted and ionic concentration increases during air exposure to avoid variations in hemolymph composition (Wood et al. 1986, Burnett 1988, Truchot 1990). Research on *M. edulis* suggests that differential resistance to prolonged air exposure may also correlate with anaerobic metabolism ability and reduced metabolic energy expenditure capacity (Widdows & Shick 1985, Demers & Guderley 1994, Marsden & Weatherhead 1998). The ability of bivalves to respire anaerobically is well documented (Brinkhoff et al. 1983, Babarro et al. 2007, Connor & Gracey 2011) and is connected to remarkably high tissue glycogen contents (Hochachka & Mustafa 1972).

If we assume that the respiration quotient between O₂ and CO₂ is 1, the mean aerial respiration rate for large mussels varied between 0.06 and 0.35 mg O₂ g AFDW⁻¹ h⁻¹ for temperatures between 11 and 18°C. Respiration rates measured in our study are similar to those reported in previous studies *i.e.* 0.02-0.05 mg O₂ g dry wt⁻¹ h⁻¹ for temperatures between 10 and 25°C (Widdows et al. 1979) and 0.5-0.4 mg O₂ h⁻¹ at 14°C (Labarta et al. 1997).

This study showed that small intertidal and subtidal *Mytilus* aerial CO₂ fluxes were similar and mainly controlled by temperature, as indicated by Arrhenius plots. Small mussels showed higher respiratory fluxes than large individuals. In animals with infinite growth, such as mollusks, it is not possible to separate the aging effect from the size effect, and any senescence metabolism modification can be masked by the continuously increasing size

(Sukhotin & Flyachinskaya 2009). A decrease in respiration rate with increasing age and weight has already been observed in oyster, limpets and mussels (Sukhotin & Pörtner 2001, Martin et al. 2006, Lejart et al. 2012). The driving influence of temperature on respiration is well known in marine mollusks (Newell 1973, Huang & Newell 2002, Martin et al. 2006). Respiration rates usually increase with temperature until a threshold is reached: the ABT, defined as the temperature above which respiration rates drop drastically. Our results showed that aerial fluxes increased with temperature until 24°C for large intertidal mussels and until 15 and 18°C for small intertidal and subtidal individuals, respectively. The reduction in CO₂ rates after ABT temperature may be caused by a limitation in respiratory mechanisms to protect animals from desiccation at higher temperatures. Even if the average monthly air temperature was always lower than 18°C, during emersion different environmental factors can control body temperature. While emerged, an organism body temperature can be influenced by solar radiation, air temperature, and convective heat exchanges (Helmuth 1998). Consequently, the body temperature in intertidal natural conditions is very likely to increase markedly during low tide (Helmuth & Hofmann 2001). Smaller animals were more sensitive to high air temperature and may resist summer temperatures (20–25°C) by reducing respiration rates and living closer to the thermal limits. In many species, stress resistance increases with the developmental stage of the animal, and different metabolic factors or shell structural properties may explain thermal tolerance variability (Wallis 1975, Sukhotin et al. 2003).

Underwater respiration

Most respiration rates given for mollusks are based on O₂ underwater measurements (Widdows 1973, Bayne et al. 1976, Simpfendorfer et al. 1995), whereas the associated carbon release is still poorly characterized. If we consider that the respiration quotient between O₂ and CO₂ is 1, mean respiration rates for the large mussels that we measured corresponded to 1.23 mg O₂ g AFDW⁻¹ h⁻¹ for the average annual temperature of 13°C. Respiration rates measured in our study are slightly higher than those given in previous studies; 0.32 mg O₂ g⁻¹ dry weight (DW) h⁻¹ at 15°C, *M. edulis* (Widdows 1973); 0.6 mg O₂ g DW⁻¹ h⁻¹ at 10°C, *M.*

edulis (Widdows et al. 1979); and 0.4–0.8 mg O₂ g⁻¹ shell-free DW h⁻¹ at 13°C, *M. galloprovincialis* (Jansen et al. 2009).

In most laboratory studies, aquatic respiration is measured at active (maximal activity) or routine rates (normal activity). In our experiment, fluxes were measured in filtered seawater where mussels cannot feed, and the respiratory rate reflected the standard or inactive rate. Our results showed that aerial respiration was strongly size dependent. As observed for aerial fluxes, underwater respiration was higher for small animals. Mussels seem unable to maintain high aerial respiration rates when body size increases.

Within the studied temperature range (9–19°C), DIC fluxes were relatively temperature independent, as reported for *Mytilus edulis* and *Mytilus californianus* (Widdows 1973, Bayne 1976). A change in the level of activity appears to be a major factor in the process of metabolic compensation in response to temperature (Widdows 1973). In this study, underwater respiration rates seemed more influenced by reproduction period and food availability. Extreme carbon fluxes (not shown in Fig. 15) of 50–60 µmol g AFDW⁻¹ h⁻¹ were recorded during gamete release and strong food availability periods (chlorophyll sea surface fluorescents data; Marel Iroise data). The variation of food expressed as chlorophyll *a* concentrations is an important factor influencing seasonal respiration patterns in *M. galloprovincialis* (Babarro et al. 2000).

Aerial/Underwater comparison

Respiration responses of mussels were strongly different between immersion and emersion period. While underwater carbon fluxes did not vary with temperature, aerial fluxes were highly influenced by temperature variations. During emersion, some intertidal bivalves breathe at a rate similar to that in water (Bayne et al. 1976, Widdows & Shick 1985); however, this is not a general feature for mussels. We found that aerial respiration represented 23% of underwater respiration for small intertidal, 19% for large intertidal and small subtidal, and only 5.6% for large subtidal mussels. A similar study in *Mytilus edulis* showed that aerial rates ranged from 14–20% of underwater rates (Widdows & Shick 1985).

Ammonium excretion

Ammonia fluxes are highly variable because of influences from several factors such as temperature, season and reproductive cycle. (Gabbott & Bayne 1973) In this study, mussel size strongly influences respiration and excretion; small mussels showed stronger excretion fluxes per biomass unit. In marine bivalves, excretion rate increases with individual biomass, while however, the rate of excretion per unit biomass decreases as an individual grows larger (Vaughn & Hakenkamp 2001). Summer and winter rates of ammonium excretion for large mussels (respectively 1.2–3.2 $\mu\text{mol g AFDW}^{-1} \text{ h}^{-1}$) were comparable to results of previous studies in *M. edulis* ($\sim 1.13 \mu\text{mol g}^{-1} \text{ h}^{-1}$) (Thomsen & Melzner 2010). Ammonia rates follow seasonal changes; in *M. edulis*, excretion is known to be maximal in spring and summer and minimal in winter (Bayne & Scullard 1977).

Calcification and calcium carbonate content

The alkalinity anomaly technique is a sensitive and appropriate technique for short-term studies of calcification fluxes in individual organisms (Chisholm & Gattuso 1991, Gazeau et al. 2007). Excretion of ammonium resulting from the catabolism potentially causes an increase in total alkalinity by 1 equivalent per mole. In this study, CaCO_3 fluxes were corrected with ammonium rates calculated during the summer and winter period, and the correction increased CaCO_3 fluxes on average by 13%. These results confirm that ammonium effects on AT are smaller than the variability observed in calcification estimates (Jacques & Pilson 1980, Chisholm & Gattuso 1991, Gazeau et al. 2007).

As reported in several studies (Malone & Dodd 1967, Lutz & Clark 1984, Martin et al. 2006, Clavier et al. 2009, Lejart et al. 2012), annual variation in invertebrate carbonate deposition is marked. This technique has been only used in a previous study that aimed to assess mussel calcification rates. The comparison with our data remains difficult because rates were expressed on a fresh weight basis (net calcification rates between -0.2 and 0.6 $\mu\text{mol CaCO}_3 \text{ g FW}^{-1} \text{ h}^{-1}$) (Gazeau et al. 2007). In our study, net CaCO_3 fluxes were clearly season dependent, with higher calcification in spring and summer and a predominance of carbonate dissolution in winter. Environmental factors, e.g. temperature and salinity, influence the

mineralogy and calcification of mussel shell (Taylor et al. 1973). During the warm summer months, regular crystals are deposited, but as water temperature declines, crystal growth ceases and the shell may even be eroded as calcium carbonate apparently buffers the acidic end-products of anaerobic metabolism (Lutz & Clark 1984). The effect of these and other factors, such as aerial exposure, on crystal growth determines the rate of shell deposition.

Our results show that small individuals precipitated more CaCO_3 per biomass unit than large individuals and that they were more influenced by seasonal variability. With increasing size, the growth rate declines due to reduced relative metabolic activity and reduced rate of water transport and food uptake in larger mussels (Bayne 1976, Kautsky 1982). Small mussels may also suffer from intraspecific feeding competition, obtaining more advantage with increasing size (Kautsky 1982).

The growth rate of *Mytilus* spp. depends on the tidal period and increases with time of submergence because during the uncovering period, calcification is not possible (Pannella 1976, Buschbaum & Saier 2001). Mussels can develop morphological variations in response to environmental conditions during their life. In our study, large subtidal mussels were much larger than intertidal animals at the same age while shells were thinner with lower calcium carbonate content. Large intertidal mussels mean hourly CaCO_3 fluxes were almost double compared to large subtidal mussels fluxes. Even if hourly calcification rates are higher for intertidal animals, daily fluxes are slightly higher for subtidal mussels, considering that intertidal individuals are immersed only 12 h per day.

Animals from the high intertidal zone exhibited lower growth rates than those permanently immersed. Previous studies have confirmed that *M. edulis* and *Perna canaliculus* (Gmelin) from higher tidal levels possess relatively thicker shells and larger adductor muscles (Lewis & Seed 1969, Hickman & Illingworth 1980). Mollusks with solid shells are more likely to withstand exposure to waves, drying and temperature variations (Vermeij 1972, Alyakrinskaya 2005). We show here that intertidal mussels have a smaller but stronger shell than subtidal animals, an important feature used to protect animals during aerial exposure.

CO₂ contribution

Annual carbon fluxes of intertidal large *Mytilus spp.* are mainly due to underwater respiration. The calcification contribution was significant with a ratio of 11% of total fluxes for intertidal and 14% for subtidal mussels. Our results show that CO₂ released by calcification processes is similar to previous values given for bivalves, 25% for *C.gigas* (Lejart et al. 2012), and 33% for *Potamocorbula amurensis* (Chauvaud et al. 2003). Further studies on intertidal hard substrate species will allow calculating the contribution of the whole intertidal community to CO₂ emissions.

Mussel beds are dense heterotrophic communities that are important economically and ecologically to the coastal zone. This study demonstrates that *Mytilus spp.* metabolism significantly contributes to CO₂ release in both the intertidal and subtidal zones.

Chapitre 2

Étude du métabolisme en émersion et en immersion de *Patella vulgata*, selon la position sur l'estran.

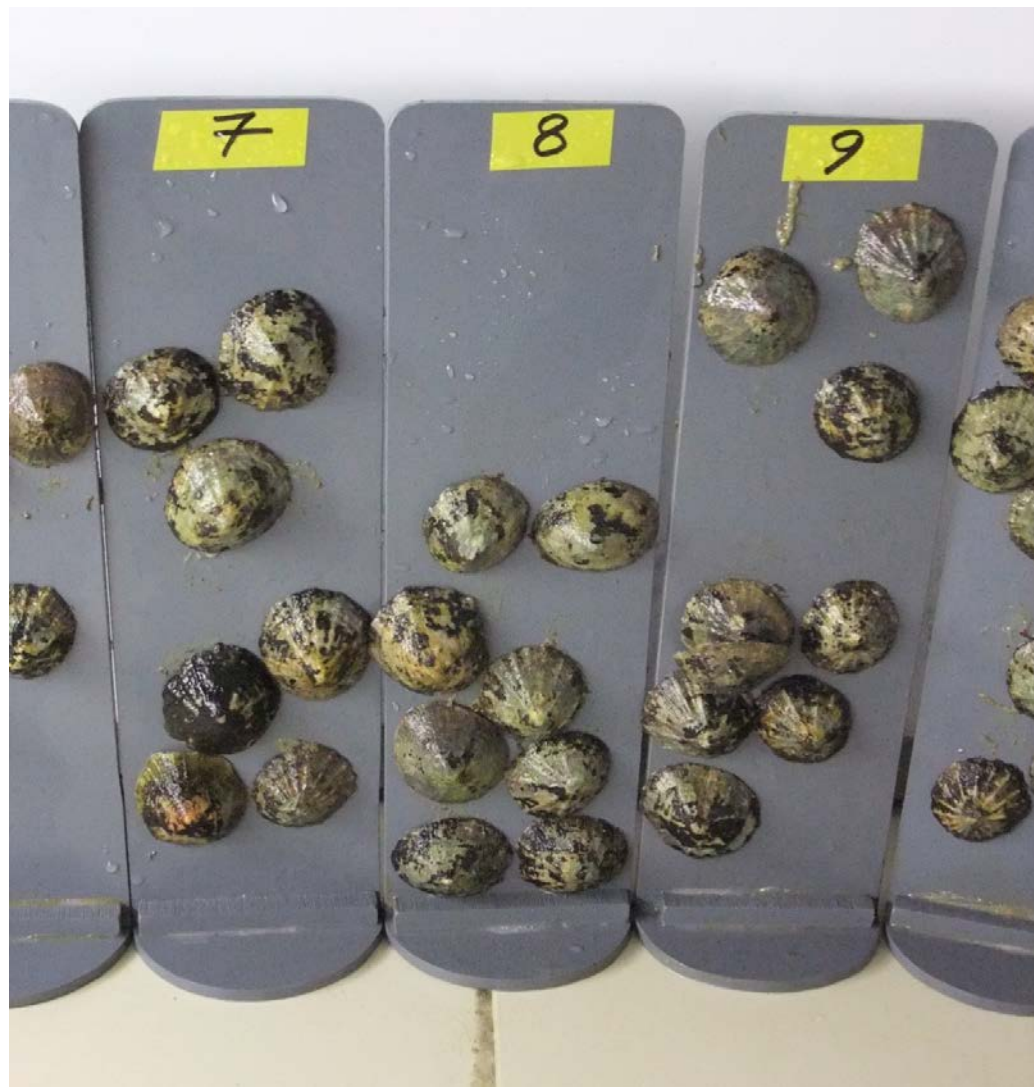


Fig. 17. Photo des patelles sur les supports pendant les mesures de métabolisme au laboratoire.

1. Contexte général et résumé

Les patelles sont rencontrées sur la totalité de l'estran (Das & Seshappa 1948, Gray & Naylor 1996). Ces gastéropodes sont bien adaptés à la vie en zone intertidale rocheuse grâce à leur stratégie comportementale et à leur morphologie.

P. vulgata est une espèce intertidale largement répandue sur les côtes de la Manche, en Mer du Nord et en Méditerranée. Cette espèce est protégée par une coquille conique non spiralée qui résiste aux impacts des vagues et aux attaques des prédateurs. La forme et la hauteur de chaque individu est influencé par ses conditions de vie. Les patelles exposées à des températures élevées produisent des coquilles hautes et avec de nombreuses aspérités (Harley et al. 2009), alors que les patelles qui vivent en zone très exposée ont des coquilles plus basses (Raffaelli & Hawkins 1999). La structure des branchies est très particulière et consiste en un ensemble de feuillets suspendu au toit de la cavité palléale ; elle lui permet de respirer à la fois à l'air et sous l'eau (Nuwayhid et al. 1978, Marshall & McQuaid 1992). Une autre adaptation morphologique importante chez cette espèce est la présence d'un pied musculaire très puissant capable d'exercer une grande force de succion ; il permet à l'animal d'adhérer fermement au substrat pour limiter les pertes en eau pendant la marée basse et de lui éviter d'être emporté par les vagues (Vermeij 1973).

Les patelles ont développé des adaptations comportementales pour se protéger des stress subis en environnement intertidal. La capacité de ces animaux à bien adhérer au substrat est aussi liée au comportement de « homing ». Certaines patelles sont en effet capables de retourner toujours à la même place avec la même orientation pour optimiser le contact de leur coquille avec le substrat (Hartnoll & Wright 1977). Dans la journée, ces brouteurs se nourrissent préférentiellement pendant la marée haute pour éviter la dessiccation et la prédation par les oiseaux. Pendant la nuit, ils sont plus actifs à marée basse car le risque de déshydratation est réduit et la prédation est surtout assurée par les crabes qui sont actifs en immersion (Hartnoll & Wright 1977, Little 1989).

P. vulgata est très résistante à la dessiccation et peut tolérer jusqu'à 60-65% des pertes en eau. Les individus plus petits, vivant plus bas sur l'estran, sont cependant sensibles au stress de dessiccation (Davies 1969). Cette espèce est aussi connue pour sa capacité de respiration à

l'air qui lui permet de maintenir un métabolisme aérobie pendant la marée basse (Brinkhoff et al. 1983). De précédentes études ont démontré que les patelles, selon leur position sur l'estran, présentaient capacités adaptatives variables en réponse à leur niveau d'exposition à l'air (Davies 1967a, White 1968, Branch 1981).

Dans ce contexte, l'objectif de ce chapitre est de comparer la respiration des animaux immersés et émergés, et d'évaluer l'effet de la position sur l'estran et des variations saisonnières sur les flux de carbone. Pour appréhender les adaptations métaboliques liées à la position sur la zone intertidale, les animaux ont été échantillonnés sur trois niveaux de l'estran. Des mesures en laboratoire ont permis d'évaluer les flux respiratoires à l'air et sous l'eau et les flux de calcification pendant la période d'immersion (Fig. 17).

Les respirations à l'air et sous l'eau sont fortement corrélées avec les variations saisonnières de la température et de la position sur l'estran. Les animaux vivant au bas de l'estran ont produit des flux de carbone supérieurs à ceux de la partie haute de l'estran. Les flux horaires sont plus élevés à l'air qu'en immersion pour toutes les patelles étudiées. La calcification est effective pendant toute l'année avec des valeurs minimales en l'hiver.

Cette étude démontre que *P. vulgata* est une espèce bien adaptée à la vie intertidale, avec de forts taux respiratoires à l'air. Les flux annuels de carbonate de calcium varient nettement avec la position des animaux sur l'estran. Pour cette raison, la calcification peut s'avérer un paramètre important, limitant la distribution des patelles sur les zones plus hautes de l'estran.

P. vulgata présente des flux de carbone différents selon sa position sur l'estran, ses adaptations métaboliques sont corrélées avec le temps d'exposition à l'air pendant la marée basse.

Aerial and underwater metabolism of *Patella vulgata* L.: Comparison of three intertidal levels.

Morgana Tagliarolo, Jacques Grall, Laurent Chauvaud, Jacques Clavier

2. Introduction

Physical conditions such as temperature, light, oxygen, nutrient availability, salinity and desiccation, as well as biological interactions including predation and competition, lead to vertical zonation of intertidal organisms on rocky shores (Vermeij 1972, Underwood 1973, Boaventura et al. 2002). Most sessile or slow-moving intertidal invertebrates cannot prevent or escape stressful events and must endure extreme environmental events. Limpets (*Patella* spp.) colonise rocky shores throughout the intertidal zone to the lowermost littoral fringe. Along the European Atlantic coasts, *Patella vulgata* L. is a homing limpet whose density increases from the high-water mark to the low-water mark, with a maximum at low-water neaps (Das & Seshappa 1948, Gray & Naylor 1996). The upper limit of the limpet distribution is considered to be restricted by desiccating conditions, temperature variations and osmotic stress (Vermeij 1972, Branch 1981, Alistair 1995). Lower limits are probably set by competition with macroalgae (Boaventura et al. 2002) and possibly by predation (Silva et al. 2008).

P. vulgata is resistant to high temperature up to 43°C (Evans 1948), and can survive for long periods in the atmospheric environment despite considerable water loss (Southward 1958). Previous studies have shown that *P. vulgata* metabolism is affected by environmental temperature, air exposure, and body size (Davies 1967a, Houlihan & Newton 1978, Santini et al. 2000). To avoid desiccation between tides, limpets use a water reservoir that is located in the extra-visceral cavity. Its volume is proportional to shell size (Vermeij 1973); hence, small animals would suffer more desiccation and would be preferentially distributed in the lower shore (Alistair 1995). Such a size gradient within limpet populations would also be maintained by migratory behaviour in response to self-species interactions, foraging, and

space competition patterns (Alistair 1995, Boaventura et al. 2003). Limpets may utilize atmospheric oxygen for respiration at low tide, exposing the mantle cavity directly to the air (Daniel 1982). Aerial respiration in *Patella* spp. is facilitated by external secondary pallial gills (Yonge 1947) that obtain oxygen via diffusion from the air into the water that is held between the body and the shell. Thus, aerial respiration in *P. vulgata* is sufficient to maintain metabolism, and the animal does not use anaerobiosis while emerged (Brinkhoff et al. 1983, Abele et al. 2010).

To date, *Patella* metabolism has been studied mainly through oxygen fluxes or heart rate (Davies 1967a, Branch 1978, Houlihan & Newton 1978, Marshall & McQuaid 1992, Santini et al. 2000), but calcification and CO₂ respiration remain poorly understood. The overall aim of this study was to investigate seasonal carbon metabolism variations and shore-level adaptations of *P. vulgata*. The following questions were addressed: Are respiration rates different in air and in water? What is the influence of seasonal temperature variation on carbon metabolism? Is *P. vulgata* physiologically adapted to different intertidal shore-level conditions? Are calcification and respiration limiting factors influencing the vertical shore distribution of *P. vulgata*?

3. Materials and methods

Sampling

P. vulgata was sampled at low tide from the rocky shore near Brest (Grand Dellec, Plouzané – 48° 21' 09 N, 4° 34' 01 W), France (Fig. 18). Here we use the term “high-shore limpets” to refer to *P. vulgata* collected from the higher distribution limit of the species (6 m above chart datum), “middle-shore limpets” for individuals sampled at mean neap tide high-

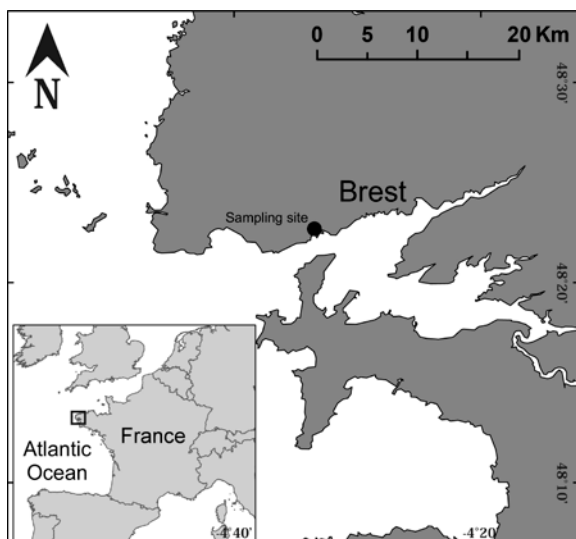


Fig. 18. Sampling site (Grand Dellec, Plouzané) for *P. vulgata* respiration measurements in Western Brittany (France).

water level (4 m above chart datum), and “low-shore limpets” for those collected at spring tide low-water (2 m above chart datum). Sampling was carried out the day before metabolic measurements. Animals of 3-4 cm in shell length (average size recorded in the field, at the sampling site) were gently removed from the rock, examined for suitability (individuals showing signs of injury or bleeding were discarded), then cleaned of epibionts and placed on polyvinyl chloride (PVC) plates. In the laboratory, animals were kept in tanks in which the natural tidal cycle was simulated. For metabolic measurements, 10 PVC supports were placed in 5.7-l bottles with increasing limpet numbers from 0 to 10. At the end of the experiment, the total biomass in each bottle was obtained by drying the limpet flesh at 60 °C for 24 hours and burning it at 450 °C for 4 hours in a muffle furnace. The ash mass was then subtracted from the dry mass to obtain the ash-free dry weight (AFDW). All biomass results are expressed in g AFDW.

Environmental parameters

Air temperature was recorded every hour close to the sampling site, at the Camaret station (Météo France). Sea surface temperature was measured every 20 min by the automated MAREL (Mesures Automatisées en Réseau pour l'Environnement et le Littoral) Iroise buoy (<http://www-iuem.univ-brest.fr/observatoire/marel.php>) near the pumping station that provided the water for our experiments.

Underwater respiration

Underwater respiration was assessed at the same time of high tide experienced in nature. Animals were incubated in the dark for 1-1.5 h in plastic bottles filled with natural filtered seawater directly pumped from the Bay of Brest. In order to maintain a constant temperature that matched the natural conditions, the bottles were immersed in running sea water for the incubation duration. Dissolved inorganic carbon (DIC) concentration was measured in water samples collected from each bottle at the beginning and end of incubation. The pH (total scale) was measured immediately using a pH-meter (Radiometer PH240) standardised with

Tris-HCl (2-amino-2-hydroxymethyl-1,3-propanediol) and 2-amminopyridine/HCl buffer solutions in synthetic seawater with a salinity of 35 part per thousand. Samples for total alkalinity (TA) measurements were filtered through 0.7 µm Whatman GF/F filters and stored in 250-ml bottles in the dark. Analyses were carried out within one week. TA (mmol kg⁻¹) was determined on 20-ml subsamples by Gran automatic potentiometric titration (Radiometer, Titrlab TIM 865) using 0.01 M HCl. Water temperature was measured at the beginning and end of the incubations. Salinity, phosphate concentration and silicate concentrations were provided by SOMLIT (Service d'Observation en Milieu Littoral, INSU-CNRS, Brest, <http://sommLit.epoc.u-bordeaux1.fr/fr/>). The DIC concentration was calculated from the pH, TA, temperature, salinity, phosphate concentrations and silicate concentrations (Pierrot et al. 2006). CO₂ dissociation constants K1 and K2 (Roy et al. 1993) were used in the computation. Underwater respiration in each bottle (R , mmol DIC h⁻¹) was calculated as follows:

$$R = \frac{\Delta DIC \times v}{\Delta t \times 10^3} - G$$

where ΔDIC is the change in the total inorganic carbon concentration (mmol DIC l⁻¹), v is the bottle volume (l), Δt is the incubation time (h), and G is the CaCO₃ flux in a bottle (mmol CaCO₃ h⁻¹).

Calcification

Calcification was estimated during immersion only, using the alkalinity anomaly technique (Smith & Key 1975) based on the observation that TA decreases by two equivalents for each mole of CaCO₃ precipitated. The following equation was utilized to estimate the net calcification rate (G) in a bottle (mmol CaCO₃ h⁻¹):

$$G = \frac{\Delta TA \times v}{2 \times \Delta t}$$

where ΔTA is the variation in TA during incubation (mmol l⁻¹), v is the net bottle volume (l), and Δt is the incubation time (h). Estimation of calcification from alkalinity changes alone may include an error because alkalinity can be influenced by other processes, since nutrient

concentration changes through excretion. Ammonium fluxes were measured in order to calculate the effect of excretion on TA; ammonium resulting from catabolism potentially increases TA by 1 equivalent per mole. We assume that in our short incubation, nitrification process variation was negligible with regard to the TA variation observed in the present study.

Ammonium excretion

The principal excretory product in aquatic molluscs is generally ammonia (Bishop et al. 1983). The rate of ammonia excretion was determined for limpets in summer and winter. Samples of water were taken at the beginning and end of the respiration incubations and were stored in 100-ml bottles. Ammonium concentration was determined according to the phenol-hypochlorite method (Solorzano 1969, Koroleff 1970). Reagents were added to the water immediately after sampling. After 24 h, concentrations were measured at 630 nm (UV-1700 PharmaSpec, UV-VIS spectrophotometer, Shimadzu, Japan) using Milli-Q water as the blank. Linear regressions of ammonia excretion rate versus AFDW were calculated for summer and winter. Ammonium excretion rates are expressed as $\mu\text{mol NH}_4^+ \text{ g AFDW}^{-1} \text{ h}^{-1}$.

Aerial respiration

Aerial respiration was measured during short incubations in an airtight opaque chamber connected via a closed circuit to an infrared gas analyser (Li-Cor, LI 820). In the circuit, an air flow of $0.8/0.9 \text{ l min}^{-1}$ was maintained by an adjustable pump. Air passed through a desiccation column filled with anhydrous calcium sulphate (Drierite, Xenia, USA). Experiments were conducted in a climatic room at the same time as during low tide experienced in nature. The indoor air in the climatic room was controlled by an aeration system directly connected with the exterior. Since laboratory is located near coastal zone the air temperature and humidity in the climatic chamber was similar to what is found in natural environment. Variations in CO_2 partial pressure (pCO_2 ; in parts per million, ppm = $\mu\text{mol CO}_2 \text{ mol air}^{-1}$) were displayed on a laptop computer and recorded at 5 s intervals for approximately 3 min. CO_2 fluxes, air temperature, and relative humidity (RH) (T200 thermo-hygrometer,

Trotec, Heinsberg, Germany) were measured every hour during emersion for the ten samples, and the control sample without limpet. Fluxes in the air correspond to the linear slope of the change in pCO₂ over time during the incubation period. Flux values were corrected for the net volume of the enclosure and the incubation time.

Data analysis

Since both fluxes and biomasses were affected by natural variability, a functional regression analysis was used to relate aerial, underwater, and calcification fluxes and AFDW biomass. CO₂ and DIC fluxes were expressed per gram biomass (mmol CO₂ or DIC g AFDW⁻¹ h⁻¹). The effect of temperature on the respiration rates of limpets in emersion and immersion was assessed through Arrhenius plots that displayed the logarithm of flux plotted against the inverse of temperature:

$$\ln Flux = \ln a - \frac{E_a}{k} \times \frac{1}{T}$$

where *Flux* is the respiration rate (Δ DIC underwater or Δ CO₂ in the air, mmol g AFDW⁻¹ h⁻¹), *a* is a normalization constant, *E_a* is the activation energy (J mole⁻¹), *k* is Boltzmann's constant (8.31 J K⁻¹ mol⁻¹), and *T* is the absolute temperature (K). Analysis of variance (ANOVA) was used to compare the slopes and intercepts of the linearised Arrhenius plots (Sokal & Rohlf 1981). If the slopes were not significantly different, the relationships between respiration rate and temperature were compared between shore levels using an analysis of covariance (ANCOVA) followed by the *post-hoc* honestly significant difference (HSD) Tukey test for samples of different sizes (Zar 2010). If data were not normally distributed, the non-parametric Kruskal-Wallis test was used. Daily fluxes were calculated for the average sea level during neap and spring tide conditions. We considered a 6-h period of aerial respiration for middle and high-shore limpets but a 3-h period for low-shore limpets, as they were emerged in nature for a maximum of three consecutive hours. To estimate CO₂ fluxes on an annual scale, average contributions were calculated for aerial and underwater mean annual temperatures. Water height was calculated every 15 min according to SHOM (Service Hydrographique et Océanographique de la Marine) tide tables. For each studied level, annual

CO_2 emissions were calculated by multiplying average hourly CO_2 fluxes in air for average emersion time and multiplying average hourly underwater and calcification fluxes for average immersion time of each studied level.

4. Results

Environmental parameters

During the study period (2010 and 2011), monthly mean temperatures of the sea surface and air ranged from 8-17 °C and from 6-17°C, respectively (Fig. 19). The average temperatures during the study period were 12 °C in the air and 13 °C in water at the sea surface. The average annual temperatures were slightly lower in 2010 (11 °C in air and 13 °C at the sea surface) than in 2011 (13 °C in air and 13 °C at the sea surface).

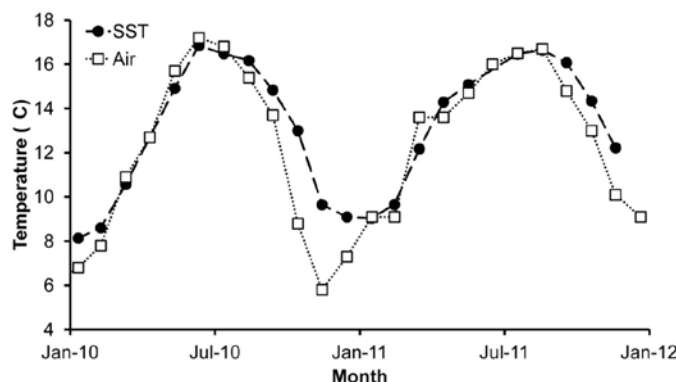


Fig. 19. Monthly variation in mean sea surface temperature (SST) (MAREL Iroise buoy) and air temperature (Air) (Météo France, Camaret station) in the study area from 2010 to 2012.

Ammonium excretion

Ammonium fluxes were measured in summer and winter for high and low-shore limpets, and only in winter for middle-shore limpets. The range of fluxes was larger during summer (2.2-0.7 $\mu\text{mol NH}_4^+ \text{ g AFDW}^{-1} \text{ h}^{-1}$) than in

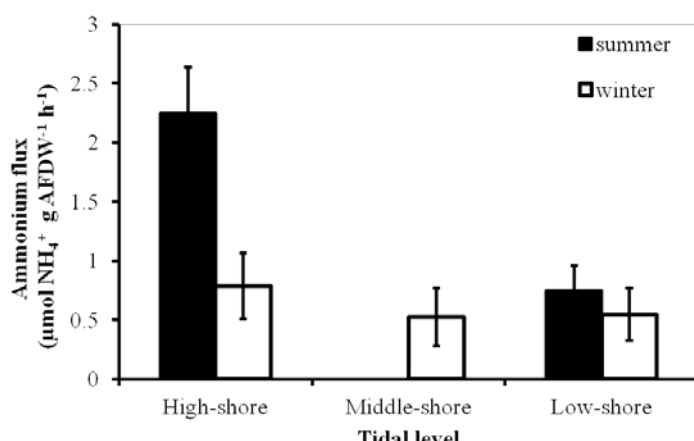


Fig. 20. *P. vulgata* ammonium excretion rates (mean \pm standard deviation, $n=10$) during summer and winter, at three tidal levels.

winter ($0.7\text{--}0.5 \mu\text{mol NH}_4^+ \text{ g AFDW}^{-1} \text{ h}^{-1}$) (Fig. 20). Excretion by high-shore limpets was significantly higher in summer than in winter (ANOVA, $p < 0.01$). Limpets from all three levels exhibited similar fluxes during the winter period (ANOVA, $p > 0.05$).

An average NH_4^+ flux was used to correct TA for measurements of low and middle-shore limpets. For high-shore limpets, calcification fluxes were obtained by correction with summer and winter ammonium values, while spring and autumn analyses were corrected with average NH_4^+ rates. For middle and low-shore animals, TA was corrected with average excretion values.

Calcification

Net calcification was positive, with CaCO_3 deposition occurring throughout the year; minimal values were recorded in winter (Fig. 21). During the study period, the average CaCO_3 deposition in immersion was stronger for high-shore limpets ($4.6 \mu\text{mol CaCO}_3 \text{ g AFDW}^{-1} \text{ h}^{-1}$) and lower for middle and low-shore limpets ($3.2 \mu\text{mol CaCO}_3 \text{ g AFDW}^{-1} \text{ h}^{-1}$ and $3.4 \mu\text{mol CaCO}_3 \text{ g AFDW}^{-1} \text{ h}^{-1}$, respectively). However, the differences between the three levels were not significant (Kruskal-Wallis, $p > 0.05$).

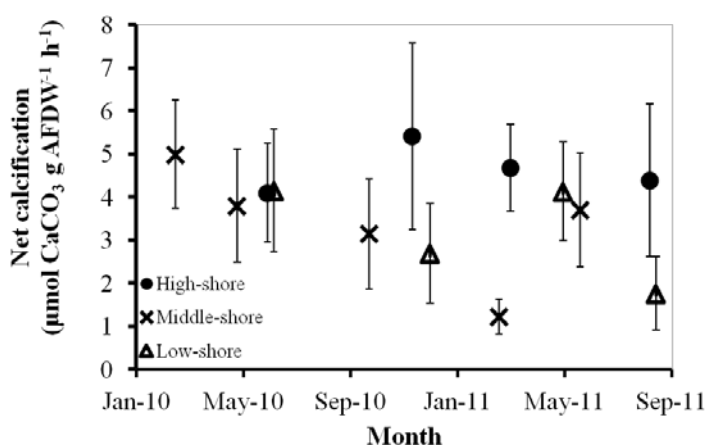


Fig. 21. Seasonal variation in *P. vulgata* net calcification rate (mean \pm standard deviation, $n=10$) at three tidal levels. Positive values correspond to calcification.

Daily net calcification fluxes were calculated for spring and neap tide conditions. During spring tide, net calcification fluxes were lower for high-shore limpets that were immersed for only 4 h d^{-1} ($0.02 \text{ mmol CaCO}_3 \text{ g AFDW}^{-1} \text{ d}^{-1}$), and higher for middle and low-shore limpets (0.04 and $0.06 \text{ mmol CaCO}_3 \text{ g AFDW}^{-1} \text{ d}^{-1}$, respectively). In neap tide conditions, high limpets were

never immersed. Middle and low-shore limpets showed calcification rates of 0.04 mmol CaCO₃ g AFDW⁻¹ d⁻¹ and 0.08 mmol CaCO₃ g AFDW⁻¹ d⁻¹, respectively.

Underwater respiration

Seasonal variations in underwater respiration were similar for the three studied levels, with minimum fluxes in winter (Fig. 22). Arrhenius plots indicated that metabolism during immersion increased with temperature from 9 °C to 18 °C. The high percentage of variance explained by the relationship indicates that temperature is a good proxy for underwater respiration (Tab. 2). Average respiration rates were slightly higher for low-shore limpets (12.9 μmol DIC g AFDW⁻¹ h⁻¹) than for high and middle-shore limpets (7.8 and 8.1 μmol DIC g AFDW⁻¹ h⁻¹, respectively). Differences between Arrhenius plot demonstrate that the three levels were significantly different (ANCOVA, p < 0.01), but only the respiration rate of low-shore limpets differed significantly from the others (HSD Tukey test, p < 0.01).

If we consider the time of immersion for each shore level, the calculated spring tide daily respiration fluxes for the mean annual temperature (13 °C) were 0.03 mmol DIC g AFDW⁻¹ d⁻¹ for high-shore limpets, 0.09 mmol DIC g AFDW⁻¹ d⁻¹ for middle-shore limpets and 0.20 mmol DIC g AFDW⁻¹ d⁻¹ for low-shore limpets. During neap tide, the high-shore limpets were never immersed. The underwater respiration rates for middle and low-shore limpets were 0.09 and 0.27 mmol DIC g AFDW⁻¹ d⁻¹, respectively.

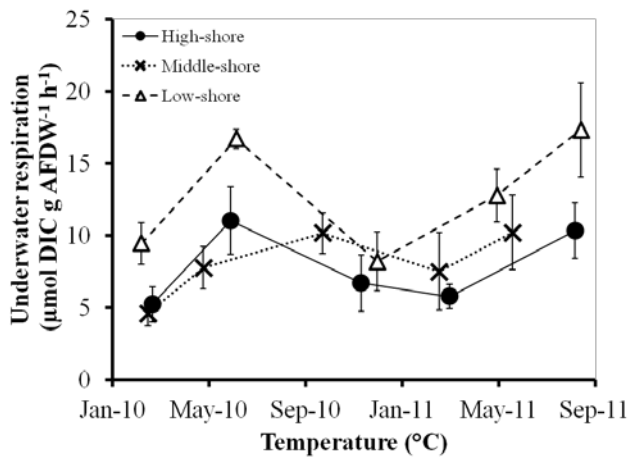


Fig. 22. Relationships between hourly underwater *P. vulgata* respiration (DIC) rates per g AFDW and temperature (mean ± standard deviation, n=10), at three tidal levels.

Tab. 2. Parameters of Arrhenius plots relating the logarithm of hourly underwater and aerial respiration rates of *P. vulgata* per g AFDW to the inverse of absolute temperature, at three tidal levels. a, normalization constant; Ea, activation energy (Joules per mole); K, Boltzmann's constant (8.31 JK⁻¹ mol⁻¹); R², coefficient of determination.

	Underwater			Air		
	High	Middle	Low	High	Middle	Low
Ln a	31.71	34.41	26.25	12.52	11.82	14.67
- E_a/K	-8.53	-9.27	-6.82	-2.83	-2.55	-3.36
R²	0.94	0.79	0.90	0.96	0.81	0.97

Aerial respiration

P. vulgata aerial CO₂ fluxes were influenced by temperature and RH conditions (Fig. 23). The respiration rates of high and middle-shore limpets were stable during a 6-h of aerial exposure when the temperature was below 30 °C (Fig. 23 a & b). Conversely, the aerial respiration rate of low-shore limpets was generally highest during the first hour of aerial exposure and decreased over the duration of low tide period (Fig. 23 c). Aerial respiration of *P. vulgata* increased with temperature from 7 °C to 35 °C (Fig. 24). Minimal respiration (8.9 µmol CO₂ g AFDW⁻¹ h⁻¹) was recorded for high-shore limpets at 7 °C and 90% RH. Low-shore limpets underwent maximal respiration (51.6 µmol CO₂ g AFDW⁻¹ h⁻¹) at 28 °C and 48% RH. Arrhenius plots demonstrate that a high percentage of variance was explained by temperature for all limpets studied (Tab. 2). Mean carbon aerial rates were 16.3 µmol CO₂ g AFDW⁻¹ h⁻¹ for high-shore limpets, 21.5 µmol CO₂ g AFDW⁻¹ h⁻¹ for middle-shore limpets and 24.8 µmol CO₂ g AFDW⁻¹ h⁻¹ for low-shore limpets. The Arrhenius plots significantly differed among the three levels (ANCOVA, p<0.01), but only high-shore limpets were significantly different from the other groups (HSD Tukey test, p < 0.01).

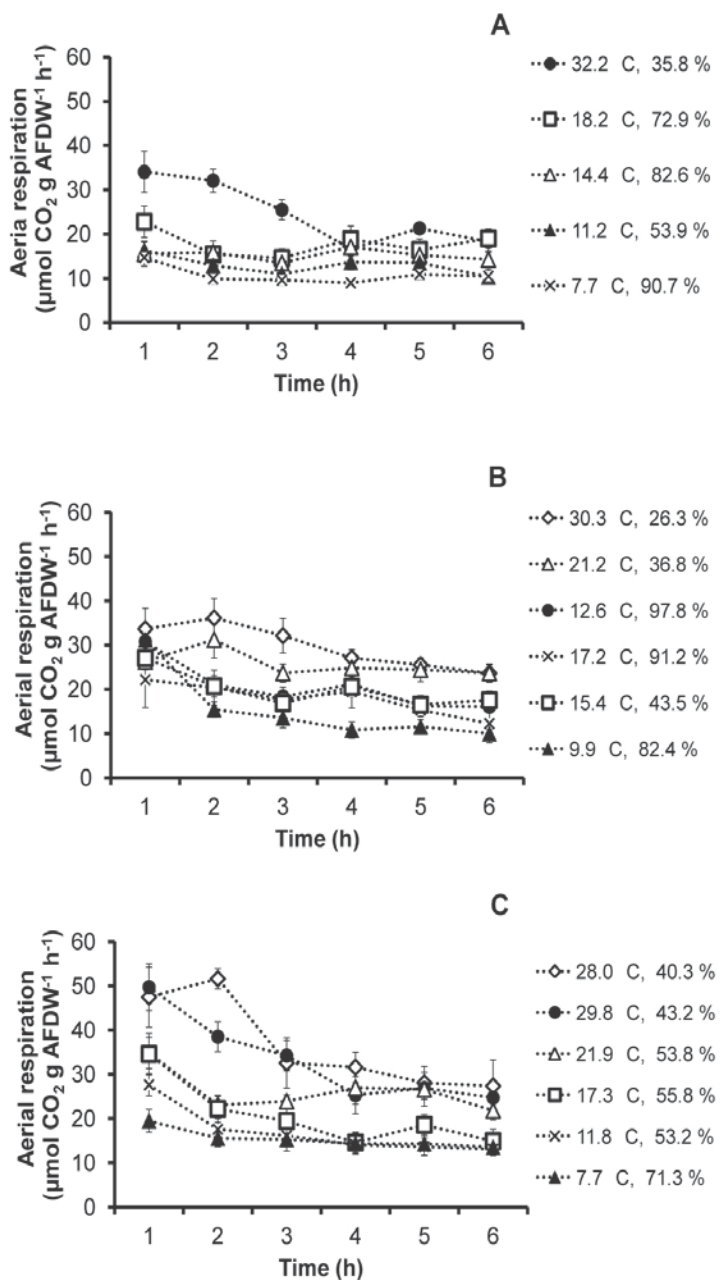


Fig. 23. Variation in aerial respiration rates of *P. vulgaris* during low tide at different temperatures (°C) and RH (%), as estimated from the variation in CO₂ concentration in incubation chambers at three tidal levels (a, high-shore; b, middle-shore; c, low-shore).

Spring tide daily fluxes were 0.28 mmol CO₂ g AFDW⁻¹ d⁻¹ for high-shore limpets, 0.22 mmol CO₂ g AFDW⁻¹ d⁻¹ for middle-shore limpets and 0.13 mmol CO₂ g AFDW⁻¹ d⁻¹ for low-shore limpets. During neap tides, low-shore limpets were never emerged. The aerial

respiration rates of middle and high-shore limpets were 0.22 and 0.33 mmol CO₂ g AFDW⁻¹ d⁻¹, respectively.

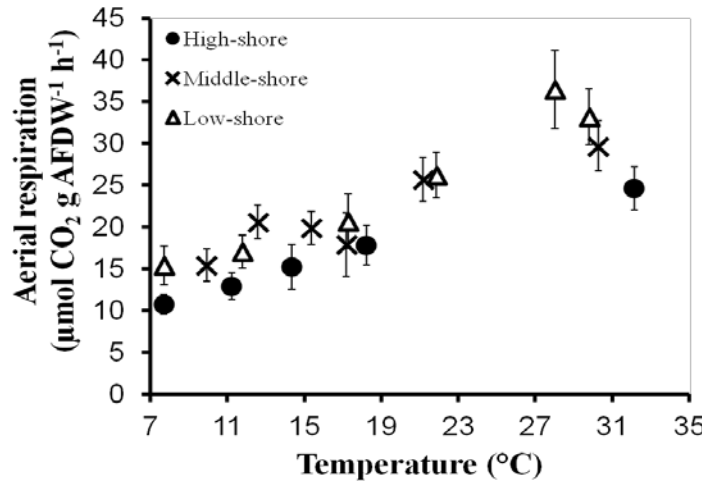


Fig. 24. Relationships between hourly aerial *P. vulgata* respiration rates per g AFDW, and temperature at three tidal levels (mean \pm standard deviation, n=10).

Respiration was higher during emersion than during submersion for all limpets and temperatures tested (Fig. 25). The Arrhenius plots for aerial and underwater respirations were significantly different both for slopes and intercept (ANOVA, p<0.05).

Annual carbon budget

Annual immersion and emersion times were calculated for each shore level. High-shore limpets spent the equivalent of 27 d y⁻¹ underwater, middle-shore limpets were immersed for a time equivalent to 170 d y⁻¹, and low-shore limpets were immersed for an equivalent of 317 d y⁻¹. The mean annual carbon emission was estimated at 120 mmol C g AFDW⁻¹ y⁻¹ for high-shore limpets, 130 mmol C g AFDW⁻¹ y⁻¹ for middle-shore limpets and 134 mmol C g AFDW⁻¹ y⁻¹ for low-shore limpets. The aerial respiration was the predominant part of total annual carbon emissions for high-shore and middle-shore limpets. The emissions from low-shore limpets were more constituted by underwater respiration (Tab. 3).

Tab. 3. *P. vulgata* aerial, underwater, and calcification carbon contributions (%) to total annual carbon emissions, at three tidal levels.

Tidal shore	% Air	% Underwater	% Calcification
High	94	4	2
Middle	65	24	11
Low	18	64	18

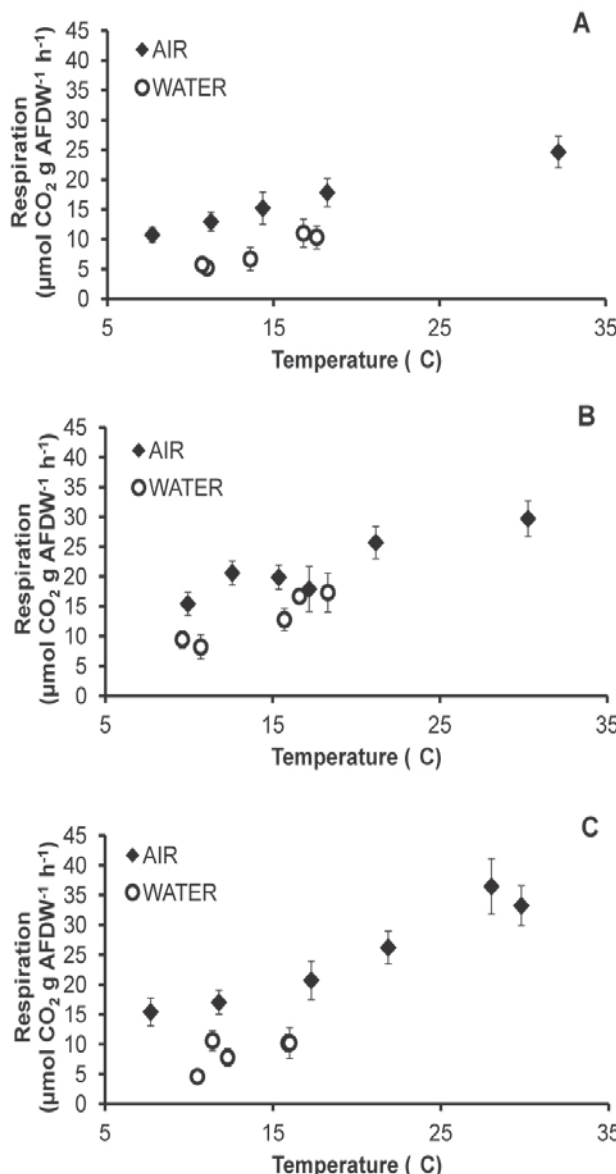


Fig. 25. Evolution of hourly underwater and aerial carbon respiration rates of *P. vulgata* per g AFDW (\pm standard deviation, $n=10$) at three tidal levels (a, high-shore; b, middle-shore; c, low-shore).

5. Discussion

Calcification and ammonium excretion

Invertebrate nitrogen excretion rates vary over tidal and seasonal cycles as a result of changes in food supply (Denny & Gaines 2007). Our results showed that excretion was maximal during summer and that high-shore limpets had stronger fluxes per biomass unit than middle-shore and low-shore limpets. Differences in ammonium excretion between sites and seasons may be related to temporal variations in food availability and quality (Clarke 1990, Obermüller et al. 2011). Previous measurements of ammonium concentration in *P. cochlear* during low tide demonstrated accumulation of

nitrogenous excretion under the shell rim (Plagányi & Branch 2000). Ammonium release during the initial period of immersion may thus be more important for limpets that spend more time in air and accumulate more waste products. This accumulation may explain our observation of higher NH_4^+ fluxes at the high-shore level.

As ammonium excretion potentially increases total alkalinity, TA fluxes were corrected with ammonium rates for the three shore levels. Ammonium correction increased the calculated values of CaCO_3 flux by an average of 7%. This study confirms that the ammonium effect is much smaller than the variation observed between calcification flux measurements (Jacques & Pilson 1980, Chisholm & Gattuso 1991, Gazeau et al. 2007).

Invertebrate carbonate deposition in mollusc shells is marked by annual variations attributed to a variety of causes, including temperature, food supply and reproductive processes (Pannella & MacClintock 1968, Lutz & Clark 1984). Generally, calcification would be minimal during winter low temperatures, whereas during summer, temperature and food supply increases would accompany an increase in calcification. Our observations agree with previous studies dealing with *Patella* spp. growth rates, which showed seasonal variations with temperature; higher levels were observed during warmer periods and lower rates occurred during winter (Blackmore 1969, Fenger et al. 2007).

Isotopic studies have indicated that intertidal air-breathing aquatic molluscs gain the carbon of their carbonates from respired CO_2 and from ambient DIC, resulting in a shell carbon composition that is intermediate between land and aquatic snails (McConaughey & Gillikin 2008). In this investigation we showed that while hourly carbonate fluxes were similar for the three tidal levels, daily and annual CaCO_3 deposition rates were lower for high-shore limpets. Growth increment is known to be controlled by tides in various intertidal mollusc species (Pannella & MacClintock 1968, Schöne et al. 2007). Sclerochronologic studies reported semidiurnal and lunar daily microgrowth increments in *P. vulgata* shells that were controlled by tide (Fenger et al. 2007). Our lower calcification rates for high-shore levels may due to calcification reduction or cessation during low-tide air exposure, probably limited by calcium reserves (Bourget & Crisp 1975).

Underwater and aerial respiration

The aerial and underwater metabolic activities of limpets have been previously studied via measurements of oxygen consumption or cardiac activity, either in the laboratory or in the field (Branch 1978, Newell 1979, Marshall & McQuaid 1992, Santini et al. 2000). The present study is the first to evaluate limpet carbon metabolism both in air and underwater. Limpets of similar size were maintained in the laboratory under tidal conditions equivalent to natural conditions, and thus our results are fully comparable across the three shore levels.

Arrhenius plots showed high correlation coefficients of respiration fluxes versus temperature for all limpet groups. The differences in *P. vulgata* metabolism between seasons were related to temperature variations and were similar at the three shore levels. Previous studies have already showed seasonal differences in *P. vulgata* activity probably related to temperature variations, food availability and reproduction period (Della Santina et al. 1995, Santini et al. 2004, Ribeiro et al. 2009).

Limpets show a wide range of feeding times that varies from locality to locality in response to tidal, day/night cycle and topography of rocky surface (Hawkins & Hartnoll 1982, Hawkins & Hartnoll 1983, Little 1989). *P. vulgata* foraging activity is minimal during day-time low tide to avoid the influence of desiccation and bird predation and during night-time high tide since crabs are mainly active at night (Hartnoll & Wright 1977, Little 1989). Our measurements were performed during day-time and animals were generally active during underwater incubation and during the first hour aerial exposure during low tide even although food was not present.

Aerial fluxes were generally higher during the first hours of aerial exposure, especially for low-shore limpets exposed to high temperature. In natural conditions, low-shore limpets are exposed to air for a maximum of three consecutive hours; therefore emersion stress related to desiccation is less important at low-shore levels than at higher levels, and limpet activity is promoted during emersion. We established that aerial respiration was significantly lower for high-shore limpets and that underwater daily respiration was stronger for low-shore limpets that spent more time immersed. Previous studies agree with our results in that metabolic rates appear to be lower in high-shore individuals than in low-level individuals from the same

limpet species (Segal 1956, Davies 1967b, White 1968). Individuals in higher intertidal zones are often inactive during emersion to reduce desiccation, thus limiting feeding times (Marshall & McQuaid 1991). Living in a highly variable environment incurs higher physiological costs for thermal adjustment and metabolic processes (Somero 2002). Depression of metabolism and implementation of energy-conserving mechanisms are important for the survival of high intertidal species (Marshall & McQuaid 1991).

Conflicting results have been described for aerial and aquatic O₂ consumption by *P. vulgata*. Previous reports have included maximal metabolic rates during air exposure (Houlihan & Newton 1978) and during submersion (Wright & Hartnoll 1981, Santini et al. 2000). In *P. granatina* aerial and underwater O₂ respiration rates were size-dependent; small animals respire faster in water while large animals respire faster in air (Branch 1978). In the present study, *P. vulgata* carbon respiration was higher in air than in water for the three shore levels studied. As previously reported, limpets appeared to be able to respire in air, therefore maintaining movement and feeding activity during low tide (Branch 1978, Abele et al. 2010). The grazing behaviour in *P. vulgata* is known to be highly variable between populations, a strategy that would minimize predation and limit desiccation, inducing activity to high tide or night time (Little et al. 2009). An active vertical migration pattern may explain why even limpets living in the lower zone are well adapted for aerial respiration.

Carbon budget

Annual limpet respiration was influenced by living position in the intertidal zone, with maximal carbon emission occurring for middle-shore limpets. The aerial contribution was predominant in the annual carbon budget for high-shore limpets but not for individuals collected at low-shore level, where underwater respiration was more important. The aerial, underwater, and calcification carbon contributions of middle-shore limpets (65%, 24%, and 11%, respectively) were similar to those reported for other intertidal organisms: 61%, 36%, and 3% respectively for *Chthamalus montagui* (Clavier et al. 2009) and 71%, 4%, and 25% respectively for *Crassostrea gigas* (Lejart et al. 2012). The relative contribution of annual calcification was important only in the low intertidal zone. These observations demonstrate

that calcification may be an important influence on vertical distribution. CaCO_3 availability may limit shell growth for aquatic animals living in higher shore levels, and thus the distribution of small limpets would be limited at the lower shore level not only by desiccation tolerance but also by shell-growth requirements. Large limpets with slower growth rates would be less influenced by CaCO_3 limitation and would actively migrate to a higher shore level, maintaining the size gradient in the intertidal zone (Alistair 1995).

Aerial and underwater results were similar for middle-shore and low-shore limpets, but high-shore limpets exhibited different metabolic adaptations that permit individuals to better tolerate stronger environmental variations. Various hypotheses may explain the benefit of upward vertical movements by limpets, including access to unexploited food sources (Little 1989, Alistair 1995), avoidance of interspecific competition (Espinosa et al. 2006), and escape to lower densities of organisms (Iwasaki 1999).

P. vulgata is a keystone species largely distributed along the northeast Atlantic coasts. This study evaluated the metabolic responses of *P. vulgata* coming from a single sampling site and submitted to similar environmental conditions. Further studies will be required at different location in order to better understand the physiological plasticity and local adaptation of this species. This study demonstrates that *P. vulgata* is well adapted to aerial exposure with respiration rates higher in air than underwater. Both aerial and underwater metabolisms are influenced by seasons and increase with temperature. The calcification process seems to be an important factor limiting the distributions of high-shore limpets. CO_2 release is strongly dependent on animal position in the intertidal zone. Further community contribution analyses should consider flux differences along the tidal zone due to different aerial exposure times and metabolic adaptations of the organisms.

Chapitre 3

Respiration et calcification comparées de neuf espèces de gastéropodes intertidaux.



Fig. 26. Photos de quelques espèces de gastéropode étudié. (*O. lineatus* ; *L. littorea* ; *N. lapillus* ; *G. magus* ; *G. umbilicalis* ; *L. saxatilis*).

1. Contexte général et résumé

La majorité des plantes et animaux vivant en zone intertidale sont d'origine marine. La zone de balancement des marées est un milieu instable où la vie est rendue possible par les capacités des différents organismes à tolérer les stress physiques (Vermeij 1972, Raffaelli & Hawkins 1999). Les effets concomitants des facteurs physiques et biologiques contrôlent la distribution verticale des animaux sur les estrans rocheux et créent des zonations par bandes horizontales (Underwood 1973, Little 1990). Les gastéropodes sont parmi les animaux les plus largement répandus sur les estrans rocheux dont ils peuvent coloniser tous les niveaux (Little 1983). La plasticité de ce groupe leur permet de s'adapter à des conditions variables et de résister aux stress environnementaux. Les stratégies de reproduction varient de la production d'œufs planctoniques comme pour *L. littorea* (Reid 1996) à l'ovoviviparité pour *L. saxatilis* (Conde-Padín et al. 2008). La forme de la coquille peut être très différente avec une tendance au développement de sculptures externes et à l'augmentation de la hauteur relative des spires pour les espèces vivant vers le haut de l'estran (Vermeij 1973). Les organes respiratoires peuvent être modifiés pour permettre une respiration à l'air plus efficace. Les espèces vivant sur les zones les plus hautes, comme *M. neritoides*, montrent ainsi une réduction des branchies et une augmentation de l'épithélium vasculaire (McMahon 1990).

La consommation en oxygène des gastéropodes intertidaux est généralement différente à l'air et sous l'eau. De nombreuses études ont comparé leur respiration aquatique et aérienne mais les résultats sont parfois discordants (Sandison 1966, McMahon & Russel-Hunter 1977, Houlihan 1979). Même si la différence entre la consommation d'oxygène en émersion et en immersion peut être liée à la position de l'espèce sur l'estran (Houlihan & Innes 1982), cette relation n'est pas générale pour tous les gastéropodes (Sandison 1966, Branch & Newell 1978). Les taux de respiration sont aussi influencés par la température et la disponibilité de nourriture (Branch 1981). Les littorines par exemple sont capables de réguler leur taux respiratoire en fonction de la température et de réduire leur métabolisme quand elles sont exposées à des températures très hautes (McMahon 1990). L'exposition à l'air sur des longues périodes peut aussi amener une réduction des flux respiratoires afin de limiter les pertes d'eau et d'éviter la déshydratation (McMahon 1988).

Dans ce contexte, l'objectif de ce chapitre est de comparer le métabolisme de neuf espèces de gastéropodes intertidaux vivant à différents niveaux de l'estran rocheux. L'influence de la variation de température saisonnière sur la calcification et la respiration à l'air et sous l'eau a été testé pour chaque espèce.

Les espèces choisies ont des caractéristiques très différentes en taille, régime alimentaire, techniques de reproduction et zone de répartition (Fig. 26).

Melarhaphe neritoides est l'espèce qui vit le plus haut sur l'estran et elle est capable de survivre à plusieurs mois d'exposition à l'air (Fraenkel 1961). Les populations sont formées de groupes parfois très denses où les individus se protègent du soleil et des prédateurs dans les failles des rochers (Fraenkel 1961).

Littorina saxatilis est aussi très résistante à la déshydratation et peut rester à l'air pendant plusieurs jours (Raffaelli & Hawkins 1999). Cette espèce peut supporter des températures très hautes (plus de 47°C) et, à l'inverse, survivre à des températures négatives (Bourget 1983, Sokolova et al. 2000).

Osilinus lineatus vit dans la zone médiolittorale supérieure et la zone supralittorale. Ces gastéropodes sont actifs pendant la marée basse et des adaptations à la respiration aérienne ont été décrites chez plusieurs espèces du genre (Micallef & Bannister 1967, Little 1989).

Gibbula umbilicalis est caractéristique de la zone médiolittorale. Cette espèce supporte les variations de température typiques de la zone intertidale grâce à sa capacité à modifier son taux d'activité en fonction de la température de l'air et de l'eau (Cornelius 1972).

Littorina littorea est rencontré en infralittoral et en médiolittoral. Ces gastéropodes peuvent rester actifs pendant la marée basse lorsque le substrat est encore humide et peuvent tolérer des températures de 40°C pendant 1 à 2 heures (Fraenkel 1961).

Nucella lapillus est la seule espèce de prédateur étudiée ; il se nourrit surtout de moules et de balanes. Le processus de prédation et de digestion peut durer plusieurs jours et être suivi par des périodes de repos (Little et al. 2009).

Gibbula pennanti, *Gibbula cineraria* et *Gibbula magus* sont les trois espèces étudiées qui vivent le plus bas sur la zone intertidale ; elles habitent également la zone subtidale (Graham 1988).

Pour chaque espèce étudiée, la respiration en émersion et en immersion à été mesurée en laboratoire dans des conditions de température identiques à celles de l'environnement naturel. De cette façon, nous avons pu évaluer les variations saisonnières des flux de carbone et comparer les différentes espèces.

La respiration à l'air et sous l'eau étaient similaires pour tous les gastéropodes étudiés et l'influence des variations de température sur les flux était maximale en immersion. Le calcul des flux annuels de carbone nous a permis de quantifier la contribution de chaque espèce en fonction de son temps d'émersion/immersion moyen. Le processus de calcification s'est avéré relativement important avec une contribution moyenne de 21% aux flux totaux de carbone.

Cette étude démontre que la respiration des gastéropodes intertidaux n'est pas directement corrélée à leur position sur l'estran mais que la taille moyenne des espèces semble être le paramètre le plus important pour expliquer les différences interspécifiques de respiration.

Calcification and respiratory rates of nine gastropod species from the intertidal rocky shore of Western Europe.

Morgana Tagliarolo, Jacques Clavier, Laurent Chauvaud, Jacques Grall

2. Introduction

The intertidal area is a transitional zone from fully marine to terrestrial conditions, characterized by increasing physical stresses (e.g., desiccation, and variations in temperature and salinity) from low to high-shore levels (Vermeij 1972). Numerous investigations have described zonation patterns of intertidal animals, with their vertical distribution along the shore varying according to local conditions and their general behavior (Underwood 1973). Sessile animals such as barnacle exhibit stable vertical zonation, whereas foraging for food or reproductive behaviour can modify distribution patterns of mobile animals such as snails at different time scales (Newell 1979). During low tide, desiccation and temperature stresses can strongly influence metabolism regulation (Sokolova & Portner 2001). Thermal stresses can also create significant energetic costs to the organism, partly explaining the vertical pattern distribution along the intertidal gradient (Somero 2002). For these reasons, intertidal organisms have adopted different morphological, behavioral, physiological, and metabolic adaptations. Very few marine species have successfully adapted to high levels on rocky shore; the most common are gastropods, the class of mollusks that include species living in the terrestrial environment (Little 1983). Intertidal gastropods are alternately exposed to aerial and aquatic conditions; they are thus adapted for respiration both in air and underwater (McMahon & Russel-Hunter 1977). Intertidal animals that can breathe in air may reduce respiration as desiccation progresses, in order to trade-off evaporative water losses (Houlihan 1979).

The literature only contains a few comparative metabolic studies on intertidal aquatic gastropods; these studies have involved few species, and most measurements have focused only on oxygen consumption. The intertidal carbon metabolism related to both aerobic and anaerobic respiration associated with calcification is yet poorly known. Previous studies comparing rocky shore invertebrate vertical distributions and aerial/aquatic respiration ratios

have displayed different and even contradictory results. Some authors have reported that a greater degree of aerial exposure is directly related to gastropod oxygen consumption in air compared with water (McMahon & Russel-Hunter 1977, Houlihan 1979); however, it appears that not all gastropods exhibit such a relationship (Sandison 1966, Branch & Newell 1978, McMahon 1990). Several studies have concluded that intertidal gastropods show strong ability to acute short-time thermoregulation of their metabolic rate through a metabolic-depressed physiology at high temperature. However, they show low ability for long-term metabolic temperature compensation, which could prevent energetically wasteful elevation of the metabolic rate during stronger warming on tidal emersion (Newell 1973, McMahon & Russel-Hunter 1977, McMahon et al. 1995, Marshall et al. 2011). It has been suggested that aerial respiration may also be influenced by the loss of mantle cavity fluid that is fundamental for maintaining gas exchanges in gill-breathing species (Houlihan 1979, Houlihan & Innes 1982).

Although intertidal species are more thermotolerant than subtidal animals, they live closer to their physiological temperature limits and have limited ability to adjust their metabolism. For these reasons, intertidal species seem more vulnerable to climate change and may serve as an early warning system for indicators of climate change (Harley et al. 2006, Helmuth et al. 2006). In the present study, we examined gastropod species that are widely distributed on rocky shore of Western Europe, with the aim of testing the influences of seasonal variations and tidal level on carbon metabolism related to calcification and both aerobic and anaerobic respiration. We investigated 1) the variation in respiration of the different species during emersion and submersion, 2) the influence of seasonal temperature variations on carbon metabolism, 3) whether calcification was influenced by height position on the shore, 4) and finally whether high intertidal species respire better in air than low-shore and shallow subtidal species.

3. Materials and methods

Sampling

Specimens of nine species of marine intertidal gastropods [*Melarhaphe neritoides* (L.), *Littorina saxatilis* (Olivi), *Osilinus lineatus* (da Costa), *Gibbula umbilicalis* (da Costa),

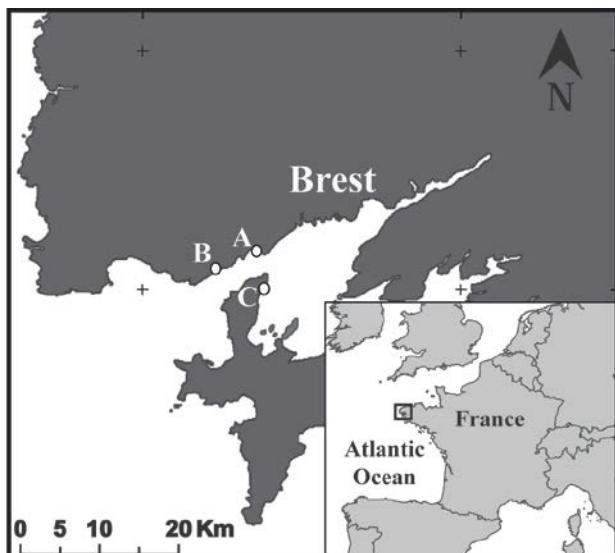


Fig. 27. Sampling sites for gastropods collection in Western Brittany (France) (A: *L. littorea*, *G. umbilicalis*; B: *M. neritoides*, *L. saxatilis*, *O. lineatus*, *G. cineraria*, *G. pennanti*, *N. lapillus*; C: *G. magus*).

Littorina littorea (L.), *Nucella lapillus* (L.), *Gibbula pennanti* (Philippi), *Gibbula cineraria* (L.), and *Gibbula magus* (L.)] were collected at low tide from rocky shore areas near Brest, France (Fig. 27). For each species, animals of similar size (in term of shell height) with few epibionts were sampled and kept in the laboratory in plastic cages equipped with polyvinyl chloride supports. Ten cages containing 1 to 10 individuals were maintained in tanks where the natural tidal cycle was simulated. Measurements were performed the day after sampling, and after metabolic experiments, the total biomass in each cage

was obtained by drying snails at 60°C for 24 hours and subsequent calcinations at 450°C for 4 hours in a muffle furnace. The ash mass was then subtracted from the dry mass to obtain the ash-free dry weight (AFDW). All biomass results are expressed in g AFDW. For each species, average size (height of the shell) was measured to the nearest 0.01 mm with a hand vernier caliper.

Aerial respiration

At low tide time, i.e. when natural populations were emerged, animals were placed on a glass table in a climatic room. The indoor air in the climatic room was controlled by an aeration system directly connected with the exterior. Since the laboratory is located by the seaside the air temperature and humidity in the climatic chamber was the same to what is found in natural environment. Animals were placed in an airtight opaque chamber connected via a closed circuit to an infrared gas analyzer (Li-Cor, LI 820) (Migné et al. 2002). Air passed through a desiccation column filled with anhydrous calcium sulphate (Drierite, Xenia, USA) and the circuit flow was maintained at of 0.8/0.9 l min⁻¹ by an adjustable pump. Measures of CO₂ partial pressure variations (pCO₂) were displayed in parts per million, ppm

= $\mu\text{mol CO}_2 \text{ mol air}^{-1}$ on a laptop computer, and recorded at 5-s intervals for approximately 3 min. CO_2 fluxes of the ten samples and the control with an empty chamber were measured every hour during the six hours of low tide. Fluxes in the air corresponded to the linear slope of the change in pCO_2 over time during the incubation period. Flux values were corrected for the net volume of the enclosure and the incubation time. Air temperature and relative humidity were measured hourly (T200 thermo-hygrometer, Trotec, Heinsberg, Germany).

Underwater respiration and calcification

Underwater respiration and calcification were assessed in the laboratory from 1–1.5 h incubations that were conducted during natural high tide. The ten samples and a control without animal were incubated in plastic bottles filled with natural filtered seawater directly pumped from the Bay of Brest. Incubations were performed in the dark, and bottles were kept immersed in running sea water to maintain constant conditions. The dissolved inorganic carbon (DIC) concentration was calculated from the pH, total alkalinity (TA), temperature, salinity, and phosphate and silicate concentrations (Pierrot et al. 2006). The CO_2 dissociation constants K1 and K2 (Roy et al. 1993) were used in the computation. Calcification was estimated using the alkalinity anomaly technique (Smith & Key 1975) based on the observation that TA decreases by two equivalents for each mole of CaCO_3 precipitated. At the beginning and end of incubation, pH, temperature, and TA were measured for water samples from each bottle. The pH (total scale) was measured using a pH meter (Radiometer PH240) standardized with Tris-HCl (2-amino-2-hydroxymethyl-1,3-propanediol) and 2-amminopyridine/HCl buffer solutions in synthetic seawater with a salinity of 35. Samples for TA measurements were filtered through 0.7- μm Whatman GF/F filters and stored in 250-ml bottles in the dark. Analyses were performed within one week. TA (mmol kg^{-1}) was determined for 20-ml subsamples by Gran automatic potentiometric titration (Radiometer, Titrlab TIM 865) using 0.01 M HCl. Salinity, and phosphate and silicate concentrations were determined by SOMLIT (Service d'Observation en Milieu Littoral, INSU-CNRS, Brest, <http://somlit.epoc.u-bordeaux1.fr/fr/>). Underwater respiration (R , mmol DIC h^{-1}) and calcification (G , mmol DIC h^{-1}) rates in each bottle were calculated as follows:

$$R = \frac{\Delta \text{DIC} \times v}{\Delta t \times 10^3} - G$$

$$G = \frac{\Delta TA \times v}{2 \times \Delta t}$$

where ΔDIC is the change in the total inorganic carbon concentration (mmol DIC l⁻¹), ΔTA is the variation in TA during incubation (mmol l⁻¹), v is the bottle volume (l), and Δt is the incubation time (h). Alkalinity can be influenced by nutrient concentration changes; therefore estimation of calcification from TA changes alone can result in errors. In our short incubation, we assumed a negligible effect of nitrification with regard to the observed TA variation; however, the effect of the ammonium excretion rate was considered to potentially increase TA by 1 equivalent per mole.

When calcification occurs in the aquatic environment, CO₂ is released into the surrounding water. The deposition of one mole of calcium carbonate releases approximately 0.6 mole of CO₂ into the seawater at 25°C temperature and 35 for salinity (Frankignoulle et al. 1995). To calculate the contribution of calcification to CO₂ fluxes we estimated the molar ratio of CO₂ released by calcification to calcium carbonate precipitated, as a function of average sea water temperature following Frankignoulle et al. (1994).

Underwater ammonium excretion

The ammonium excretion rate was measured for each gastropod species in summer and winter. The ammonium concentration in the surrounding water was determined using the phenol-hypochlorite method (Koroleff 1969, Solorzano 1969). Samples of water were taken at the beginning and end of the respiration incubations in 100-ml bottles. Reagents were immediately added to the samples and to two control bottles filled with Milli-Q water, and these bottles were stored in the dark for 24 h. Concentrations were measured at 630 nm (UV-1700 PharmaSpec, UV-VIS spectrophotometer, Shimadzu, Japan) using Milli-Q water as the blank. Linear regressions of the ammonia excretion rate versus AFDW were calculated for summer and winter. Ammonium excretion rates were expressed as $\mu\text{mol NH}_4^+ \text{ g AFDW}^{-1} \text{ h}^{-1}$.

Calcium carbonate content

Calcification rates may be influenced by between-species differences in shell thickness. The calcium carbonate proportion of the shell was assessed for each studied species. Soft tissues were removed, and the dried shell was pestled to obtain fine powder. To ensure measurable CaCO₃ content, 0.35 g shell DW was treated for all samples. The calcium carbonate of the sample was treated with an excess of hydrochloric acid, and the volume of carbon dioxide gas released was measured using a Bernard apparatus (Hulseman 1966). Results were compared to the volume of CO₂ released by pure CaCO₃. The carbonate content was expressed in weight percentage.

Data analysis

Aerial, underwater, and CaCO₃ fluxes were related to AFDW through a functional regression analysis that considered the natural variability of both fluxes and biomass. Respiration fluxes were expressed per gram biomass (mmol CO₂ or DIC g⁻¹ h⁻¹). Arrhenius plots were utilized to evaluate the temperature effects on respiration rates during emersion and immersion. Arrhenius plots displayed the logarithm of flux plotted against inverse temperature as follows:

$$\ln Flux = \ln a - \frac{E_a}{k} \times \frac{1}{T}$$

where *Flux* is the respiration rate (Δ DIC underwater or Δ CO₂ in the air, mmol g⁻¹ h⁻¹), *a* is a normalization constant, *E_a* is the activation energy (J mole⁻¹), *k* is Boltzmann's constant (8.31 J K⁻¹ mol⁻¹), and *T* is the absolute temperature (K). Analysis of variance (ANOVA) was used to compare the slopes and intercepts of the linearized Arrhenius plots (Sokal & Rohlf 1995). If the slopes were not significantly different, the relationships between respiration rate and temperature were compared between species using an analysis of covariance (ANCOVA) followed by the *post-hoc* honestly significant difference (HSD) Tukey test for samples of different sizes (Zar 2010). The Pearson correlation coefficient was used to evaluate correlations of carbon fluxes with shell size, average individual biomass (AFDW), and average shore height. In order to evaluate the influence of body mass on metabolic rates, the

relationship between aerial and underwater metabolic rate and body mass was expressed by the equation:

$$R = aM^b$$

Where R is the metabolic rate of each species calculated for the average annual temperature of 13°C, M is the average body mass calculated for each species, a is the scaling coefficient and b is the scaling exponent. Whereas a varies with the type of organism, b are simple multiple of $\frac{1}{4}$ following the quarter-power biological law (Seibel 2007, Banavar et al. 2010).

When samples were too small, not normally distributed or variances were not equal, the Mann-Whitney non-parametric test was performed.

To estimate carbon fluxes on an annual scale, average contributions of aerial and underwater fluxes were calculated for aerial and underwater mean annual temperatures. Average shore position (Fig. 28) was estimated for each studied species using data from the

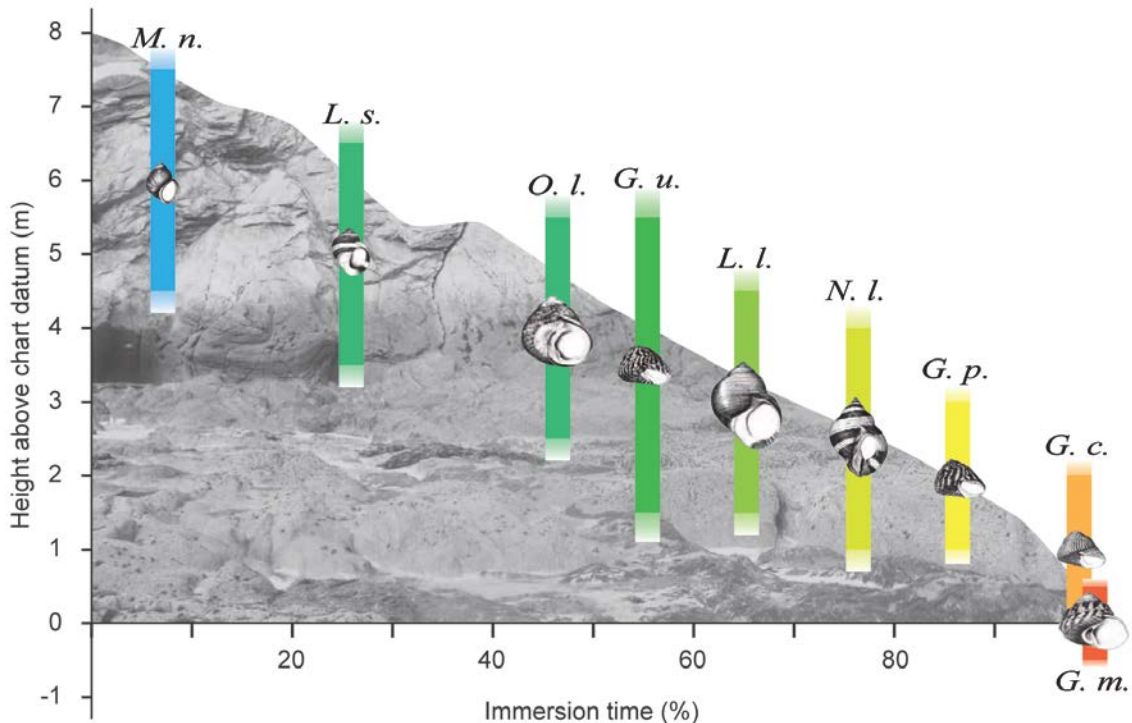


Fig. 28. Average vertical distribution and percent immersion time of studied species (*M. n.*, *M. neritoides*; *L. s.*, *L. saxatilis*; *O. l.*, *O. lineatus*; *G. u.*, *G. umbilicalis*; *L. l.*, *L. littorea*; *N. l.*, *N. lapillus*; *G. p.*, *G. pennant*; *G. c.*, *G. cineraria*; *G. m.*, *G. magus*).

literature (Fretter & Graham 1962, Little & Kitching 1996). Water height was calculated every 15 min according to SHOM (Service Hydrographique et Océanographique de la Marine) tide tables. For each studied species, annual CO₂ emissions during low tide were calculated by multiplying average hourly CO₂ fluxes by average time spent in air. Underwater annual carbon emissions were calculated by multiplying average hourly underwater and CaCO₃ fluxes by average time spent underwater for each species. The ratios between aerial and underwater respiration rates were calculated for each species using the average annual environmental temperature of the study area (13°C).

4. Results

Aerial and underwater respiration

Both aerial and underwater carbon fluxes were influenced by temperature variations (Fig. 29). Arrhenius plots (Tab. 4) demonstrated that a high percentage of variance was explained by temperature for all species, except for underwater fluxes of *M. neritoides*. Aerial respiration rate was generally stable during the 6-h aerial exposure for all species except for *M. neritoides*, for which the highest fluxes occurred during the first hour of aerial exposure and decreased for the rest of low-tide. Comparisons of Arrhenius relationships demonstrated that aerial CO₂ fluxes significantly differed between species (ANCOVA, p < 0.01). Post-hoc analyses revealed that *M. neritoides* respiration was significantly higher than that of the other gastropods, and that *L. saxatilis* respiration was significantly different from that of *L. littorea*, *N. lapillus* and *O. lineatus* (HSD Tukey test, p < 0.01 for both).

Tab. 4. Parameters of Arrhenius plots relating the logarithms of the hourly underwater and aerial respiration rates of each studied species per g AFDW to the inverse of absolute temperature (°K), at three tidal levels.

	Air			Underwater		
	Ln (a)	Ea/K	R ²	Ln (a)	Ea/K	R ²
<i>Melarhaphe neritoides</i>	29.97	7.65	0.74	11.47	2.37	0.01
<i>Littorina saxatilis</i>	6.69	1.07	0.51	27.61	7.13	0.47
<i>Osilinus lineatus</i>	27.21	7.15	0.88	28.16	7.30	0.62
<i>Gibbula umbilicalis</i>	16.84	3.99	0.94	47.52	12.89	0.97
<i>Littorina littorea</i>	16.33	4.07	0.72	43.28	11.71	0.82
<i>Nucella lapillus</i>	36.40	9.79	0.90	41.22	11.08	0.84
<i>Gibbula pennanti</i>	22.68	5.75	0.96	55.28	15.07	0.96
<i>Gibbula cineraria</i>	13.98	3.21	0.57	25.76	6.59	0.74
<i>Gibbula magus</i>	34.01	9.14	-	46.85	12.73	0.97

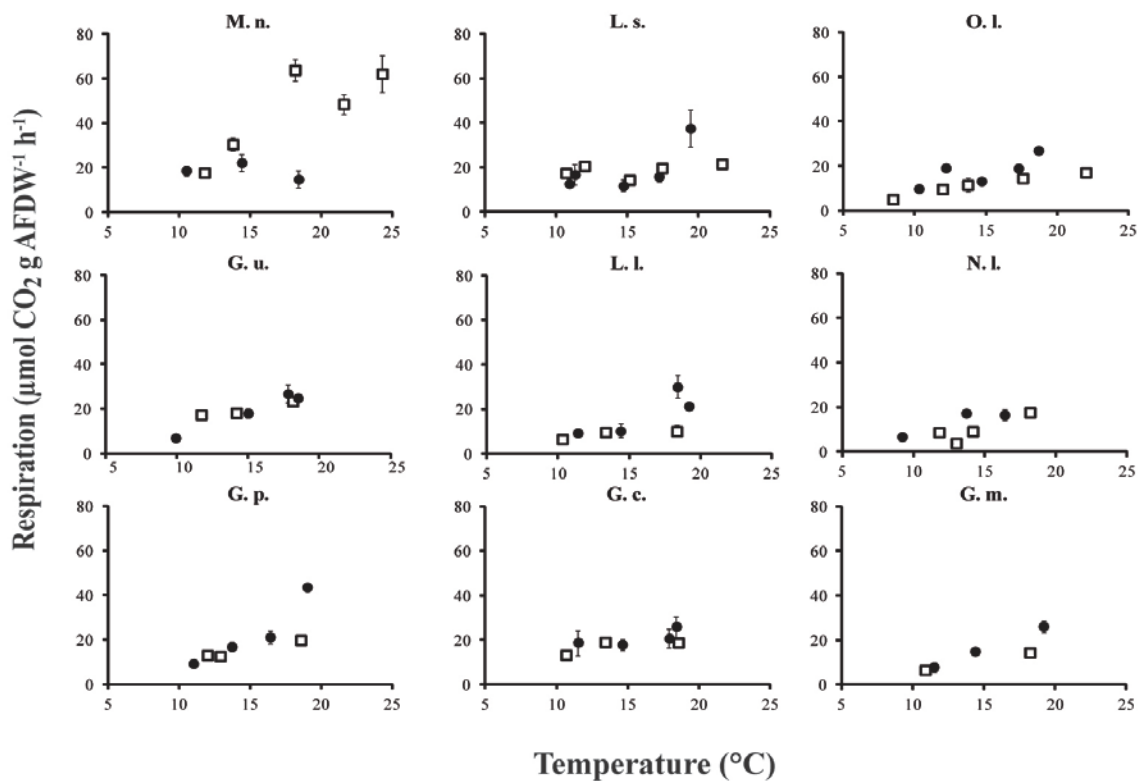


Fig. 29. Relationships between temperature and hourly underwater (white squares) and aerial (black circles) respiration rates per g AFDW (mean \pm standard deviation) for studied species (*M. n.*, *M. neritoides*; *L. s.*, *L. saxatilis*; *O. l.*, *O. lineatus*; *G. u.*, *G. umbilicalis*; *L. l.*, *L. littorea*; *N. l.*, *N. lapillus*; *G. p.*, *G. pennant*; *G. c.*, *G. cineraria*; *G. m.*, *G. magus*).

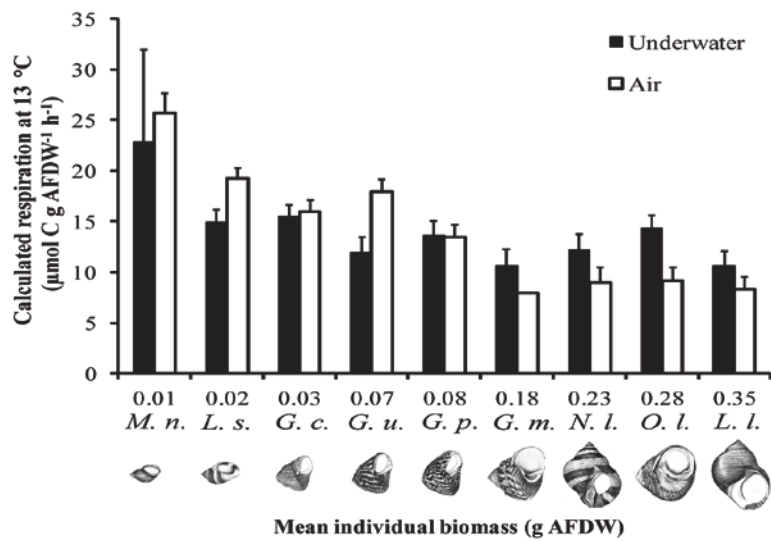


Fig. 30. Variation of hourly underwater and aerial carbon respiration rates at 13°C, calculated per g AFDW as a function of the average individual biomass of the gastropod species (*M. n.*, *M. neritoides*; *L. s.*, *L. saxatilis*; *O. l.*, *O. lineatus*; *G.u.*, *G. umbilicalis*; *L. l.*, *L. littorea*; *N. l.*, *N. lapillus*; *G. p.*, *G. pennant*; *G. c.*, *G. cineraria*; *G. m.*, *G. magus*).

The influence of body mass on mass specific aerial CO₂ fluxes, normalized for the average annual temperature of 13°C, follow the “quarter power law” because the scaling coefficient not significantly different from -0.25 (b=-0.30, R²=0.88) (Fig. 30). Conversely, the slope of log transformed underwater mass specific fluxes against body mass were significantly different from quarter power coefficient (b=-0.14, R²=0.65). The correlation between the average shell length and body biomass can be described by an exponential model (R²=0.97), except for *N. lapillus* significantly different shape (higher length for same weight). Linear regression between aerial and aquatic hourly fluxes and species shore position showed a slight correlation (R²=0.42 and 0.41, respectively).

Underwater carbon fluxes were compared for all studied species except *M. neritoides* for which the data did not fit the Arrhenius model. Arrhenius relationships for underwater fluxes were not significantly different between species (ANCOVA, p > 0.05), with an average value of $20 \pm 12 \mu\text{mol DIC g AFDW}^{-1} \text{ h}^{-1}$. Underwater respiration of each species was compared to average shore height, shell size, and biomass but no significant correlations were found.

The slopes of the Arrhenius plots for aerial and underwater respirations were not significantly different, except for those for *G. pennanti* and *G. umbilicalis* (ANOVA, $p < 0.05$). Respiration was similar in emersion and immersion at a same temperature for all gastropod species (Fig. 30).

The aerial to aquatic ratio of hourly rates of carbon fluxes was not directly related to the degree of aerial exposure in the rocky shore. *G. umbilicalis* and *L. saxatilis* exhibited stronger aerial/aquatic ratios while lower ratios were recorded for *O. lineatus* and *N. lapillus*.

Ammonium excretion

Ammonium fluxes were measured in summer and winter for each studied species, except for *M. neritoides* for which only winter fluxes were available (Fig. 31). Excluding *M. neritoides* ($12.1 \mu\text{mol NH}_4^+ \text{ g AFDW}^{-1} \text{ h}^{-1}$), the range of average NH_4^+ fluxes was $0.8\text{--}2.5 \mu\text{mol NH}_4^+ \text{ g AFDW}^{-1} \text{ h}^{-1}$, with an average value of $1.9 \pm 0.8 \mu\text{mol NH}_4^+ \text{ g AFDW}^{-1} \text{ h}^{-1}$. Summer and winter ammonium fluxes were compared to average shore height, shell size, and biomass but no significant correlations were found.

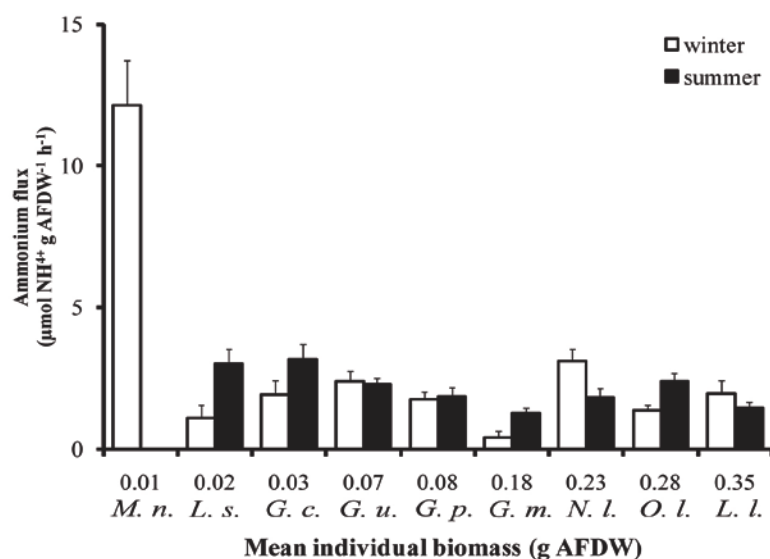


Fig. 31. Ammonium excretion rates (mean \pm standard deviation) during summer and winter as a function of the average individual biomass of the gastropod species (*M. n.*, *M. neritoides*; *L. s.*, *L. saxatilis*; *O. l.*, *O. lineatus*; *G. u.*, *G. umbilicalis*; *L. l.*, *L. littorea*; *N. l.*, *N. lapillus*; *G. p.*, *G. pennanti*; *G. c.*, *G. cineraria*; *G. m.*, *G. magus*).

Excretions did not significantly differ between summer and winter (Mann-Whitney, $p > 0.05$), with average values of $2.1 \pm 0.7 \mu\text{mol NH}_4^+ \text{ g AFDW}^{-1} \text{ h}^{-1}$ and $1.7 \pm 0.8 \mu\text{mol NH}_4^+ \text{ g AFDW}^{-1} \text{ h}^{-1}$ in summer and winter, respectively. Therefore, the average values of NH_4^+ flux between summer and winter were used to correct TA for each studied species.

Calcification and calcium carbonate content

Tab. 5. Percentage of calcium carbonate in the shell of each studied.

	% CaCO ₃
<i>Melarhaphe neritoides</i>	81.7
<i>Littorina saxatilis</i>	99.1
<i>Osilinus lineatus</i>	91.7
<i>Gibbula umbilicalis</i>	94.8
<i>Littorina littorea</i>	98.1
<i>Nucella lapillus</i>	98.5
<i>Gibbula pennanti</i>	85.0
<i>Gibbula cineraria</i>	83.2
<i>Gibbula magus</i>	89.3

Net calcification was positive for all species throughout the year (Fig. 32). High-shore species showed stronger and more variable calcification, with average CaCO₃ depositions of 19 and 16 $\mu\text{mol CaCO}_3 \text{ g AFDW}^{-1} \text{ h}^{-1}$ for *M. neritoides* and *L. saxatilis*, respectively. CaCO₃ fluxes were significantly different between species (ANOVA, $p < 0.05$). HSD Tukey post-hoc tests revealed significant differences between the fluxes of *M. neritoides* and *O. lineatus*, *N. lapillus* and *L. littorea*, and *L. saxatilis* and *O. lineatus*. Average calcification was statistically correlated to the average body biomass of the species (Pearson correlation coefficient, $r = -0.82$, $p < 0.05$). The average percentage of CaCO₃ content in gastropods

shells (Tab. 5) was 92.5%, and varied from 81.7% for *M. neritoides* to 99.1% for *L. saxatilis*.

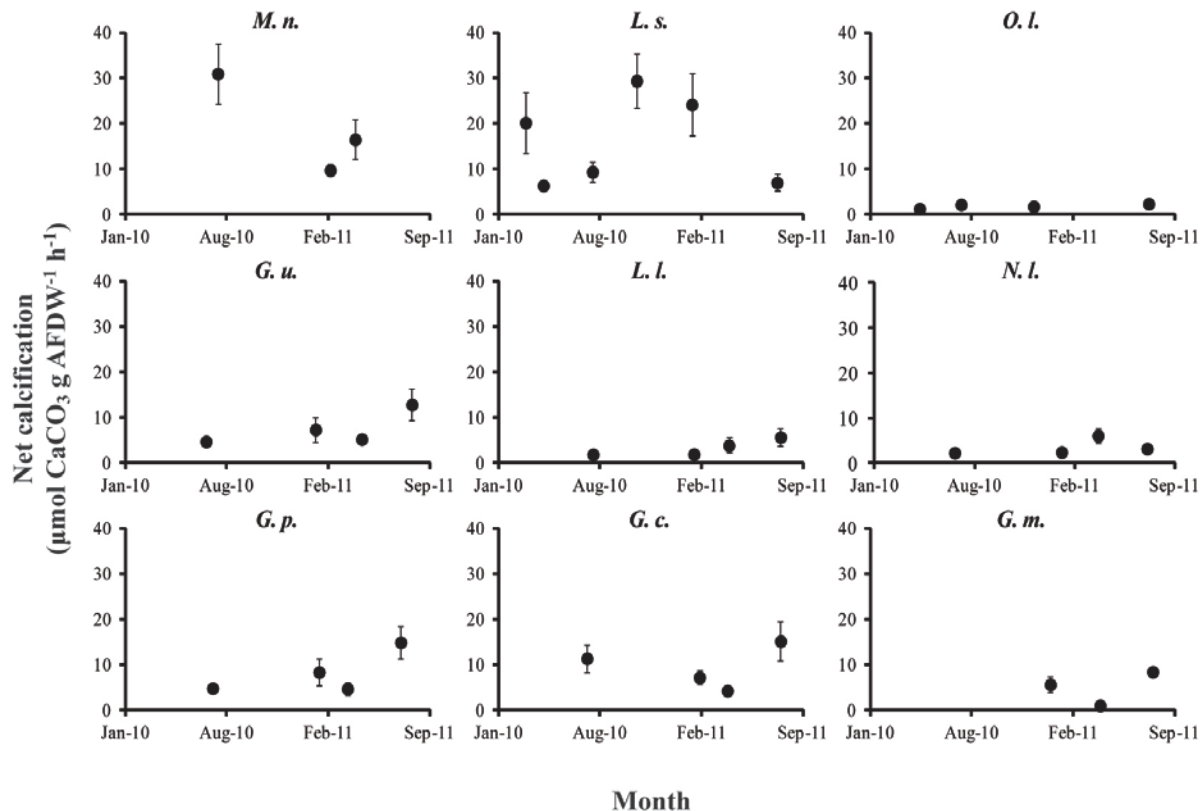


Fig. 32. Seasonal variation in net calcification rate (mean \pm standard deviation) for all studied species. Positive values correspond to calcification (*M. n.*, *M. neritoides*; *L. s.*, *L. saxatilis*; *O. l.*, *O. lineatus*; *G. u.*, *G. umbilicalis*; *L. l.*, *L. littorea*; *N. l.*, *N. lapillus*; *G. p.*, *G. pennant*; *G. c.*, *G. cineraria*; *G. m.*, *G. magus*).

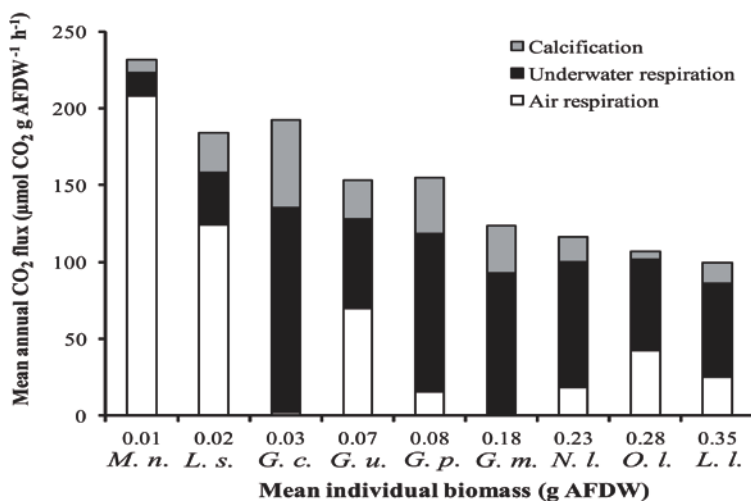


Fig. 33. Average annual carbon emissions due to calcification, and aerial and underwater respiration as a function of the average individual biomass of the gastropod species (*M. n.*, *M. neritoides*; *L. s.*, *L. saxatilis*; *O. l.*, *O. lineatus*; *G. u.*, *G. umbilicalis*; *L. l.*, *L. littorea*; *N. l.*, *N. lapillus*; *G. p.*, *G. pennant*; *G. c.*, *G. cineraria*; *G. m.*, *G. magus*).

Annual carbon budget

Annual cumulated air exposure was maximal for *M. neritoides* with 338 d y^{-1} in emersion, minimal for *G. cineraria* with 5 d y^{-1} , and nil for *G. magus*. The calculated mean annual CO₂ emission was maximal for *M. neritoides* with 232 mmol CO₂ g AFDW⁻¹ y^{-1} and minimal for *L. littorea* with 99 mmol CO₂ g AFDW⁻¹ y^{-1} (Fig. 33). Both log transformed total annual CO₂ emissions and average individual biomass were significantly correlated together biomass ($b=-4.5$, $R^2=0.95$). The contributions of calcification to total carbon fluxes ranged from 4% for *M. neritoides* to 30% for *G. cineraria*, with an average value of 16%.

5. Discussion

Aerial and underwater respiration

A number of studies have dealt with aerial and underwater metabolism of intertidal gastropods (McMahon & Russel-Hunter 1977, McMahon 1990, Sokolova & Portner 2001); however, the different methodologies used may have influenced the results. The present study is the first to have used similar techniques to investigate the aerial and underwater carbon respiration fluxes of nine intertidal gastropod species, and to relate the results to their vertical distribution. All studied individuals were subjected to the same sampling stress, and all animals showed similar activity levels during measurements. Gastropods were normally active, with maximal activity levels during immersion and reduced activity during aerial exposure.

The rocky shore of the north-east Atlantic is characterized by a semidiurnal macrotidal regime (maximum tidal amplitude: 8 m; tidal periodicity: 12 h 15 min). *M. neritoides* is among the species living highest in the intertidal zone of this region, and was the only species whose fluxes significantly differed from all others both in air and underwater. *M. neritoides* produced higher carbon fluxes in air than in water, especially during the first hours of aerial exposure. High-shore littorinids like *M. neritoides* are well adapted to the aerial environment; they have gills with very few leaflets, and significant oxygen uptake occurs across the mantle surface (Little & Kitching 1996). In a previous study, *M. neritoides* showed stronger heat resistance in air than underwater (Fraenkel 1961). We found that *M. neritoides* metabolism

during submersion seemed less efficient and not influenced by seasonal temperature variations. Conversely, seasonal temperature fluctuation strongly influenced the respiration rates of most species, which generally increased with temperature both in emersion and in submersion. The temperature influence was higher underwater than in air, which may be an adaptation to the rapid temperature changes occurring in air (Petersen & Johansen 1973, Petersen et al. 1974). The responses to seasonal temperature variations differed between species. Aerial respiration increased quickly with temperature for *M. neritoides*, *N. lapillus* and *G. magus*; minimal increases were recorded for *L. saxatilis*; and all other species showed similar intermediate responses. Although *L. saxatilis* and *M. neritoides* both live on the upper part of the shore, they showed very different metabolic adaptations. Previous studies comparing the two species have shown *L. saxatilis* to be more vulnerable to desiccation and less euryhaline than *M. neritoides* (Kronberg 1990).

All studied species are predominantly herbivorous (scrapers) except dogwhelks (*N. lapillus*), which are among the most common predators on rocky shores (Little & Kitching 1996). Dogwhelks feed on barnacles and mussels; search for prey only during tidal immersion and take several hours to more than a day to handle each item (Dunkin & Hughes 1984). Dogwhels metabolism is influenced by feeding behavior, with maximal rates during feeding and declining rates between meals (Bayne & Scullard 1978). Our results show that *N. lapillus* aerial respiration was greatly influenced by temperature.

In the present study, aerial carbon fluxes were strongly influenced by species means size and biomass. Within most taxa, metabolism increases with body mass which means that the mass-specific metabolic rate is higher in small organisms than in large ones (Makarieva et al. 2005). In the present study, species have similar lifestyle and activity level, and belong to the same taxonomic class. Hence we avoid the “signal-to-noise” due to comparing animals of very different biological traits and living in very different conditions (Seibel & Drazen 2007). While aerial fluxes seem in accord with the quarter theory, underwater respiration is less influenced by body mass variations. Environmental factors can profoundly affect the scaling of metabolic rate in animals (Glazier 2007). In aerial gas exchange, smaller animals may have an advantage from their higher surface-volume ratio since aerial diffusion occurs through mantle surface area (Fretter & Graham 1962, Houlihan 1979). Underwater respiration that occurs thought gills resulted less influenced by increase of species body mass.

We did not observe a clear pattern of aquatic respiration that could be related to the level on the shore. The aerial/aquatic ratios we established for temperate rocky shore gastropods ranged between 0.4–2.3 and were generally lower than the previously reported ratio for mangrove snails of 2.5–2.9 (Houlihan 1979). All intertidal gastropods seemed to have similar underwater respiration capacity by biomass unit, but a different metabolic response to the aerial environment. Respiratory mechanisms that are efficient in water often do not function as well upon emersion. The ability to maintain similar aerial and aquatic respiration fluxes is correlated with a reduction of gill surface area and mantle wall vascularization (Fretter & Graham 1962, McMahon 1988).

Calcification and ammonium excretion

Aquatic gastropods are primarily ammonotelic during immersion (Bishop et al. 1983). Little is known about the excretion of intertidal gastropod species (Needham 1935, Taylor & Andrews 1988, Aldridge et al. 1995). The high ammonium fluxes that we measured for *M. neritoides* may be related to longer aerial exposure that leads to greater accumulation of the excreted products, which would be released during the initial period of immersion.

TA fluxes for each species were corrected with ammonium rates since ammonium excretion would increase TA. Ammonium correction increased the calculated values of CaCO₃ flux by an average of 18%. Our findings confirm that the ammonium effect is much smaller than the variation observed between CaCO₃ flux measurements (Jacques & Pilson 1980, Chisholm & Gattuso 1991, Gazeau et al. 2007).

This is the first study to report seasonal CaCO₃ fluxes for these nine intertidal gastropods. Calcification seemed to depend on animal size and shore-height. Smaller species living in high shore, such as *M. neritoides* and *L. saxatilis*, showed stronger and more variable CaCO₃ fluxes during immersion, whereas larger species living in low shore, such as *O. lineatus* and *N. lapillus*, showed minimal calcification rates per biomass unit. High-shore species growth can be reduced or stopped during aerial exposure, probably by calcium depletion (Bourget & Crisp 1975). Therefore, species living in higher intertidal levels should accelerate the calcification process when underwater. The stronger calcification of *M. neritoides* contrasted with a lower shell calcium carbonate content due to a shorter immersion period. Conversely,

L. saxatilis, which spends more time immersed and had similar strong calcification rates, showed higher shell calcium carbonate content and a solid shell.

Annual carbon budget

The total annual carbon emission by intertidal gastropods was indirectly correlated with average individual biomass, with maximal values for smaller species and minimal values for larger species. Different theory could explain the observed relationship: larger species would spend more energy on breathing mechanisms than smaller species (Makarieva et al. 2008) and the cost of transport and energy saving would increase in large animals (Glazier 2007, Seibel 2007).

Calcification-related carbon emission varied to between 4% and 30% of the total annual carbon budget, according to animal size and immersion time. This important contribution of annual calcification for all studied species indicates that each species is able to regulate the calcification process according to their position on the intertidal zone.

In summary, both aerial and underwater metabolisms were influenced by seasons and increased with temperature. Aerial respiration fluxes were predominant in the annual carbon budget for high-shore snails that spend more time in emersion. Although high-shore species, like *M. neritoides* and *L. saxatilis*, appeared better adapted to aerial respiration, mean species body size is the predominant factors influencing intraspecific intertidal gastropod carbon emission.

Partie II

**Production primaire, respiration et
calcification des communautés
intertidales de substrat rocheux.**

Chapitre 4

Variation saisonnière du métabolisme des communautés intertidales de substrat rocheux semi-exposé.

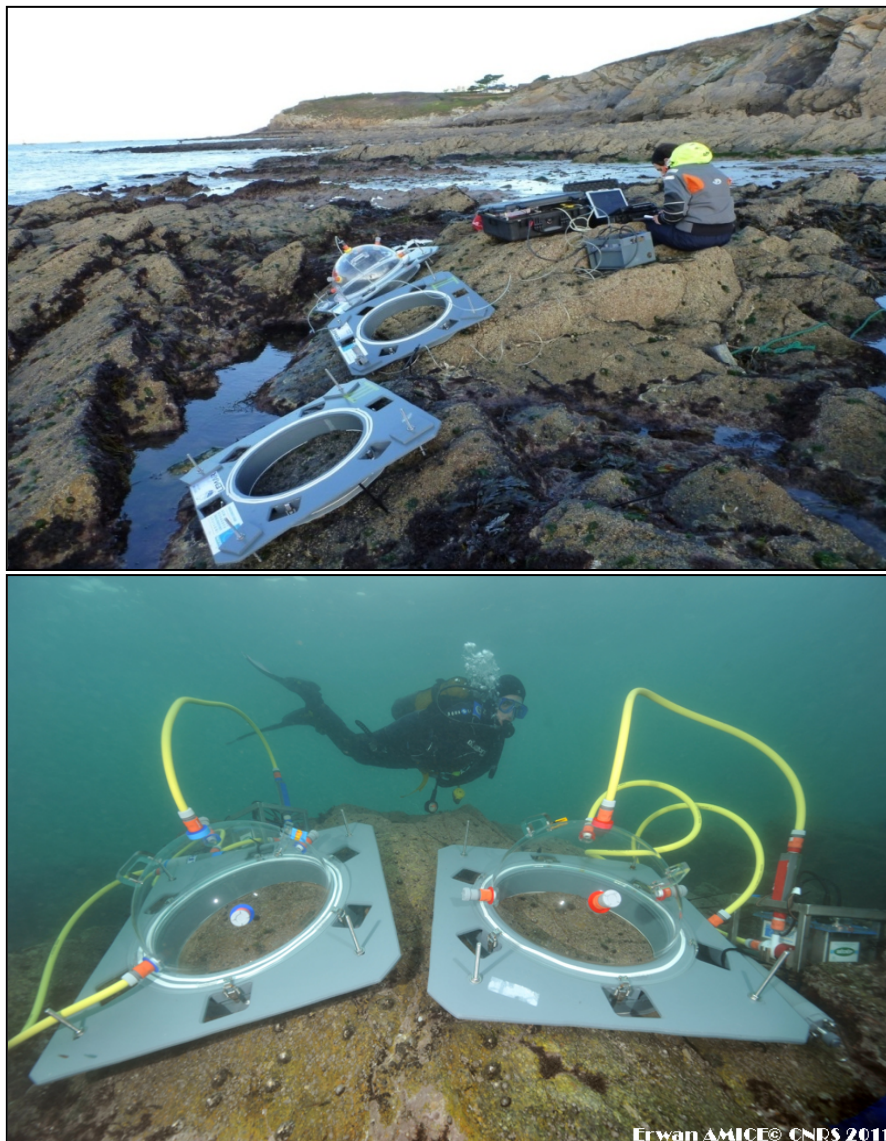


Fig. 34. Chambres benthiques disposées sur le niveau bas de l'estran, pendant la marée basse (photo du haut) et pendant la marée haute (photo du bas).

1. Contexte général et résumé

Le métabolisme des communautés est un concept central dans les recherches sur les bilans du carbone. Les mesures effectuées au niveau communautaire permettent de considérer la contribution de tous les organismes (autotrophes et hétérotrophes) vivant sur l'estran et d'établir si le bilan de carbone de la communauté est positif ou négatif. Ce bilan dépend de l'équilibre entre la production primaire brute (GPP, community gross primary production) et la respiration de l'ensemble des organismes (CR, community respiration). La production nette de carbone d'une communauté (NCP, net community production) est la différence entre l'assimilation de carbone par l'activité photosynthétique et les pertes par la respiration (Fig. 35) (Woodwell & Whittaker 1968).

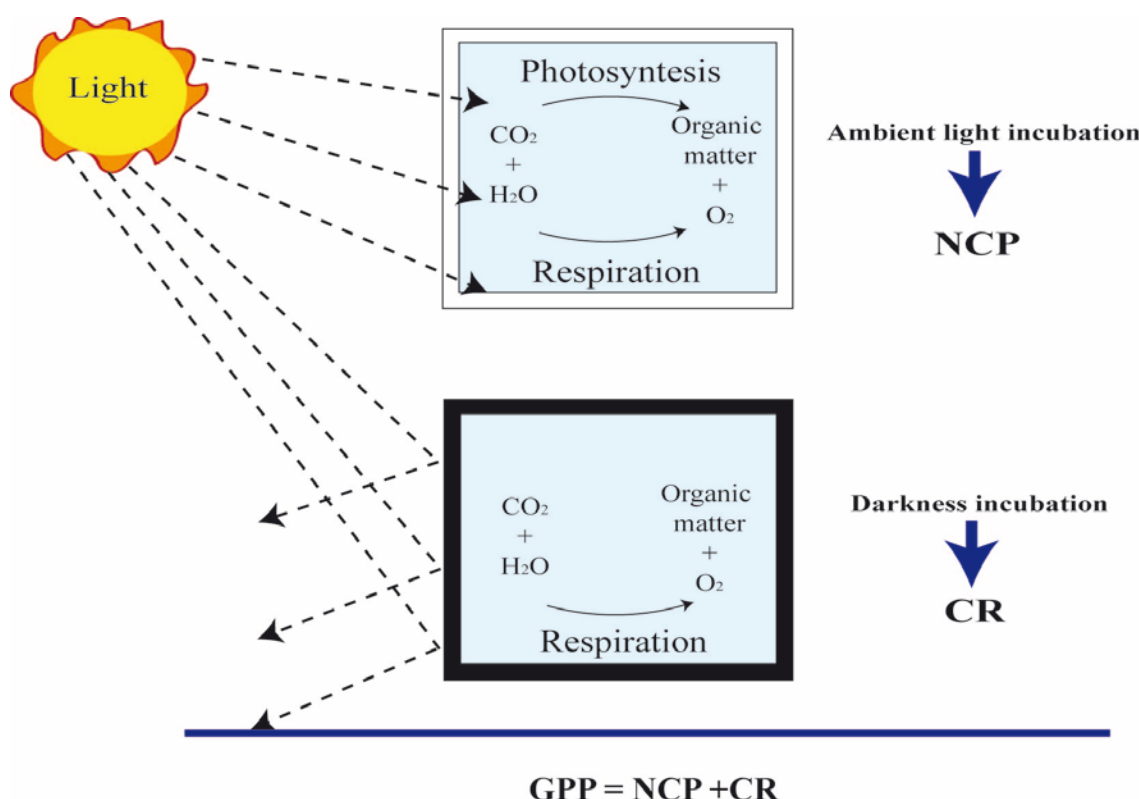


Fig. 35. Illustration schématique des processus étudiés.

NCP est une mesure du bilan énergétique de la communauté qui permet d'établir si elle est une source ou un puits de carbone pour son environnement. Dans les systèmes dits

« autotrophes », les nutriments inorganiques sont assimilés et la matière organique produite peut être exportée, au contraire dans les systèmes « hétérotrophes » la matière organique est minéralisée sur place et les nutriments inorganiques sont exportés (Middelburg et al. 2005).

Les communautés benthiques dominent souvent le métabolisme des écosystèmes côtiers, notamment dans les zones peu profondes. L'approche la plus directe pour mesurer leur respiration et leur production consiste à isoler une partie du milieu dans des chambres benthiques et à calculer les taux de respiration à travers les flux de gaz (Middelburg et al. 2005). En zone intertidale, l'estimation des flux de carbone doit tenir compte des fortes variations des paramètres abiotiques lors de l'alternance entre immersion et émersion. En effet, un certain nombre de facteurs vont contrôler la GPP et la CR:

- **La lumière** est très importante pour les organismes autotrophes, elle est le moteur de la photosynthèse. La réponse des végétaux aux différentes irradiances peut être décrite par des modèles non linéaires photosynthèse/irradiance (Vermaat & Verhagen 1996, Migne et al. 2009, Clavier et al. 2011). Des mécanismes de photoinhibition ou de photoadaptation sont susceptibles de se manifester sous de fortes irradiances. Les taux d'activité à court terme des animaux peuvent aussi être influencés de manière indirecte par les variations d'irradiance, notamment pour se protéger contre la déshydratation (Miller & Denny 2011).
- **La température** agit sur le métabolisme des tous les organismes, mais les réponses peuvent être très différentes selon les espèces.
- **La salinité** peut être un paramètre important en zone intertidale ou la pluie et l'évaporation pendant la marée basse peuvent conduire à des fortes variations osmotiques.

D'autres facteurs vont aussi contrôler les émissions de carbone des différentes zones côtières comme la disponibilité en nutriments, l'hydrodynamisme, le marnage et la composition des différentes communautés. Le NCP ainsi que le flux de CO₂ en zone côtière vont donc montrer une forte variabilité. La composition des communautés de milieu rocheux intertidal et leur interactions sont bien connues mais les difficultés liées à leur étude *in situ* n'ont pas encore permis de quantifier pleinement leur métabolisme (Golley et al. 2008).

Dans ce contexte, l'objectif de ce chapitre est d'introduire une nouvelle approche méthodologique (Fig. 34) pour l'étude *in situ* des communautés des estrans rocheux et d'estimer la contribution de la communauté rocheuse intertidale aux flux de carbone.

L'étude a été effectuée sur un estran rocheux semi-exposé où les balanes sont dominantes et les macroalgues sont rares en raison d'un hydrodynamisme fort. Trois niveaux de l'estran ont été comparés et les mesures ont été répétées pour les quatre saisons.

Les résultats de CR montrent que la communauté est bien adaptée à la respiration aérienne qui n'est pas significativement différente de celle en immersion. La calcification prévaut sur la dissolution des carbonates tout au long de l'année. NCP varie beaucoup en fonction des paramètres environnementaux selon la situation émergée ou immergée. Pendant la marée haute, la photosynthèse est principalement influencée par l'irradiance, alors qu'en émersion d'autres paramètres comme l'humidité de l'air et la température semblent jouer un rôle important en concomitance avec l'irradiance.

Cette étude démontre que les communautés intertidales de substrat rocheux semi-exposé sont surtout hétérotrophes et peuvent constituer une source de carbone pour l'atmosphère.

Aerial and underwater metabolism in an intertidal rocky shore community.

Morgana Tagliarolo, Jacques Clavier, Jacques Grall, Erwan Amice, Marion Maguer, Anne Donval, Aude Leynaert, Sorin Moga, Philippe Lenca, Laurent Chauvaud

2. Introduction

Rocky shores are found worldwide and experience vastly different climates, water qualities, as well as wave and wind exposure conditions. Despite this wide range of conditions, tidal cycle is the overriding factor determining emersion and immersion, and controlling the distribution of organisms living on rocky shores (Little & Kitching 1996). Vertical distribution patterns are obvious on exposed shores, where mussels, barnacles and lichens form a series of bands (Lewis 1964). The general vertical structure of benthic communities on northern Europe exposed rocky shores consist of lichens and small gastropods such as *Melarhaphe neritoides* (L.) in the upper part of the shore, several species of barnacles at mid shore and macroalgae and limpets at the lower part of the shore, which is exposed to air only during low spring tide (Lewis 1964).

The timing of low tides plays a key role in determining the exposure of intertidal organisms to variable and potentially stressful conditions. Because most intertidal organisms evolved from marine origin, most biological functions (feeding, reproduction, respiration, etc.) occur during immersion (Newell 1979). Nevertheless, many intertidal organisms such as gastropods and barnacle are able to breath and feed during low tide (McMahon & Russel-Hunter 1977, Little 1989, Clavier et al. 2009). Due to the huge differences of environmental conditions between immersion and emersion community metabolism may differ (Migne et al. 2009, Clavier et al. 2011).

Metabolism of rocky shore organisms have mostly been studied in the laboratory where each species was studied separately (Branch 1978, Houlihan & Newton 1978, Babarro et al. 2000, Clavier et al. 2009, Lejart et al. 2012). The study of community metabolism is however essential to understand the response of the whole community to environmental variation.

Species composition, position on the shore and physical conditions (temperature, irradiance, salinity, air humidity etc.) are hypothesized to be important factors influencing respiration and primary production.

The use of benthic chambers allows estimation of respiration and photosynthesis through *in situ* measures of carbon fluxes. This technique is known to be effective to measures the whole community metabolism, including macro and microorganism present in the enclosed volume (Migné et al. 2002). Several estimations of intertidal benthic community carbon fluxes have been performed through the use of benthic chamber method, but the majority of studies were focused on soft substrate (Spilmont et al. 2007, Davoult et al. 2009, Ouisse et al. 2010, Clavier et al. 2011). Only two previous studies have been performed on both primary production and respiration of rocky shore communities; the first on a macroalgae dominated shore (Golley et al. 2008), the second on isolated rocky blocks (Lejart 2009).

To our knowledge, primary production and respiration measurements of exposed rocky shore communities are poorly known. For this reason we have performed *in situ* measurements of carbon fluxes at three different vertical shore levels of an intertidal exposed rocky shore. This paper thus investigates benthic metabolism comparing primary production and respiration in the air and underwater, and evaluating seasonal effect on carbon fluxes.

3. Material and methods

Study site

The study was carried out in western Brittany (France) on the intertidal rocky shore community of Porsliogan ($48^{\circ}20'55''$ N, $4^{\circ}46'20''$ W). It is characterized by a macrotidal regime with a spring-tide range of about 8 m. The experimental site has an exposed gently sloping rocky bottom. Three vertical shore levels were selected: we will further use the terms “high-shore” to refer to measurements performed at 5 m above chart datum, “middle-shore” for those at 3 m above chart datum and “low-shore” for those at 1.5 m above chart datum. The benthic community metabolism was measured in January, Mars, June, October 2011 and Mars 2012 to assess seasonal variability.

Environmental parameters

The percentage of relative humidity (RH) was measured near the rocky surface during low tide (T200 thermo-hygrometer, Trotec, Heinsberg, Germany). During emersion, a quantum sensor (Li-192SA, Li-COR) and an air temperature sensor (LI 1400-101, LI-COR) were connected to an L1 1400 logger to evaluate photosynthetically available radiation (PAR, 400-700 nm) and air temperature, respectively. During underwater experiments, PAR was measured using a quantum sensor (LI-192SA, LI-COR) connected to a L1 1400 logger placed in a watertight casing. A third PAR sensor was deployed on land near the sampling site to record the daily evolution of irradiance in the air. Irradiance ($I, \mu\text{mol m}^{-2} \text{s}^{-1}$) and temperature ($^{\circ}\text{C}$) were sampled every 5 s, then averaged every minute.

Carbon flux measurements

Community respiration, production and calcification were investigated by *in situ* incubation experiments using benthic enclosures. Three rocky areas, as smooth as possible, were chosen at each shore level. Circular grooves of 1-2 cm depth, the size of benthic chamber bases, were dug and smoothed with concrete five months prior to the beginning of measurements in order to avoid perturbation of communities. Benthic chambers (50 cm in diameter, 0.2 m^2 surface, Fig. 36) were constituted by a polyvinyl chloride (PVC) base of 10 cm height attached to threaded rod sealed in the rocky substratum to resist wave action. The airtightness between the basis and the rock substrata was ensured

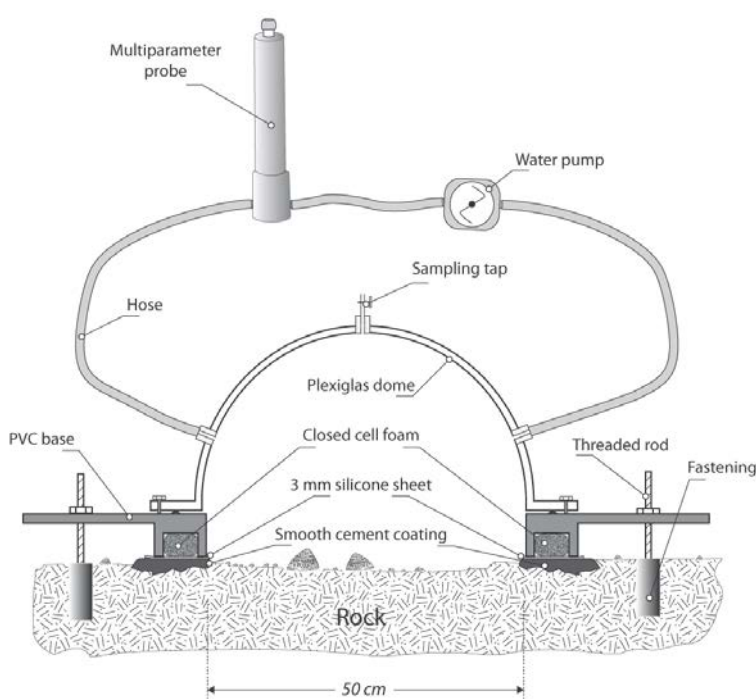


Fig. 36. Schematic representation of the experimental apparatus.

Multiparameter probe and water pump were used during underwater measurements.

using a 3 mm silicone sheet and closed cell foam. Bases were assembled for each level during low tide and filled with water to check the system for leaks. Transparent (Perspex) or opaque (PVC) dome were fit to each basis and fastened by clamps. The airtightness between the chamber and the basis was obtained using a rubber joint. The transparent dome was thus used to assess net community production (NCP) and calcification in daylight, and an opaque dome was used to estimate community respiration (CR) and calcification in dark conditions. Gross community production (GCP) was estimated subtracting CR from NCP with the assumption that CR is equivalent under light and dark conditions.

CO₂ fluxes during emersion were measured at the rock-air interface during short-time incubations using an infrared gas analyzer (Li-Cor, LI 820) (Migné et al. 2002). Air passed through a closed circuit with a desiccation column filled with anhydrous calcium sulphate (Drierite, Xenia, USA). The air flow was maintained at of 0.8/0.9 l min⁻¹ by an adjustable pump. The air enclosed in the dome was homogenized using a small battery-operated fan. The CO₂ concentration (pCO₂; in parts per million, ppm = $\mu\text{mol CO}_2 \text{ mol air}^{-1}$) was displayed on a laptop computer and recorded at 5 s intervals for approximately 3 min. The dome was opened for at least 5 min between successive incubations to restore ambient conditions, thus temperature variations in the chamber was negligible. The CO₂ fluxes were calculated using the slope of CO₂ concentration ($\mu\text{mol CO}_2 \text{ mol}^{-1}$) against time (min). Fluxes were expressed at the community level (mmol CO₂ m⁻² h⁻¹) taking into account the volume of the enclosure and the enclosed surface area.

During spring, different humidity treatments were tested on the three benthic chambers at the middle-shore level in order to evaluate the effect of desiccation on aerial carbon fluxes. Natural drying, splashing (sea water) and raining (freshwater) were simulated for about 3 hours of aerial exposure and measures were repeated both with clear and opaque dome.

During immersion, one-hour incubations were performed at the rocky-water interface. Water in each enclosure was homogenized by an adjustable submersible pump at 2 L min⁻¹ connected to a battery enclosed in a waterproof casing. A multiparameter probe (YSI 6920) was placed in the water circuit to measure oxygen concentration (mg O₂ l⁻¹), temperature (°C), salinity (practical salinity unit) and depth (m) (Fig. 36). Dissolved inorganic carbon (DIC) concentration (mmol DIC l⁻¹) was calculated from pH, TA, temperature, salinity, phosphate and silicate concentrations (Pierrot et al. 2006). CO₂ dissociation constants K1 and K2 (Roy et

al. 1993) were used in the computation. Calcification was estimated using the alkalinity anomaly technique (Smith & Key 1975) based on the observation that TA decreases by two equivalents for each mole of CaCO_3 precipitated. Seawater samples were collected from the benthic chambers, using 450 ml syringes at the beginning and at the end of incubations. Seawater pH (total scale) was measured immediately using a pH-meter (Radiometer PH240) standardised with Tris-HCl (2-amino-2-hydroxymethyl-1,3-propanediol) and 2-amminopyridine/HCl buffer solutions in synthetic seawater with a salinity of 35. Water samples for total alkalinity (TA) were filtered through 0.7 μm Whatman GF/F filters and stored in 250-ml bottles in the dark. Analyses were carried out within one week. TA (mmol kg^{-1}) was determined on 20-ml subsamples (6-replicate) by Gran automatic potentiometric titration (Radiometer, Titrilab TIM 865) using 0.01 M HCl (Merck Titrisol). Salinity, phosphate and silicate concentrations were provided by SOMLIT (Service d'Observation en Milieu Littoral, INSU-CNRS, Brest, <http://sommelit.epoc.u-bordeaux1.fr/fr/>). The CR, NCP and net community calcification (CG) were calculated for each incubation, according to the equations:

$$\text{NCP or CR (O}_2\text{)} = \frac{(\Delta O_2 \times v)}{s \times \Delta t}$$

$$\text{NCP or CR (DIC)} = \frac{(\Delta DIC \times v)}{s \times \Delta t} - CG$$

$$CG = \frac{\Delta TA \times v}{2 \times s \times \Delta t}$$

Where ΔO_2 is the change on the concentration of dissolved O_2 during incubation (mmol l^{-1}), v is the chamber volume (l), s is the enclosed surface area (m^2), Δt is the incubation time (h), ΔDIC is the change in the total inorganic carbon concentration (mmol l^{-1}), CG is the net community calcification ($\text{mmol CaCO}_3 \text{ m}^{-2} \text{ h}^{-1}$), ΔTA is the variation in TA during incubation (mmol l^{-1}).

Community description

The sampling site was a barnacle dominated shore where algal cover was negligible. Macrofauna composition and abundance were assessed seasonally using non-destructive methods at each studied site. Five photographs of 25cm² quadrats were taken randomly within the location of each basis using a Panasonic Lumix FT3 (at 10 cm from the rock surface). Photo analysis was performed using Quantum GIS software to assess macrofauna (barnacles and gastropods) composition and abundance. Animals were identified to the lowest practical taxon and numbered. Additionally, the maximum shell length of enclosed limpets was measured in-situ to the nearest 1 mm using a hand vernier caliper. Average biomass for each level and season was calculated using average individual biomass (ash free dry weigh) together with the abundance of each species. To calculate average individual biomass of each species, five groups with 1 to 5 individuals of the same species were dried at 60°C for 24 hours and subsequent calcinations at 450°C for 4 hours in a muffle furnace. Average individual biomass was calculated from the regression between biomass and individuals number.

Regarding photosynthetic pigment assessment, rock fragments of 20-40 cm² were taken close to experimental location for each level and season. The pigments were extracted from these samples in 90% acetone for 12h under agitation at 4°C in a dark room. The extract was analyzed using two methods; High Performance Liquid Chromatography (HPLC) and fluorimetry. HPLC method (Agilent Technologies 1200 series) and the injection was performed on Zorbax Eclipse XDB-C8 column (3x150mm, 3,5µm particule size). Pigments were separated and quantified following the method originally described by Van Heukelem & Thomas (2001) and improved for a better sensitivity according to Hooker et al. (2009). Separation was based on a linear gradient established between a 70:30, methanol 28mM Tributyl acetate ammonium mixture and a 100% methanol solution. Detection was carried out for two different wave lengths, 450 nm (carotenoids, chlorophyll *b* and *c*), 667nm (chlorophyll *a* plus associated allomers and chlorophyllide *a*). The majority of pigments (Chl C2, Chl *a*, phaeophorbid *a*, phaeophytin *a*, β-carotene, fucoxanthin, lutein, zeaxanthine, violaxanthin, Chl *b*) were identified comparing the absorption spectrum with a spectral library previously created using standard pigments. The other pigments (scytonemin and red scytonemin) were identified following Mueller et al. (2005). Pigments were quantified from

the peaks of spectral library, but for violaxanthin, scytonemin and red scytonemin standard peaks were not available consequently only presence/absence data are available.

Since fluorimetry method is simpler and more rapid than HPLC, routine measurements of Chl *a* concentration were performed by fluorimetry during the studied period for each season and shore level. Samples were centrifuged and fluorescence was measured with a Turner Design fluorometer.

Data analysis

A Michaelis-Menten model was fitted using a non-linear regression between immersed NCP fluxes and PAR irradiance measured underwater (PI curve), according to the following equation:

$$NCP = \frac{P_{\max} \times I}{K_{\max} + I} - CR$$

Where P_{\max} is the gross maximal photosynthetic rate ($\text{mmol C m}^{-2} \text{ h}^{-1}$), I is irradiance, K_m is the half saturation constant ($\mu\text{mol PAR m}^{-2} \text{ s}^{-1}$). The F-test was used to compare CR , K_m

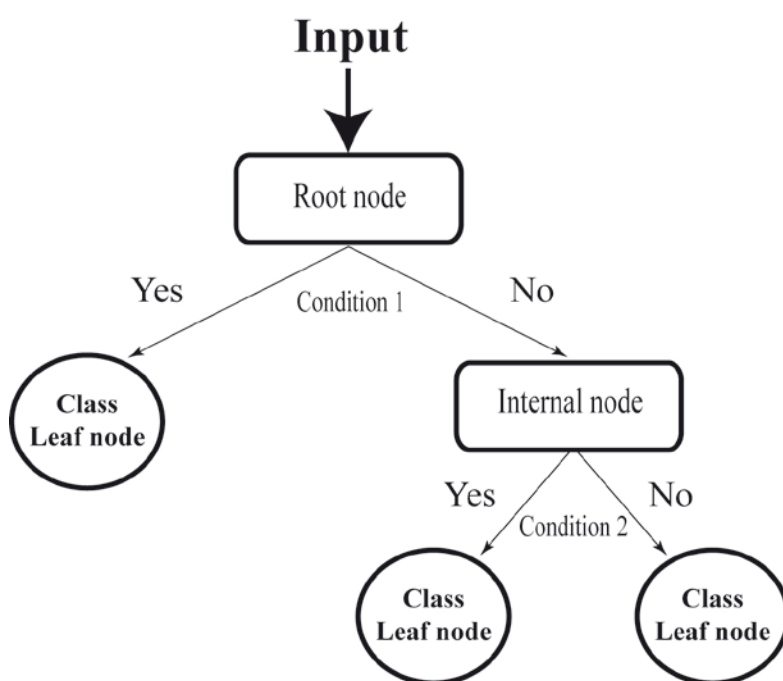


Fig. 37. An example regression tree.

and P_{\max} parameters of regression models obtained for the different seasons and shore levels according to Ritz & Streibig (2008). These parameters were used to calculate average underwater daily fluxes for each season and shore-level during a complete tidal cycle (spring-neap tide). In order to better estimate daily fluxes, aerial and underwater fluxes were calculated in function of water

height estimated every 15 min according to SHOM (Service Hydrographique et Océanographique de la Marine) tide tables. Underwater PAR irradiance was estimated for each level from irradiance measured in air and the extinction coefficient (k) calculated for each season and level according to Beer-Lambert equation.

The analyses of variance (ANOVA), followed by a post hoc honestly significance difference (HSD Tukey) was used to compare results from the different levels and seasons. If data were not normally distributed, the non parametric Kruskal-Wallis and Mann-Whitney test was used.

Results from aerial CO₂ fluxes were analyzed through the decision tree method. Decision tree is a model technique which can provide qualitative discrete outputs of a system under conditions represented by parameters (Solomatine & Dusal 2003, Witten & Frank 2005). It splits parameters' domain into sub-domains, and the system output for each sub-domain is learned through historical records. When new condition comes up, the system output is predicted by looking up which sub-domain it belongs to. A split point is a node and the corresponding output is a leaf (Fig. 37). A node can be further split, and the whole procedure results in a tree-like modeling structure (Chen & Mynett 2004).

The non-commercial data mining tools RapidMiner 5.2 and Weka were chosen to run the model. For the prediction of aerial NCP from available data on air temperature (°C), air relative humidity (RH), irradiance ($\mu\text{mol m}^{-2} \text{s}^{-1}$) and emersion time (min), we used W-REPTree algorithm. From the full set of NCP values, 2/3 of the 404 instances were used for learning process and 1/3 to test prediction accuracy of the regression trees constructed. A cross validation was performed, the pruning was set to default values, a number of 5 minimal instances per leaf were fixed and 4 maximal levels were allowed. The pruning procedure produces a sequence of possible trees of different size, and we chose the best fit for a given tree size and model complexity. The quality of a tree is measured by the mean squared error between the actual and the predicted value of a class (Breiman et al. 1984, Loh 2011).

4. Results

Environmental parameters

Average aerial and underwater PAR irradiances established for a tidal cycle vary between seasons and shore levels (Fig. 38). The maximal air irradiance value was of $1926 \mu\text{mol m}^{-2} \text{s}^{-1}$ during summer. The extinction coefficient (k) calculated for underwater irradiances at each shore-level and season varied between 0.3 and 1.2. Underwater irradiances were similar in autumn for the three different levels but differed significantly in winter, summer and spring

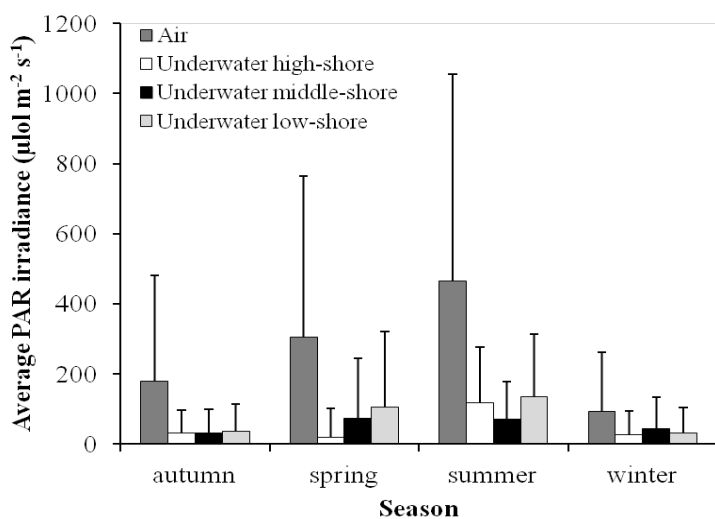


Fig. 38. Average seasonal variation of aerial and underwater PAR at the three sampling sites.

(ANOVA, $p<0.05$). During the studied period (from January 2011 to March 2012) air temperature above rocky shore varied from 7.3°C to 16.7°C with an average value of 12.6°C . Water temperature varied from 17°C to 9°C with an average value of 13°C (Fig. 39).

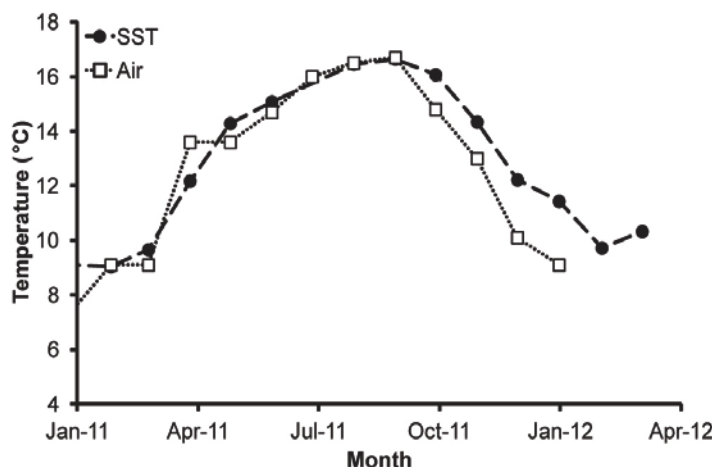


Fig. 39. Average monthly variation of mean sea surface (Mare Iroise Station) and air temperature (Météo France, Camaret station) from January 2011 to April 2012.

Community respiration

Underwater CR (Fig. 40) was not significantly different between season and shore level (Kruskal-Wallis, $p>0.05$), in contrast with aerial CR (Kruskal-Wallis, $p<0.05$). High and middle-shore level had similar aerial fluxes, while low-shore had higher respiratory fluxes during emersion. Winter aerial CR showed statistically lower aerial

CR than the other seasons (HSD Tukey $p<0.05$).

Aerial and underwater average fluxes were not significantly different (Wilcoxon's signed ranks test, $p>0.05$). The highest underwater mean CR was observed in autumn at low-shore level ($2.8 \text{ mmol C m}^{-2} \text{ h}^{-1}$) and the lowest in summer at middle-shore level ($0.8 \text{ mmol C m}^{-2} \text{ h}^{-1}$). During emersion, the highest average CR rate was in summer at low-shore level ($2.7 \text{ mmol C m}^{-2} \text{ h}^{-1}$) and the lower was in winter at middle-shore level ($0.4 \text{ mmol C m}^{-2} \text{ h}^{-1}$).

Underwater community production

Underwater NCP fluxes were strongly influenced by irradiance variation (Fig. 41). The P_{max} , K_m and CR parameters of PI curve did not differ significantly between levels (F-test, $p>0.05$) while seasonal variations were significant (F-test, $p<0.05$). Results from the three levels were then grouped for each season and a Michaelis-Menten model was fitted (Fig. 41). No photoinhibition was observed and irradiance explains more than 80% of net flux variance.

Underwater NCP fluxes varied between 3.8 and $-18.0 \text{ mmol m}^{-2} \text{ h}^{-1}$ with an average value of $-3.3 \text{ mmol m}^{-2} \text{ h}^{-1}$.

Oxygen and DIC fluxes (Fig. 42) were highly related ($N = 147$, $R^2 = 0.88$), the slope of the regression is 0.94.

Estimated daily NCP fluxes during immersion varied seasonally from -23.5 to $23.8 \text{ mmol m}^{-2} \text{ d}^{-1}$ (Fig. 43). NCP was positive during all year long for high-shore level,

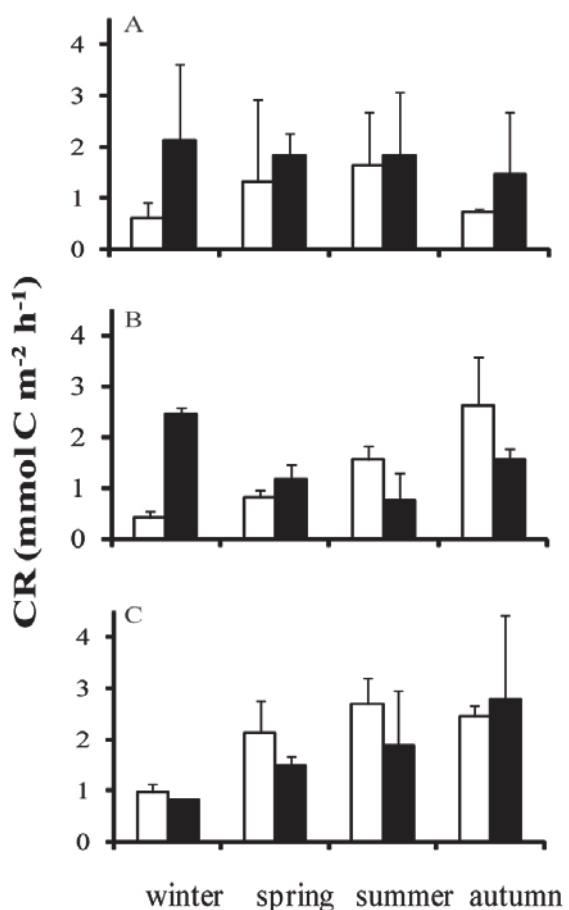


Fig. 40. Seasonal variation of community respiration ($\text{mmol C m}^{-2} \text{ h}^{-1}$) at the different shore-levels. White bars represent aerial respiration and black bars represent underwater respiration. (A, High-shore; B, Middle-shore; C, Low-shore).

indicating that CR was predominant. Negative values of NCP during spring at the middle-shore level as well as in summer at middle and low-shore levels reveal a predominance of primary production.

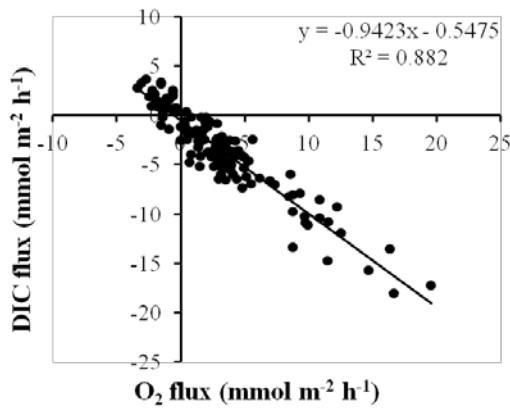


Fig. 41. Linear relationship between net ΔO_2 and ΔDIC (dissolved inorganic carbon).

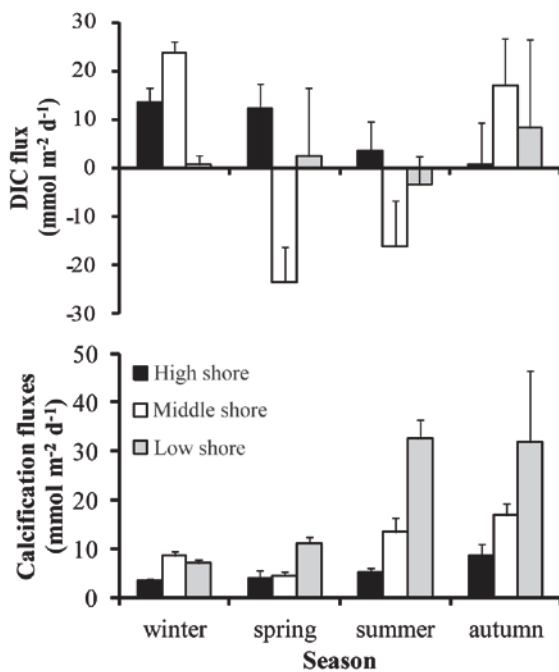


Fig. 42. Seasonal variation of average daily DIC and CaCO_3 fluxes at the different shore levels.

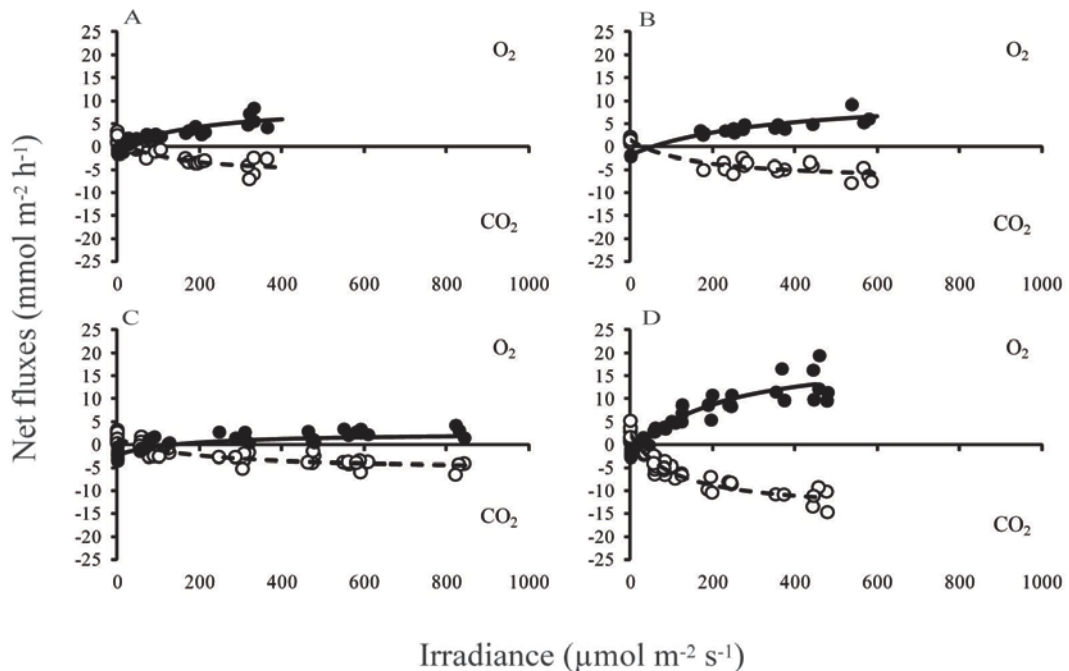


Fig. 43. Relationships between irradiance and underwater net community production (NCP) measured as O_2 emission (black dots) or CO_2 consumption (white dots). A, winter; B, spring; C, summer; D, autumn.

Underwater community calcification

Underwater CaCO_3 fluxes were strongly influenced by irradiance variation (Fig. 44). P_{max} , K_m differ significantly between seasons (F-test, $p<0.05$). PI curves were similar at the three shore levels during winter and spring, conversely P_{max} and K_m was significantly different between levels during autumn and P_{max} during summer (F-test, $p<0.05$). Irradiance explains more than 70% of the CaCO_3 fluxes variation. Seasonal community daily calcification was estimated for each shore level (Fig. 43). Daily fluxes were higher during summer and autumn with maximal values for low-shore level ($32 \text{ mmol m}^{-2} \text{ d}^{-1}$); minimal values were recorded during winter and spring at high-shore level ($3 \text{ mmol m}^{-2} \text{ d}^{-1}$).

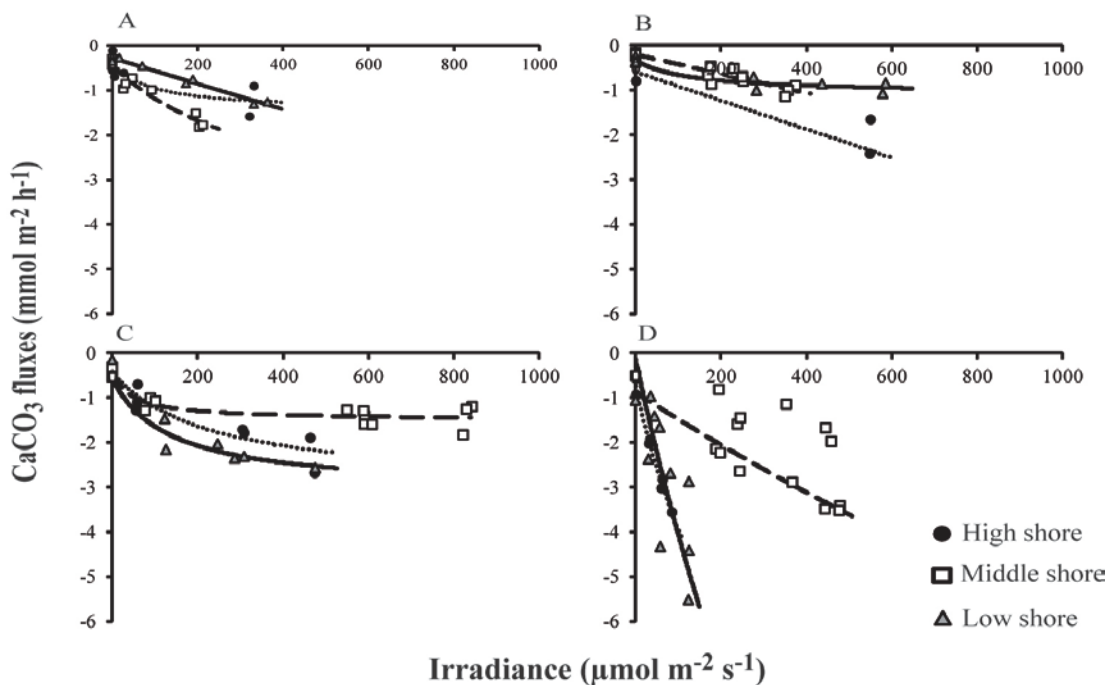


Fig. 44. Relationship between net community CaCO_3 fluxes and irradiance at the three shore levels. (A, winter; B, spring; C, summer; D, autumn).

Aerial community production

Aerial NCP varied between -14 to 6 mmol m⁻² h⁻¹ with an average value of -2 mmol m⁻² h⁻¹. NCP fluxes were significantly different between seasons (Kruskal-Wallis, p<0.05) with minimal photosynthesis contribution during summer (average NCP of 0.03 mmol m⁻² h⁻¹) and maximal in autumn (average NCP of -3.36 mmol m⁻² h⁻¹). The three shore-level NCP fluxes were also significantly different (Kruskal-Wallis, p<0.05) with stronger CO₂ consumption at the low-shore level.

Irradiance variations alone only account for 23% of the variation in NCP (Fig. 45, A). Four parameters were considered to explain aerial NCP variation: irradiance, relative air humidity, temperature and emersion time. Irradiances varied between 0 and 2077 μmol m⁻² s⁻¹ with maximal values recorded during summer (Fig. 45, A). Temperature varied

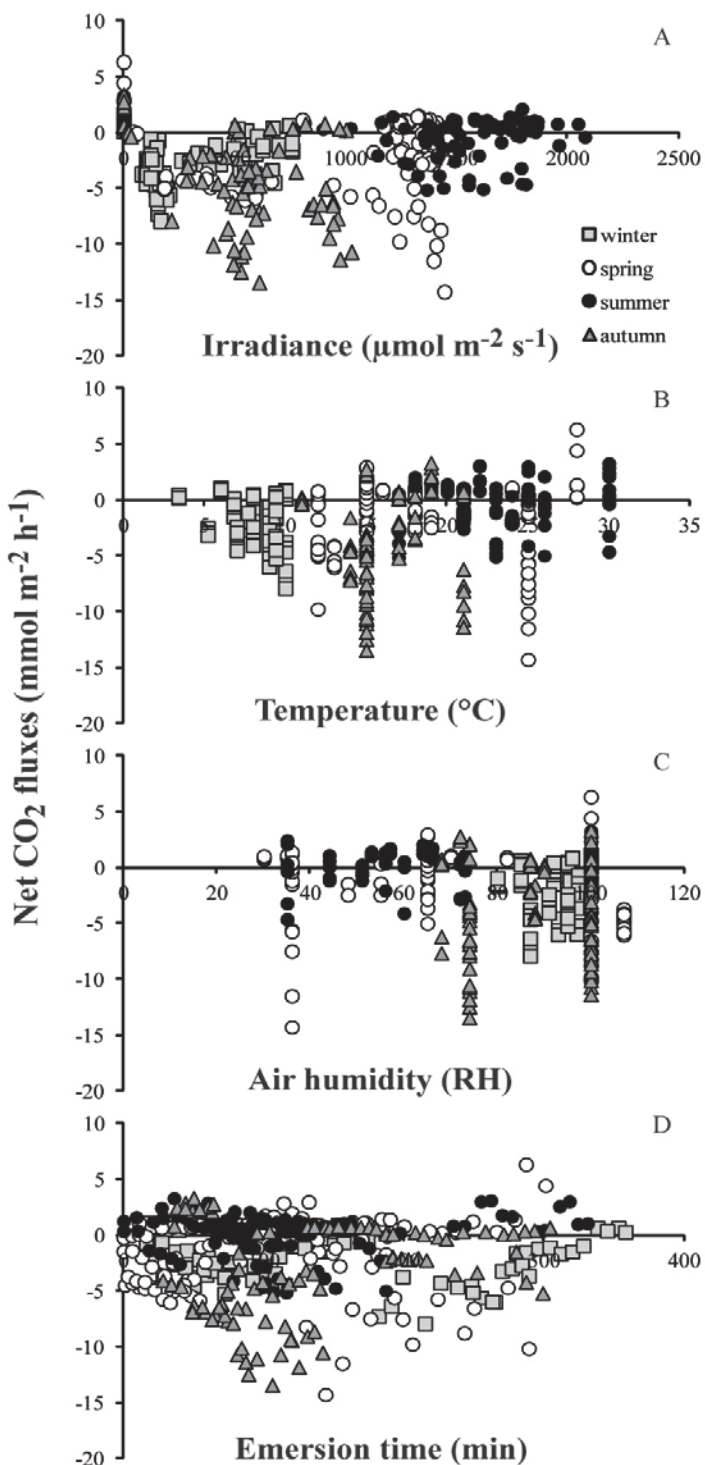


Fig. 45. Relationships between net aerial CO₂ fluxes and the four parameters measured *in situ* (A, irradiance; B, temperature; C, air humidity; D, emersion time).

seasonally with maximal values during summer (Fig. 45, B). Air humidity varied between 30 and 100% during raining events (Fig. 45, C). The emersion time is the time (min) spent in aerial condition; this parameter depends on tide conditions during measurement (Fig. 45, D).

Regression tree was used to model aerial NCP using the four physical variables measured. The model (Fig. 46) suggests that three parameters are enough to explain NCP (irradiance, air humidity and air temperature). Irradiance was the most important parameter explaining NCP variability (root of tree) and it allows discriminating incubation in dark or low irradiance from all other measures. For irradiances below $81 \mu\text{mol m}^{-2} \text{s}^{-1}$, the temperature was however the most important parameter to explain NCP increase. At highest irradiances, air humidity was the most important, and maximal NCP fluxes (average $-7.45 \text{ mmol m}^{-2} \text{ h}^{-1}$) occurred between 73.5 and 77 RH.

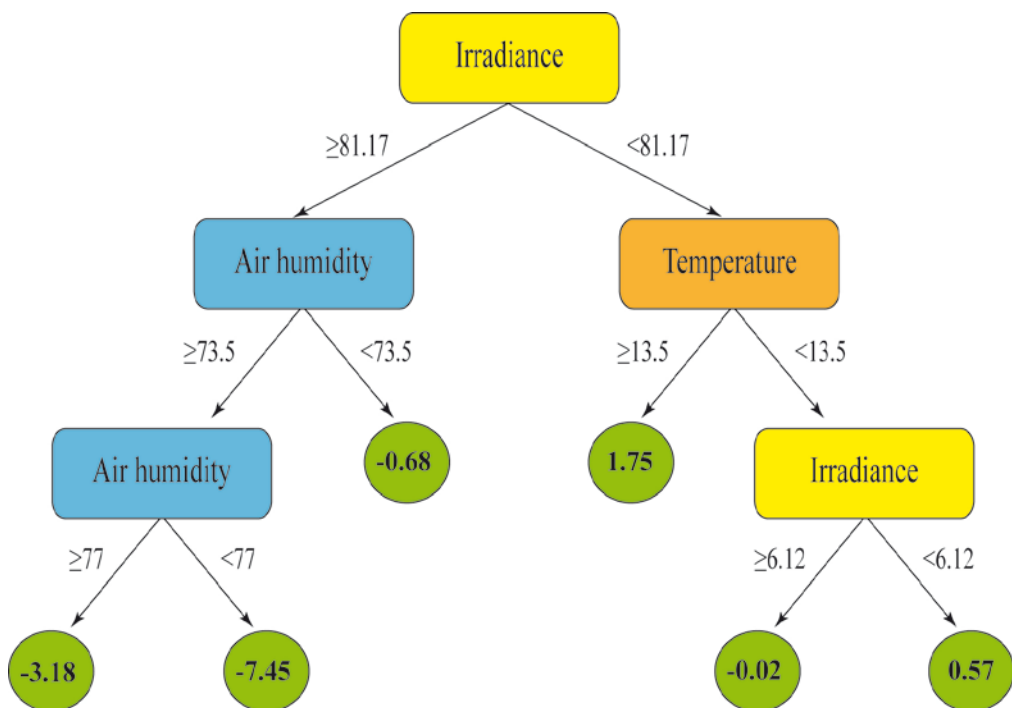


Fig. 46. Regression tree for aerial NCP fluxes produced using REPTree algorithm. Average NCP values ($\text{mmol m}^{-2} \text{ h}^{-1}$) calculated for each terminal leaf are in green circles.

The regression plots between aerial CR (Fig. 47, A) and emersion time for the three humidity treatments tested were not significantly different for slopes (ANOVA, $P>0.05$). Conversely, regression plots between aerial NCP (Fig. 47, B) and emersion time were significantly different for slopes with natural drying values significantly different from the other two treatments (ANOVA, $P<0.05$).

Community description

Four species of barnacles (*Chthamalus stellatus* (Poli), *Chthamalus montagui* (Southward), *Semibalanus balanoides* (L.), *Elminius modestus* (Darwin)), five species of gastropod (*Melarhaphe neritoides* (L.), *A. Littorina saxatilis* (Olivi), *Littorina obtusata* (L.), *Littorina compressa* (Jeffreys), *Patella* sp.), and the bivalve *Mytilus* spp. were identified on the three studied shore levels.

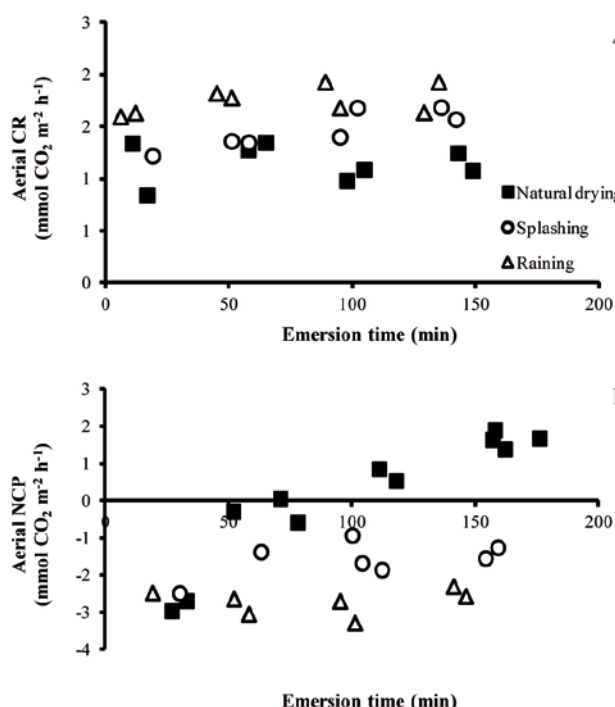


Fig. 47. Relationships between aerial carbon fluxes measured on natural drying, splashing and raining simulated conditions and emersion time (A, CR-dark incubations; B, NCP-light incubations).

Even if macrozoobenthic community composition varied between seasons and shore levels (Tab. 6), the average macrozoobenthos biomass was not significantly different between seasons and shore-levels (Kruskal-Wallis, $p>0.05$). Average animal biomass was maximal at high level ($150 \text{ g AFDW m}^{-2}$), conversely middle and low-shore level showed similar values (77 and 80 g AFDW m^{-2} , respectively).

Pigment concentrations varied between seasons and shore-levels (Tab. 7). Chl *a* was the most important pigment, followed by β -carotene. Red scytonemin and scytonemin were characteristic of the high-shore, conversely phaeophorbide *a* was present only at the middle and low-shore levels. As Chl *b* presented an unusual retention time we named this pigment

Chl *b*-like, the spectrum probably results from the co-elution of Chl *b* and Chl *d* (Kashiyama et al. 2008).

Tab. 6. Average macrozoobenthos biomass for each season and level (g AFDW m⁻²) at the three studied shore levels.

	High-shore				Middle-shore				Low-shore			
	Win	Spr	Sum	Aut	Win	Spr	Sum	Aut	Win	Spr	Sum	Aut
Barnacle	82.2	99.2	125.1	119.1	55.7	63.5	67.7	64.0	34.8	42.3	38.3	40.8
<i>M. neritoides</i>	24.6	33.6	11.4	30.6	0.2	-	0.9	-	4.1	-	-	-
<i>L. saxatilis</i>	1.6	18.5	27.0	11.2	1.6	-	2.0	-	-	-	-	-
<i>L. compressa</i>	0.7	0.2	-	0.5	3.01	7.42	2.4	1.0	16.0	19.4	41.1	7.8
<i>L. obtusata</i>	1.1	-	-	-	2.1	-	-	-	3.2	-	-	-
<i>Mytilus</i> spp.	-	-	-	-	-	-	-	-	1.1	1.1	1.1	-
<i>Patella</i> sp.	0.3	0.1	-	-	5.2	9.9	6.0	7.9	8.8	12.9	17.4	18.6
Total	125.6	151.7	163.4	161.7	67.9	80.8	79.1	80.4	77.4	75.8	97.9	67.2

Tab. 7. Pigment concentration at the three shore-levels during winter (Win), summer (Sum) and autumn (Aut) (mg m⁻²). For violaxanthin, scytonemin and red scytonemin only presence/absence data are available (*=presence).

Values for summer are not available at the high-shore.

	High-shore			Middle-shore			Low-shore		
	Win	Sum	Aut	Win	Sum	Aut	Win	Sum	Aut
Chl C2					1.4	2.4		2.7	0.6
Phaeophorbide <i>a</i>				1.5	0.2	1.0	2.1	3.4	2.1
Fucoxanthin	0.2		1.0	8.7	5.9	10.5	5.8	18.1	17.1
Zeaxanthin	0.6		1.3	0.7	1.0	1.2	2.0	3.2	2.2
Lutein	0.6		0.9	0.7	0.5	0.8	2.0	1.9	1.7
Chlorophylle <i>b</i> -like	0.9		2.3	0.9	2.8	2.7	4.8	5.7	4.4
Phaeophytin <i>a</i>	0.7		9.0	1.3	0.9	2.8	3.0	4.1	3.6
B-carotene	2.5		7.1	4.3	2.3	5.4	7.9	8.1	10.1
Chl <i>a</i>	10.8		34.1	29.5	25.3	70.7	49.6	105.3	95.8
Violaxanthin				*	*	*	*	*	*
Red scytonemin	*		*						
Scytonemin	*		*						

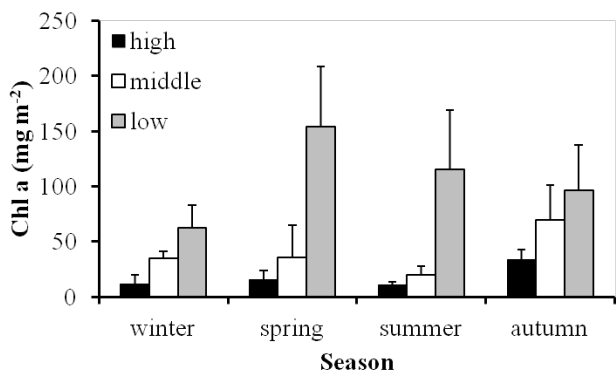


Fig. 48. Chl *a* concentration measured through fluorimetric method at the three levels and for the four seasons.

rocky surface (average 0.61 mg m^{-2}) and barnacles shell (average 0.58 mg m^{-2}) showed that the two substrate were not significantly different (Mann-Whitney, $p>0.05$).

Fluorimetric methods (Fig. 48) revealed that Chl *a* concentration was significantly different between shore levels (Kruskal-Wallis, $p<0.05$) and followed the shore gradient with maximal fluxes at the low-shore level (average 107 mg m^{-2}) and minimal at the high-shore level (average 18 mg m^{-2}). Differences between seasons were not significant (Kruskal-Wallis, $p>0.05$). Comparison of Chl *a* content between

5. Discussion

Community respiration

Community respiration measured through benthic chamber technique permits to quantify the contribution of all organisms present on the rock surface (animals, algae, lichens, bacteria). In this study, average aerial and underwater respirations are similar in emersion and immersion for the three studied shore-levels. This indicates that benthic community is well adapted to both aerial and underwater respiration. Anyway CR in emersion seems more variable and more influenced by temperature and shore level position. Low-shore level, which is emerged only for a short time period during spring water tides, showed the highest aerial respiration. Organisms living at low-shore level are less affected by desiccation and can maintain their activity during low tide; conversely high-shore species must limit their aerial activity during emersion to prevent important water loss (Newell 1973).

Since respiration can be influenced by light, our estimates of CR in darkness could underestimate the daily respiration estimates (Middelburg et al. 2005). Previous studies had established that CR of intertidal temperate communities may vary according to substrata,

wave exposure and species composition. In the intertidal seagrass dominated shore CR varies between 79.1 and 186.3 mg C m⁻² h⁻¹ (Ouisse et al. 2011), those of rocky intertidal canopy-forming algae during emersion varied between 122.1 and 615.6 mg C m⁻² h⁻¹ (Golley et al. 2008) and oyster dominated rocky shores between 16.56 and 205.92 mg C m⁻² h⁻¹ (Lejart 2009). In this study, CR results (between 4.9 and 32.2 mg C m⁻² h⁻¹) were generally lower than obtained in other shore studies but in the same order of magnitude as those measured on intertidal rock without oyster colonization (between 20.4 and 39.5 mg C m⁻² h⁻¹) (Lejart 2009) or on a rocky community after elimination of macroalgae canopy (between 2.5 and 75.6 mg C m⁻² h⁻¹) (Golley et al. 2008).

Even while macroalgae could be responsible for most of the respiratory carbon fluxes in intertidal rocky shore (Golley et al. 2008), at our study site only very small macroalgae, lichens or microalgae were present and CR fluxes seemed mostly influenced by macrozoobenthos activity.

Underwater community calcification

In the present study, CaCO₃ fluxes were estimated by the alkalinity anomaly method that is considered the most convenient for short time incubation (Gattuso et al. 1998). Estimation of alkalinity changes alone may include an error because alkalinity can be influenced by other processes, such as nutrient concentration changes through excretion. As different studies have confirmed that ammonium excretion effect on TA is smaller than the variability observed in calcification estimates, we does not consider excretion influence in our results (Jacques & Pilson 1980, Chisholm & Gattuso 1991, Gazeau et al. 2007, Tagliarolo et al. 2012b, Tagliarolo et al. 2012c). The nitrification process may also be considered as negligible in our short time incubations. Underwater CaCO₃ fluxes were significantly related to irradiance since photosynthesis and calcification processes are linked (Bensoussan & Gattuso 2007, Martin et al. 2007). The presence of algae may facilitate calcification during daytime by increasing the pH by photosynthesis, conversely the respiration process in night reduce pH (Lombard et al. 2010).

Estimation of daily fluxes showed that calcification was positive throughout the year while strongly influenced by season. Carbonate deposition on animals and algae is known to be marked by seasonal variation due principally to temperature influence (Martin et al. 2007, Clavier et al. 2009, Lejart et al. 2012, Tagliarolo et al. 2012b, Tagliarolo et al. 2012c).

Shore position seemed an important factor influencing daily calcification fluxes since growth increment is known to be controlled by tidal regime in wide variety of intertidal species (Pannella & MacClintock 1968, Fenger et al. 2007, Schöne et al. 2007).

Net community production

In the present study we have used a non-destructive technique to monitor short-term variations in aerial and underwater NCP and community calcification. This allows us to evaluate seasonal variability for the same community. Such a monitoring of the same zone through metabolism measurement should allow to detect changes in ecosystem functioning and estimate anthropic impact on intertidal rocky shore benthic communities.

The underwater GPP varied between 0.1 and 19.5 mmol C m⁻² h⁻¹ which is in the same range of those measured in emersion on rocky intertidal community after elimination of macroalgae canopy (between 0.1 and 6.34 mmol C m⁻² h⁻¹).

Variations in underwater NCP fluxes were explained principally by irradiance parameters using a Michaelis-Menten model; conversely aerial fluxes were very variable and irradiance accounts for 23% only. In order to explain the influences of different physical parameter on aerial NCP the decision tree model technique was then applied.

The machine learning methods often exhibit great power for explaining and predicting ecological patterns, but this techniques are seldom used in ecology (Olden et al. 2008). The regression decision tree is an automated model construction based on intelligent software, able to detect some structure in the data (Dalaka et al. 2000). The model is designed to search for the dependency between a dependent and a number of attribute variables. This type of model is transparent and easily interpreted; conversely other learning methods such as neural network, are more complex and constitute a “black box” that deliver results without an explanation of how these results were derived (Dreiseitl & Ohno-Machado 2002). The regression decision tree model has already been used to fit photosynthesis process for terrestrial plants and was considered as a very powerful modeling alternative to ordinary curve fitting methods (Dalaka et al. 2000).

During emersion, intertidal communities are submitted to various stresses associated with a number of environmental factors such as extreme temperature, desiccation or high light levels (Helmuth et al. 2002). Regression tree results suggest that air humidity and solar

irradiance are the two most important environmental factors explaining NCP during emersion. Even if photosynthesis process is directly correlated with light, desiccation can also significantly affect algal physiological performance (Williams & Dethier 2005, Lamote et al. 2012). When light was dim, NCP was principally influenced by temperature; when temperature were above 13°C carbon fluxes decrease. High temperature could lead to faster desiccation, and benthic species would be forced to limit gas exchanges and activity levels to avoid water losses (Little et al. 2009).

Results obtained comparing the three humidity treatments showed that while aerial CR seemed little influenced by drying or freshwater wetting, NCP depends strongly on hydration conditions. Raining and splashing simulation gave similar NCP. Intertidal macroalgae are known to be highly resistant to osmotic pressure and photosynthesis is reduced only after extensive freshwater exposure (Schagerl & Möstl 2011). In this study, natural drying condition strongly limited photosynthesis and the respiration became predominant after only one hour aerial exposure.

Average fluxes in immersion were generally lower in the air than underwater and seasonal variations were significant in both conditions. The contribution of planktonic organisms can be assumed as negligible in temperate intertidal zone (Santos et al. 2004), consequently the difference between aerial and underwater fluxes is due to different community metabolism adaptation. The differences between average aerial and underwater NCP were stronger during autumn (-3.36 and -6.15 mmol m⁻² h⁻¹, respectively) than during winter (-1.86 and -1.15 mmol m⁻² h⁻¹, respectively). Seasonal variation in photosynthesis rates of intertidal communities has already been observed (Golley et al. 2008, Ouisse et al. 2010). Light intensity and temperature are generally the two most important factors determining seasonal patterns of primary production (Dawes et al. 1978). Contrary to previous studies that exhibit maximal aerial photosynthetic production during summer, our results showed maximal rates in autumn. During the study period, while air temperature was maximal during summer and lower during autumn, sea surface temperatures reached higher values in autumn. The relationship between environmental temperature and organism body temperature during emersion is complex and influenced by other factors (irradiance, wind, body form...) (Helmuth 1998). Even if pigment concentration measured on rocky surface was similar during summer and autumn, higher desiccation stress would limit photosynthetic performance in summer during emersion, accounting for the observed results.

The three shore-levels showed significantly different NCP fluxes during emersion but not during immersion. The studied low-shore that is emerged only for short time experience less desiccation stress, which leads to higher photosynthetic production (Lamote et al. 2012).

Estimation of daily fluxes for each season and shore-level were performed only in immersion, fluxes in emersion are very variable and further model needs to be developed in order to calculate daily and annual total carbon emission. Results for underwater NCP fluxes showed that intertidal exposed rocky shore communities are predominantly heterotrophic systems that are source of CO₂ for their surrounding environment.

Community description

The studied zone was a barnacle dominated shore that typically occurs under conditions which are too severe for fucoid algae but not exposed enough for mussels (Lewis 1964). Two gastropod species (*M. neritoides* and *L. saxatilis*) characterize the high intertidal zone, conversely limpets and mussels are present only in lower levels. The winter period showed lower biomass values at the three shore levels; animals seem to be limited by their sensitivity to low winter temperature (Franke & Gutow 2004). Even if species diversity varies between the three shore levels biomasses were not significantly different.

Epilithic micro-algal biofilm are assemblages of bacteria, diatoms, cyanobacteria, other unicellular algae and the spores and germinal stages of macro-algae (Murphy et al. 2005). Pigment analysis can provide information on the phylogenetic composition of algae present on rocky surface (Millie et al. 1993, Paerl et al. 2003). In our samples, the occurrence of fucoxanthin associated with Chl *c2*, violaxanthin, zeaxanthin and β-carotene suggests the presence of brown algae at low and middle-shore levels (Zacharias 2012). The second most important group at lower intertidal zone was the chlorophyceae (chl *b*, xanthophylls, lutein, violaxanthin) that may be represented by micro and macroalgae species (Brown & Jeffrey 1992). Numerous studies performed on intertidal macroalgae support the finding that net photosynthesis is generally lower in emersion than in immersion, and that desiccation has a negative effect on net photosynthesis (Skene 2004, Williams & Dethier 2005, Sampath-Wiley et al. 2008, Brown 2009). Consequently air humidity level could be an important parameter influencing metabolism and growth of macroalgae (Martínez et al. 2012).

Because of zeaxanthin is generally considered as the biomarker of cyanophyceae, we can conclude that this group was always present at the three shore levels. The high-shore is characterized by the presence of scytonemins (specific pigments of cyanophyceae), these molecules are often synthesized in response to UV exposure forming a stable protective layer (Singh et al. 2012). Biofilm in shallow waters consists primarily of photosynthetic organisms, such as diatoms, cyanobacteria, and macroalgal germlings (Underwood 1984, Hill & Hawkins 1991). In intertidal exposed rocky shore, the photosynthetic microbial assemblage is strongly influenced by environmental stresses such as insulation and desiccation, but grazing intensity seems also an important factor regulating microbial assemblages biomass (Thompson et al. 2004).

The high concentration of β -carotene in the high-shore indicates the presence of lichens (Niall 2012). Lichens are among the organisms adapted to harshest environment and are able to colonise intertidal rocky shores and resist to salt and dry stresses (Grube & Blaha 2005). Lichen's photobionts are able to stop photosynthetic activity when dehydrated (Bukhov et al. 2004) and could protect them against UV thanks to anti-oxidant production (de la Coba et al. 2009).

This study demonstrates that while NCP of intertidal rocky shore community are different in emersion and immersion, the CR is similar in the two conditions. The underwater NCP seems influenced exclusively by irradiance; conversely aerial fluxes depend strongly on desiccation. Calculation of seasonal carbon fluxes suggests that intertidal exposed rocky shores communities are heterotrophic systems that are sources of CO₂ for their surrounding environments.

Since the community species composition of the studied zone is typical of temperate macrotidal exposed rocky shore, carbon fluxes measured in this study could be considered representative for this type of coastal ecosystem. For this reason, results could use for calculation of carbon budget at regional scale.

Chapitre 5

Contribution de la macrofaune de substrat rocheux exposé aux flux de carbone sur une échelle régionale. Évaluation de l'effet du réchauffement climatique sur les flux respiratoires.

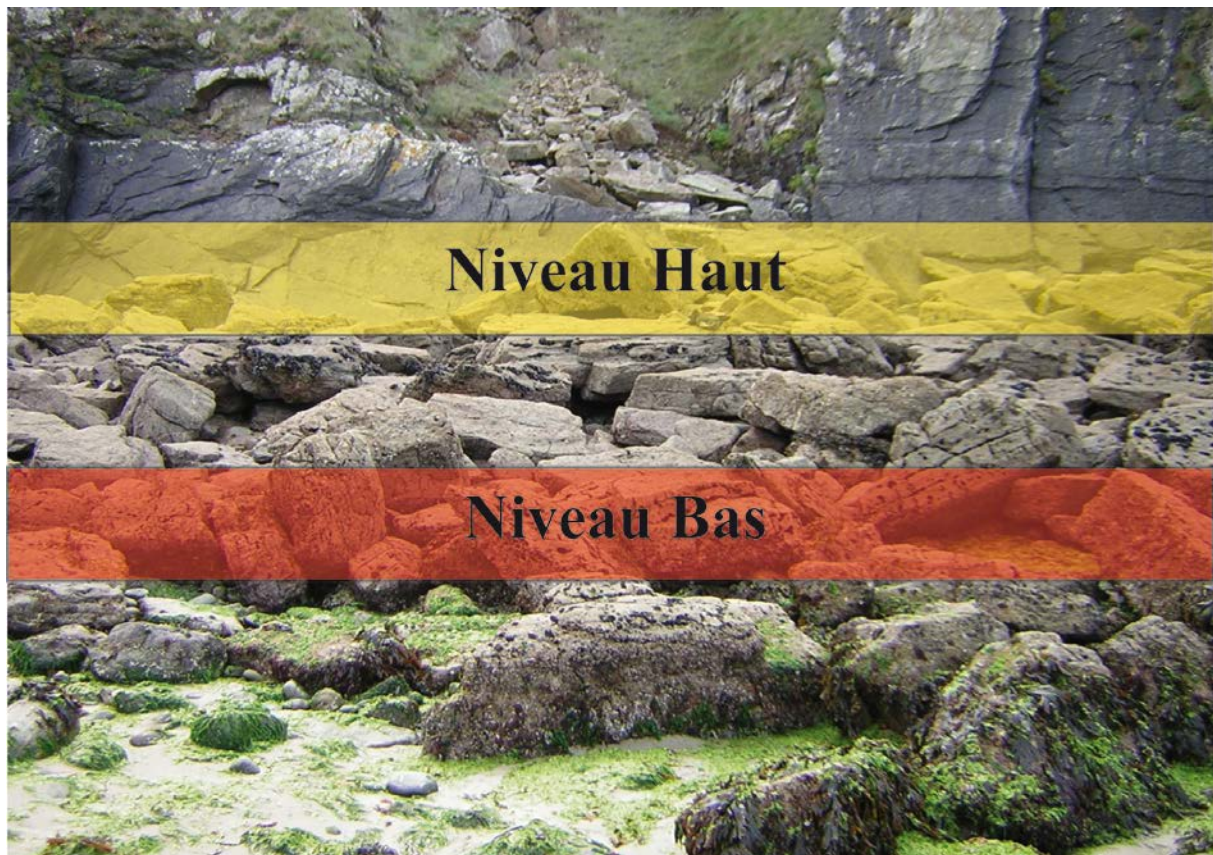


Fig. 49. Positionnement représentant les deux niveaux de l'estran choisis pour le suivi de la faune benthique dans le cadre du programme REBENT.

1. Contexte général et résumé

Le rôle de la zone côtière dans les cycles globaux du carbone n'a pas encore été entièrement clarifié. Les communautés y sont diverses et elles peuvent constituer soit une source soit un puits de carbone pour l'atmosphère (Siefert & Plattner 2004). Les écosystèmes benthiques côtiers sont caractérisés par une forte hétérogénéité spatiale et temporelle (Middelburg et al. 2005) et la quantification des taux globaux de respiration est rendu difficile par une connaissance imparfaite de la contribution de ces communautés benthiques côtières.

L'estimation des flux de carbone annuels sur la zone rocheuse intertidale nécessite la prise en compte de l'alternance des phases d'immersion et d'émergence, des variations des paramètres abiotiques et de la composition en espèces des communautés. Pour calculer des bilans à l'échelle d'un écosystème côtier, il faut prendre en compte les variations géographiques de la composition et de la biomasse des différentes communautés, qui peuvent varier géographiquement selon les conditions environnementales et les impacts anthropiques. De plus, les paramètres physiques et chimiques peuvent être influencés par des variations à plus large échelle comme celles qui sont liées au réchauffement climatique (Borges 2011).

Pour cette raison nous proposons, dans ce chapitre, une première estimation des variations spatiales et temporelles du métabolisme de la faune benthique de substrat rocheux à une échelle régionale. Les résultats de cette estimation sont ensuite utilisés pour évaluer l'impact du réchauffement climatique sur les flux de carbone.

Pour cela, nous avons calculé des bilans de carbone par extrapolation à partir des mesures d'abondance d'espèces sur neuf sites répartis autour de la Bretagne. Les temps d'immersion et d'émergence et les différentes températures moyennes annuelles de l'air et de la surface de la mer, ont été considérés. Les données d'abondance de la faune intertidale ont été fournies par le programme REBENT (REseau de surveillance BENThique).

L'objectif du réseau REBENT est d'acquérir des connaissances sur la faune et la flore benthique de la zone côtière françaises, et de mettre en place un système de surveillance pour détecter l'évolution de leurs habitats. Le programme est actif en Bretagne depuis 2003 et considère les habitats rocheux et meubles intertidaux et subtiaux.

Les données obtenues par le réseau REBENT nous ont permis de travailler sur deux niveaux de l'estran (Fig. 49), significativement différents à la fois par leur composition spécifique et les flux de carbone liés à leur métabolisme. Les flux de carbone se sont, en effet, avérés très variables entre les différents sites, et les variations annuelles de l'abondance des espèces ne semblent pas les influencer sensiblement.

L'effet des changements de température sur les taux respiratoires a été estimé en simulant une fluctuation des températures sur chaque site. Une augmentation de 1°C provoquerait ainsi un accroissement d'environ 4% des émissions de carbone par les zones rocheuses intertidales étudiées. En conséquence, à l'échelle régionale, les communautés intertidales peuvent être considérées comme une source potentielle de carbone sous l'influence du réchauffement climatique.

Carbon production of intertidal exposed rocky shore animal communities.

Morgana Tagliarolo, Jacques Grall, Laurent Chauvaud, Jacques Clavier

2. Introduction

Coastal marine ecosystems are among the most ecologically and socio-economically vital on the planet (Harley et al. 2006). Although the continental margins, considered here to extend from the coastline to a depth of 200m, occupy only a little over 7% of the seafloor and less than 0.5% of the ocean volume, they play a major role in oceanic biogeochemical cycling (Chen & Borges 2009). Unfortunately, the contribution of coastal zone to carbon global cycles is not yet clarified, as coastal ecosystems are characterised by a strong temporal and spatial heterogeneity (Middelburg et al. 2005). Different studies indicate that continental margins could be a source of CO₂ to the atmosphere (Smith & Mackenzie 1987, Smith & Hollibaugh 1993, Mackenzie et al. 2000) even if benthic community living in this zone could be a sink or a source for the atmospheric carbon (Siefert & Plattner 2004). In this situation, the estimation of total carbon emissions still requires further investigation.

Compared to other coastal communities, intertidal rocky shore is characterized by a large biodiversity and various adaptations to aerial exposure. Quantification of carbon fluxes from intertidal rocky shore communities requires the consideration that immersion and emersion succession cause variation of different physic-chemical parameters (such as temperature, light, desiccation, salinity), and changes in community composition along the coast. Since organisms' metabolism is generally influenced by temperature, carbon emissions will change depending on temperature variations.

According to the Fourth Assessment Report of the Intergovernmental Panel on Climate Change (IPCC-2007), the global mean surface air temperature increased by 0.74°C while the global mean sea surface temperature (SST) rose by 0.67°C over the last century (Trenberth & Josey 2007). However, the warming has been neither steady nor the same at different locations. Thus European seas have experienced an rapid increase in temperature of about

0.67-0.80 °C between 1982 and 2006 (Belkin 2009). Measurements performed in the English Channel for the period 1986-2006 indicate that warming is not homogeneous in this area and that the central part of the channel and the western part of French Brittany exhibit a lower warming rate (about 0.6°C) than the Northern part (Saulquin & Gohin 2010). Reliable predictions of climate change in the immediate future are difficult, especially at the regional scale, where natural climate variations may amplify or mitigate anthropogenic warming (Lean & Rind 2009). In long-term projections extending towards the end of this century and beyond, a large part of the uncertainty is associated with the trend of anthropogenic greenhouse gas emissions and the resulting external forcing of the climate system. The mean global warming estimated by IPCC multi-model vary between 1.1°C to 6.4°C (Meeht & Stocker 2007). Mean temperature in Europe is predicted to increase more than the global average. The largest climate warming is expected in the northern Europe, especially in winter, while cooling would occur in southern Europe throughout the year as well as in central Europe in summer (Christensen et al. 2007).

Increasing concentrations of CO₂ and other greenhouse gases in the atmosphere are considered as the major cause of global-mean surface air temperature rise during the twentieth century and are projected to accelerate the rate of global warming (Meeht & Stocker 2007). The present study is based on available carbon fluxes estimated for the main macrozoobenthic species, and their abundance on the coasts of Brittany, to estimate the contribution of intertidal exposed rocky shore communities to CO₂ emission. The importance of both respiration and calcification during immersion and emersion period was evaluated for different species. Fluxes were calculated at two shore level and spatial and temporal natural variation was examined at a regional scale. The effect of temperature variation on carbon emissions was tested.

3. Material and methods

Sampling strategy

The abundance of the studied benthic species were provided by REBENT network (REseau BENThique). The main goal of this network is to define a reference state and

provide a monitoring of coastal benthic habitats to detect changes at various scales over time and space (Ehrhold et al. 2006). The Brittany coast (France) was chosen as a pilot region to test protocols and methods.

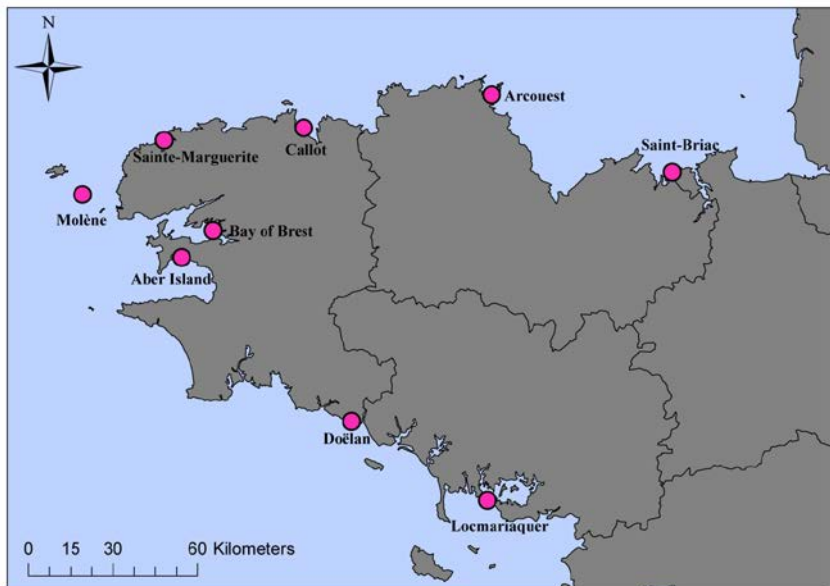


Fig. 50. REBENT sites for intertidal rocky shore communities monitoring.

community living in the upper eulittoral zone and “low-shore” for animals living in the lower part of the eulittoral zone.

Non-destructive methods are used annually to estimate the macrozoobenthic community composition and abundance in each studied zone since 2004. Ten quadrats of 0.1 m^2 divided in 40 smaller quadrats of 25 cm^2 are sampled once a year at the same position on the shore. On each 0.1 m^2 quadrat, large macrofauna abundance is evaluated directly *in situ*. Photographs of five randomly selected 25 cm^2 quadrats are taken on each 0.1 m^2 quadrat and photo analysis is performed using Quantum GIS software to assess barnacle and small gastropod abundances.

Some records are not available because of technical problems or poor weather conditions, during sampling. In this study, we have used data from six years’ monitoring (2004-2005-2006-2007-2009-2010). To uniform data species abundance was averaged from 7 quadrats of 0.1 m^2 for large species and 21 quadrats of 25 cm^2 (3 for each 0.1 m^2 quadrat) for small animals. Carbon fluxes were estimated for five species groups: barnacles (*Semibalanus balanoides*, *Elminius modestus*, *Chthamalus stellatus*, *Chthamalus montagui*), limpets

REBENT is monitoring rocky intertidal fauna at 9 sites (Fig. 50). They have similar hydrodynamic conditions and they are representative of exposed or moderately exposed shores where algal cover is limited or nil. The monitoring was performed at two shore levels; here we use the term “high-shore” to refer to

(*Patella vulgata*, *Patella depressa*, *Patella ulyssiponensis*), mussels (*Mytilus* spp.), oyster (*Crassostrea gigas*), and gastropods (*Gibbula pennanti*, *Gibbula umbilicalis*, *Littorina littorea*, *Littorina obtusata*, *Littorina saxatilis*, *Nucella lapillus*).

Environmental parameters

Immersion/emersion times as well as aerial and underwater temperature were considered to extrapolate carbon fluxes on an annual scale. Water height was calculated every 15 min according to SHOM (Service Hydrographique et Océanographique de la Marine) tide tables. The high-shore was immersed for 640 h year⁻¹ and the low-shore for 4103 h year⁻¹. Average annual air and sea surface temperature was calculated from data recorded in the vicinity of each sampling site from Météo-France and PREVIMER (IFREMER).

Carbon fluxes

Carbon fluxes were calculated for immersion and emersion periods considering both respiration and calcification processes. For each species average biomass at each level and season was calculated by multiplying the average individual biomass (g ash free dry weigh) by the number of individuals. To obtain more accurate biomass estimates, limpets and mussels were divided in two size classes (more or less than 2.5 cm) during photo analysis, and the average individual biomass was estimated accordingly.

Respiration was estimated as a function of temperature and average biomass using Arrhenius parameters. Data were provided by previous studies conducted on the same geographical area during both high and low tide period (Tab. 8) (Clavier et al. 2009, Lejart et al. 2012, Tagliarolo et al. 2012a, Tagliarolo et al. 2012b, Tagliarolo et al. 2012c). Since mussels underwater respiration is not influenced by temperature (Tagliarolo et al. 2012b), average fluxes were utilized in calculations. Mussels' carbon fluxes are known to be different between large and small individuals. Respiration and calcification parameters were then chosen for each year and site, in function of the predominant mussels size, according to the results of Tagliarolo et al. (2012b). Since data were not available for *L. obtusata*, parameters measured for *G. pennant*, that has a similar size and distribution, were utilized (Tagliarolo et al. 2012a).

Calcification contribution to carbon fluxes during immersion was calculated using average annual fluxes available for the different species (Tab. 8) (Clavier et al. 2009, Lejart et al.

2012, Tagliarolo et al. 2012a, Tagliarolo et al. 2012b, Tagliarolo et al. 2012c). When calcification occurs in the aquatic environment, CO₂ is released into the surrounding water. The deposition of one mole of calcium carbonate releases approximately 0.6 mole of CO₂ into the seawater at 25°C temperature and 35 for salinity (Frankignoulle et al. 1995). To calculate the contribution of calcification to carbon fluxes, we estimated the molar ratio of CO₂ released by calcification to calcium carbonate precipitated, as a function of average sea water temperature (Frankignoulle et al. 1994).

To tentatively estimate the effect of temperature on average annual carbon fluxes, calculations were repeated for mean temperature of ± 0.5, 1, 1.5 and 2 °C from the studied year, for each year and sampling site, and results were averaged by shore level.

Tab. 8. Mean calcification and parameters of Arrhenius plots relating the logarithm of hourly underwater and aerial respiration rates per g AFDW to the inverse of absolute temperature. *a*, normalization constant; *Ea*, activation energy (Joules per mole); *K*, Boltzmann's constant (8.31 JK-1 mol-1).

	Underwater respiration		Aerial respiration		Mean calcification μmol CaCO ₃ g ⁻¹ h ⁻¹	Reference
	Ln a	Ea/k	Ln a	Ea/k		
Barnacles	29.6	7.86	28.75	7.63	1.01	(Clavier et al. 2009)
<i>Gibbula pennanti</i>	55.28	15.07	22.68	5.75	6.84	(Tagliarolo et al. 2012a)
<i>Gibbula umbilicalis</i>	47.52	12.89	16.84	3.99	7.56	(Tagliarolo et al. 2012a)
<i>Littorina littorea</i>	43.28	11.71	16.33	4.07	3.36	(Tagliarolo et al. 2012a)
<i>Littorina obtusata</i>	55.28	15.07	22.68	5.75	7.56	(Tagliarolo et al. 2012a)
<i>Littorina saxatilis</i>	27.61	7.13	6.69	1.07	16.12	(Tagliarolo et al. 2012a)
<i>Melarhaphe neritoides</i>	11.47	2.37	29.97	7.65	19.11	(Tagliarolo et al. 2012a)
<i>Mytilus</i> spp. Large (>3cm)	26.4	μmol DIC g ⁻¹ h ⁻¹	49.15	13.77	4.3	(Tagliarolo et al. 2012b)
<i>Mytilus</i> spp. Small (<3cm)	35.9	μmol DIC g ⁻¹ h ⁻¹	54.95	14.99	15.7	(Tagliarolo et al. 2012b)
<i>Nucella lapillus</i>	41.22	11.08	36.4	9.79	3.50	(Tagliarolo et al. 2012a)
<i>Osilinus lineatus</i>	28.16	7.3	27.21	7.15	1.92	(Tagliarolo et al. 2012a)
<i>Ostreidae</i> spp.	56.44	15.53	27.74	8.02	4.5	(Lejart et al. 2012)
<i>Patella</i> spp.	34.41	9.26	11.82	2.55	3.2	(Tagliarolo et al. 2012c)

4. Results

Environmental parameters

The average annual air temperature in Brittany coastal zone vary between 11.2°C in 2010 and 12.3°C in 2007 (Tab. 9). Minimal values were recorded near Brest and maximal values near the monitoring site Arcouest. Sea surface average annual temperatures range between 12.2 °C in 2010 and 13.8 in 2007 (Tab. 9). Minimal values were recorded in the north of Brittany and maximal in the south.

Tab. 9. Annual variation of average sea surface (above value) and air (below value) temperatures in °C from 2004 to 2010 (Météo-France and PREVIMER (IFREMER)). See Fig. 50 for location of sites.

	2004	2005	2006	2007	2008	2009	2010
Callot	13.04 11.63	13.02 11.89	12.82 12.07	13.41 11.93	12.88 11.63	12.67 11.68	12.20 10.96
Doelan	13.85 12.16	13.79 12.22	13.69 12.58	13.87 12.39	13.50 11.68	13.39 11.82	13.20 11.02
Île de l'Aber	13.45 11.53	13.47 11.77	13.28 12.04	13.46 11.89	13.05 11.41	12.86 11.53	12.50 10.70
l'Arcouest	13.04 12.53	13.02 12.75	12.82 12.80	13.41 12.92	12.88 12.38	12.67 12.33	12.20 11.60
Locmariaquer	13.85 12.50	13.79 12.80	13.69 12.78	13.87 12.40	13.50 12.05	13.39 12.53	13.20 11.59
Molene	13.45 12.16	13.47 12.30	13.28 12.55	13.46 12.53	13.05 12.11	12.86 12.02	12.60 11.63
Rade de Brest	13.45 11.53	13.47 11.77	13.28 12.04	13.46 11.89	13.05 11.41	12.86 11.53	12.50 10.70
Saint Briac	13.04 11.81	13.02 12.06	12.82 12.32	13.41 12.15	12.88 11.65	12.67 11.62	12.20 10.84
Sainte Marguerite	13.04 12.34	13.02 12.44	12.82 12.50	13.41 12.59	12.88 12.25	12.67 12.08	12.20 11.58

Spatial and temporal natural variation of carbon fluxes

Total annual carbon emissions at the two shore levels are not significantly different between the six studied years (Kruskal-Wallis >0.05). Conversely, carbon fluxes varies significantly between sites (Kruskal-Wallis <0.05 for both shore levels) (Fig. 51). High and low-shore carbon fluxes are maximal at Doëlan site (27.1 and 59.9 mol C m⁻² yr⁻¹, respectively) and minimal at Molene (0.7 and 0.9 mol C m⁻² yr⁻¹, respectively).

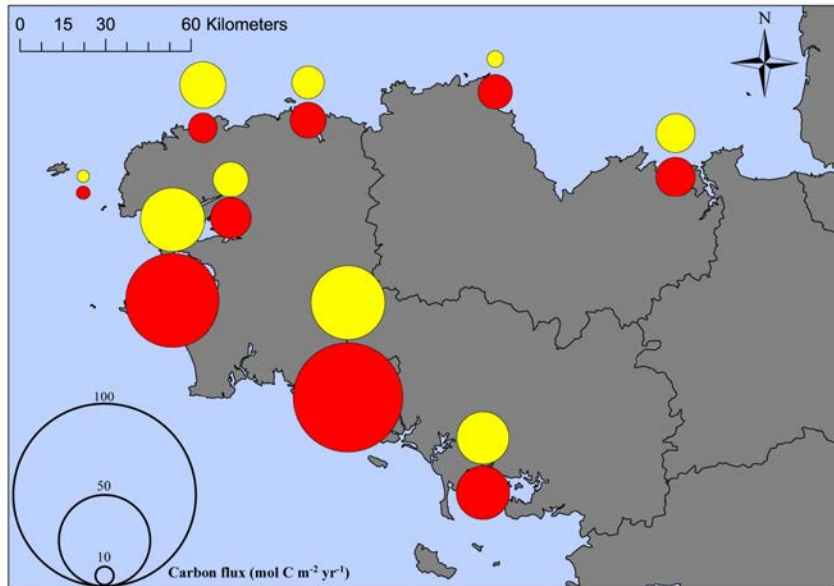


Fig. 51. Geographical variation of average annual carbon fluxes ($\text{mol C m}^{-2} \text{ yr}^{-1}$) in high-shore (yellow point) and low-shore (red point).

11). Barnacles are present in all studied sites and their average contribution to total average fluxes is important (4.3 and $4.2 \text{ mol C m}^{-2} \text{ yr}^{-1}$, in high and low-shore respectively); conversely, mussels showed a patched distribution with higher abundance, and thus fluxes, at Doëlan and Aber Island sites (Tab. 10 and Tab. 11). Limpets are largely distributed on all sites but their contribution to total carbon fluxes is less important.

Tab. 10. Carbon fluxes ($\text{mol C m}^{-2} \text{ yr}^{-1}$) calculated at high-shore level for each site and species group (aerial respiration-underwater respiration-calcification) and total values.

	Barnacle	Mussel	Limpet	Oyster	Gastropod	Total
Callot	2.6-0.2-0.0	/	0.3-0.0-0.0	/	2.0-0.1-0.1	5.3
Doelan	5.2-0.5-0.0	/	0.5-0.0-0.0	/	18.5-1.6-0.8	27.1
Aber Island	7.7-0.7-0.1	/	2.4-0.1-0.0	/	8.5-0.7-0.4	20.7
l'Arcouest	0.5-0.0-0.0	/	0.7-0.0-0.0	/	0.1-0.0-0.0	1.4
Locmariaquer	5.6-0.5-0.0	/	/	/	6.5-0.5-0.3	13.5
Molene	0.2-0.0-0.0	/	/	/	0.4-0.0-0.0	0.7
Bay of Brest	4.7-0.5-0.0	/	/	/	1.0-0.1-0.0	6.3
Saint Briac	3.7-0.3-0.0	0.1-0.1-0.0	0.8-0.0-0.0	/	2.2-0.2-0.1	7.5
Sainte Marguerite	4.2-0.4-0.0	/	3.5-0.1-0.0	/	2.2-0.2-0.1	10.7

The contribution of the five species' groups to the total carbon fluxes is different between sites and between levels at the same site. While barnacles carbon fluxes are important at both shore levels, emission due to gastropods are stronger

at high-shore and those due to mussel at the low-shore level (Tab. 10 and Tab.

Mean carbon fluxes from high-shore ($10.7 \text{ mol C m}^{-2} \text{ yr}^{-1}$) are mostly due to aerial respiration (90% of total fluxes), underwater respiration plus calcification process were less important (8 and 2%, respectively). In low-shore, underwater respiration is predominant (58% of total fluxes), aerial respiration represents 30% and calcification 12% of total carbon fluxes.

Tab. 11. Carbon fluxes ($\text{mol C m}^{-2} \text{ yr}^{-1}$) calculated at low-shore for each site and species group (aerial respiration-underwater respiration-calcification), and total values.

	Barnacle	Mussel	Limpet	Oyster	Gastropod	Total
Callot	1.6-1.6-0.1	/	1.3-0.5-0.1	/	0.5-0.7-0.1	6.5
Doelan	3.6-3.9-0.3	9.1-27.2-8.2	1.3-0.5-0.1	/	2.4-2.3-1.2	59.9
Aber Island	2.8-3.0-0.2	3.1-29.3-3.5	0.9-0.4-0.1	/	0.2-0.2-0.1	43.8
l'Arcouest	1.6-1.5-0.1	0-0.1-0	1.1-0.4-0.1	0-0.4-0.2	0.1-0.2-0	5.9
Locmariaquer	2.9-3.0-0.2	0.3-0.7-0.2	1.7-0.7-0.2	0.1-1.4-0.4	0.9-1.0-0.3	14.0
Molene	/	/	0.6-0.2-0.1	/	/	0.9
Bay of Brest	2.3-2.4-0.2	/	1.2-0.5-0.1	0.1-0.9-0.3	0.1-0.1-0	8.4
Saint Briac	1.7-1.7-0.1	/	1.0-0.4-0.1	/	1.0-1.0-0.5	7.7
Sainte Marguerite	1.0-1.0-0.1	/	1.3-0.5-0.1	/	0.2-0.2-0.1	4.4

Effect of temperature variation on carbon fluxes

The average carbon emission calculated for the different studied years and monitoring sites is of $10.3 \text{ mol C m}^{-2} \text{ yr}^{-1}$ at the high-shore and $17.1 \text{ mol C m}^{-2} \text{ yr}^{-1}$ at the low-shore level. Simulation of temperature effect on carbon fluxes shows a linear increase for both levels (Fig. 52). The two levels exhibits similar responses to temperature changes and regression slopes are

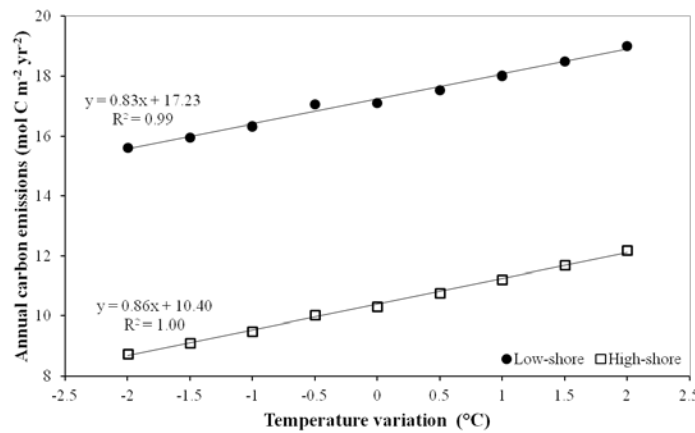


Fig. 52. Estimated annual carbon fluxes ($\text{mol C m}^{-2} \text{ yr}^{-1}$) for exposed rocky shore communities in function of temperature variation. 0 correspond to the average annual temperature calculated for the studied period.

not significantly different (ANOVA<0.05) with an increase of about $10 \text{ g C m}^{-2} \text{ yr}^{-1}$ for each 1°C change in temperature.

5. Discussion

Spatial and temporal natural variation of carbon fluxes

In this study, carbon fluxes were calculated from direct measurements in the laboratory using closed chambers in immersion (dissolved inorganic carbon fluxes) and emersion (CO_2 fluxes) (Clavier et al. 2009, Lejart et al. 2012, Tagliarolo et al. 2012a, Tagliarolo et al. 2012b, Tagliarolo et al. 2012c). Calcification and respiration related carbon fluxes were calculated for each species as a function of the average annual temperature of air and sea surface. The average total annual carbon emission was of $10.7 \text{ mol C m}^{-2} \text{ yr}^{-2}$ ($129 \text{ g C m}^{-2} \text{ yr}^{-2}$) in low-shore and of $17.8 \text{ mol C m}^{-2} \text{ yr}^{-2}$ ($213 \text{ g C m}^{-2} \text{ yr}^{-2}$) in high-shore. These estimations of community carbon production are similar to the annual community respiration calculated in intertidal sandy and muddy system ($14\text{-}188 \text{ g C m}^{-2} \text{ yr}^{-2}$) (Migne et al. 2009) but less important than respiration measured on maerl beds ($407 \text{ g C m}^{-2} \text{ yr}^{-2}$) (Martin et al. 2007).

Rocky shores support a variety of habitat and are characterized by highly heterogeneity due to different physical conditions (Kostylev et al. 2005). Estimation of coastal system fluxes depends on measures of different costal community and on their respective surface area (Laruelle et al. 2010). Little was known about the contribution of intertidal exposed rocky shore communities, and the present study has considered both temporal and special variability in order to give an evaluable estimation of carbon emission of this type of habitat.

While annual variation in community composition seems not to affect significantly carbon fluxes, the geographical variability is significant. In exposed shores, local factors such as temperature, water currents, substrate type and biological interactions may explain the variability between sites (Lewis 1964).

Our study evaluated the contribution of the major population of fauna living in exposed rocky shores; algae respiration and production were not considered. Algae and microalgae were indeed not studied during the REBENT program on exposed rocky shore community,

because they were mostly absent from the monitored sites. The contribution of bacteria to carbon fluxes can also be important, and *in situ* measurements would be necessary to evaluate the entire ecosystem respiration and primary production contribution to carbon fluxes (Golley et al. 2008).

High and low-shore community showed a different community composition and, while high-shore is immersed for average 26 days per year on average, low-shore is mostlyimmerged (average 171 days per year). At high-shore level, population of barnacles and of *M. neritoides* are predominant and their contribution to total fluxes are 40 and 51%, respectively. At low-shore level, mussels contribute to 55% of the total fluxes but they are present only on a few sites. Mussels can form extensive beds of juvenile on wave-exposed shores, with patchy distribution with gaps in the overall cover (Little et al. 2009). Conversely limpets and the other gastropods are largely distributed on both shore levels and were recorded at all studied sites.

The different contribution of high and low-shore levels to aerial and underwater fluxes is mainly due to their different air/water exposition time. Since we postulate that calcification process is possible only underwater (Pannella 1976, Buschbaum & Saier 2001), carbon production from calcification is higher at the low-shore than at the high-shore level. At low-shore level, the carbon originating from calcification corresponds to 12% of the total carbon emission. This is in accordance with previous measurements in similar tidal conditions for each studied species (11% for limpets, 25% for oyster, 3% for barnacles, between 7 and 14% for mussels and between 13 to 23% for the other gastropods) (Clavier et al. 2009, Lejart et al. 2012, Tagliarolo et al. 2012a, Tagliarolo et al. 2012b, Tagliarolo et al. 2012c). However, previous studies based on estimation of carbon fluxes from biomass and calcimass values provided substantially higher estimates of the contribution of calcification process to total carbon production (between 47 and 82%) (Golley et al. 2008, Hily et al. in press).

Effect of temperature variation on carbon fluxes

The response of communities to the changes in temperature involves biological-mediated metabolic processes. Animals respiration is directly correlated with temperature and can be described by Arrhenius equation, whereas carbon released from calcification process also depends on sea water temperature (Frankignoulle et al. 1994).

The contribution of intertidal exposed rocky shore to carbon production, calculated from temperature and community abundances from 2004 and 2010, vary between 11 and 18 mol C m⁻² yr⁻² and seems not influenced by annual temperature and variations in community composition. From 2004 to 2010, the annual temperature range was 1.2 °C at sea surface and of 1.5°C in the air.

According to the IPCC estimations, global air and sea surface temperature have risen in the past century and warming trends are expected to accelerate in the current century (Trenberth & Josey 2007). In our study, the impact of a variation of ±2°C was tested in order to evaluate the response of benthic community to temperature variations. The two eulittoral levels showed similar responses with a variation of 0.8 mol C m⁻² yr⁻² for each 1°C shift in temperature. The potential feedback to an increase of 1°C could lead to an increase of 4% of carbon emission from intertidal exposed rocky shore community.

Global change can promote coastal community metabolism through changes in coastal physics, increase in terrestrial inputs and shift in carbonate chemistry by pH modification. Carbon fluxes estimated in this study may contribute to understand metabolic responses to climate warming. However, we did not consider the possible influence of temperature variation on community composition and the effect of a possible ocean acidification induced by the increase of atmospheric CO₂ (Harley et al. 2006, Byrne 2011). Many marine organisms live close to their thermal tolerance and an increase in temperature can negatively impact the performance and survival of marine organisms (Somero 2002). In the present study, we have showed that even if community composition varies between years, CO₂ fluxes remain relatively constant. Although species composition may changes because of global warming, the carbon emission calculated for a site will remain roughly the same.

Intertidal rocky shore assemblages are generally accessible and easy to monitoring. They are thus considered suitable to study the effect of global changes on coastal areas (Cruz-Motta et al. 2010). *In situ* estimations of carbon fluxes are possible but they are yet complicated and expensive, for these reasons they have been used for short-term and small-scale assessments only (Golley et al. 2008, Tagliarolo et al. in preparation). The method used in this study is rather simple and require only species abundances to monitor large surface and different sites. Because of the important spatial variability of intertidal communities, large-scale studies for

global carbon estimations are required; carbon fluxes estimated in our study could be considered representative for temperate barnacle dominated rocky shore.

Responses of coastal ecosystem to climate changes are unpredictable, but the influence of global warming for community metabolism is clearly important. The responses of intertidal exposed rocky shore invertebrate to temperature increases could intensify CO₂ emission and consequently climate change process.

Synthèse générale et perspectives

L'océan est considéré globalement comme un puits de CO₂ atmosphérique (Sabine et al. 2004), alors que le statut des zones côtière reste encore, de ce point de vue, mal connu. Plusieurs études ont tenté d'établir si cette zone pouvait être considérée globalement comme une source ou un puits de CO₂ pour l'atmosphère, mais les résultats se sont avérés très dépendants des caractéristiques de la zone d'étude, notamment du type d'écosystème (Chen & Borges 2009, Borges 2011). Des approches à différents échelles temporelles et spatiales sont donc nécessaires pour pouvoir appréhender l'hétérogénéité et la variabilité des flux de carbone de la zone côtière.

Le travail développé dans cette thèse a permis de quantifier les émissions de carbone des estrans rocheux, à travers des mesures en laboratoire à l'échelle spécifique et des mesures *in situ* à l'échelle de la communauté.

Comparaison des flux de carbone des différentes espèces macrozoobenthiques intertidales

Les mesures de flux de carbone en laboratoire nous ont permis de comparer les principales espèces de faune vivant à différents niveaux de l'estran. Les techniques employées avaient déjà été mises en œuvre pour mesurer le métabolisme des balanes (Clavier et al. 2009) et des huîtres (Lejart et al. 2012) dans les mêmes environnements. Les mesures que nous avons réalisées viennent donc compléter cette approche et nous disposons maintenant de suffisamment d'informations pour caractériser le métabolisme de la macrofaune des zones intertidales rocheuses de la zone étudiée. Nous avons ainsi pu mettre en évidence des différences inter et intra-spécifiques importantes entre les flux respiratoires en émersion et en immersion (Fig. 53).

Afin de pouvoir évaluer l'effet de la température sur le métabolisme des différentes espèces étudiées, les flux de carbone en émersion et en immersion ont été calculés pour trois températures. Les températures utilisées dans les calculs sont la valeur moyenne mensuelle minimale (6°C), moyenne (13°C) et maximale (18°C) relevée pendant la période d'étude. Le rapport entre la respiration en émersion et en immersion diminue avec la température pour la majorité des espèces, à l'exclusion de *Melarhaphe neritoides* et *Mytilus* spp. dont la

corrélation entre la respiration en immersion et la température n'a pas été établie. Pendant la marée basse, les animaux intertidaux peuvent se fermer hermétiquement et empêcher les échanges gazeux ou bien exposer leurs branchies pour permettre une respiration aérobie. Une telle respiration à l'air est avantageuse pour la conservation de l'énergie mais elle expose les animaux à d'importantes pertes en eau par évaporation (Widdows et al. 1979, McMahon 1988, Sokolova & Portner 2001). Avec l'augmentation de la température, le risque de dessiccation augmente et les animaux tendent à minimiser les échanges avec l'extérieur et à diminuer leur taux métabolique. Les individus appartenant à des espèces où la respiration aérienne est très faible (rapport air/eau inférieur à 1), sont généralement inactifs pendant l'émergence, ce qui diminue leur dépendance vis-à-vis de la température (Houlihan 1979, Houlihan & Innes 1982).

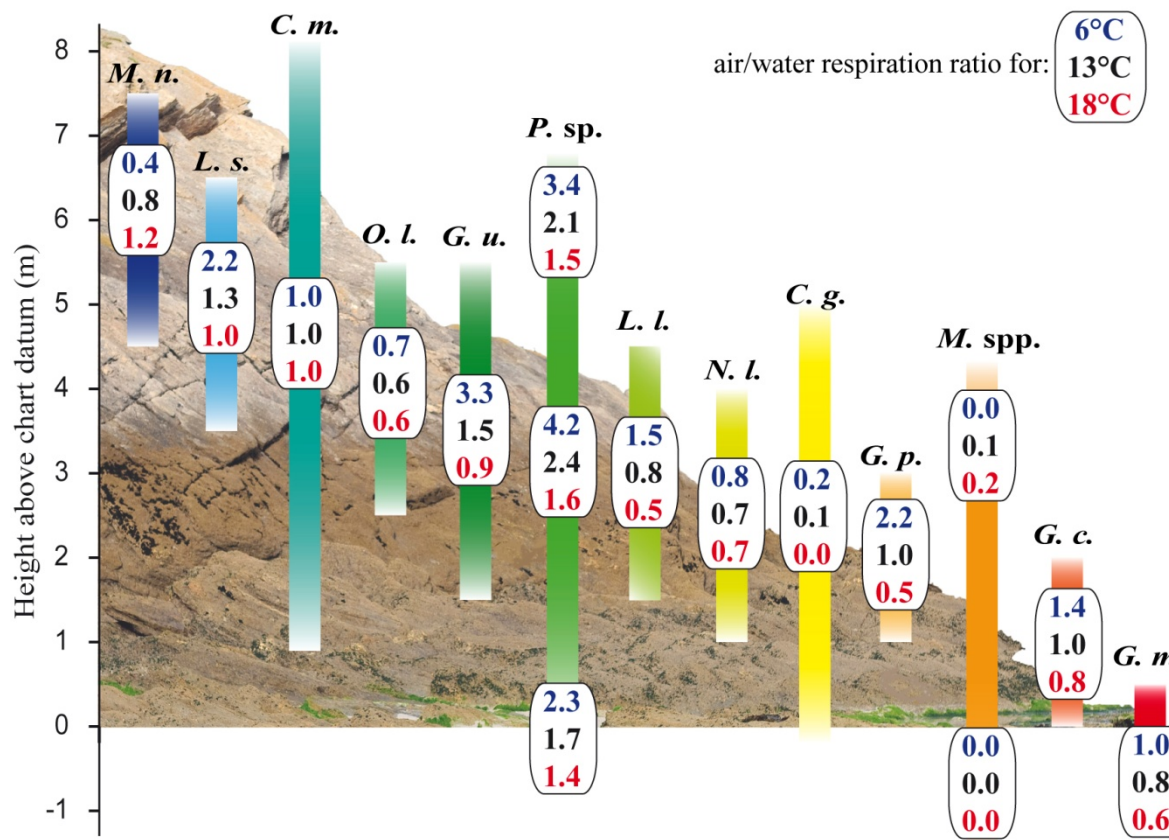


Fig. 53. Rapport respiratoire air/eau en fonction de la position sur l'estran et de la température. Les rapports ont été calculés pour trois températures : 6°C, bleu ; 13°C, noir ; 18°C, rouge. (*M. n.*, *M. neritoides*; *L. s.*, *L. saxatilis*; *C. m.*, *Chthamalus montagui*; *O. l.*, *O. lineatus*; *G. u.*, *G. umbilicalis*; *P. sp.*, *Patella* sp.; *L. l.*, *L. littorea*; *N. l.*, *N. lapillus*; *C. g.*, *Crassostrea gigas*; *G. p.*, *G. pennanti*; *M. spp.*, *Mytilus* spp.; *G. c.*, *G. cineraria*; *G. m.*, *G. magus*).

Les résultats que nous avons obtenus montrent que le rapport entre la respiration dans l'air et dans l'eau n'est pas corrélé avec le niveau de vie sur l'estran. Des facteurs morphologiques ou comportementaux, autres que la position sur l'estran, contrôlent donc probablement les flux respiratoires sur la zone intertidale rocheuse (Alyakrinskaya 2002, 2004). La comparaison des flux respiratoires établis pour les gastéropodes (à l'exclusion de *Patella* sp.) montre que la biomasse moyenne est le paramètre plus important pour expliquer les différences interspécifiques.

Du point de vue intraspécifique, nos résultats sur les moules et les patelles ont établi que le rapport respiratoire air/eau dépend de la position sur l'estran, avec une meilleure adaptation à la respiration aérienne pour les individus vivant dans les niveaux les plus hauts.

Les mesures de calcification ont montré que, même si le dépôt de CaCO₃ varie avec la saison, la calcification l'emporte sur la décalcification tout au long de l'année chez la plupart des espèces étudiées, ce qui valide la méthode utilisée. Seules les balanes ont montré une prévalence de dissolution des carbonates en hiver (Clavier et al. 2009). Même si le processus de calcification est similaire chez les mollusques et les balanes, la composition de la partie organique contenue dans leurs structures calcifiées est différente (Watson et al. 1995). La coquille des mollusques est généralement composée de calcite et/ou d'aragonite qui se forment dans le liquide extrapalléal, contenu entre le manteau et la coquille (Chave 1984). Les plaques des balanes ont une composition complexe avec différentes couches; leur croissance n'est pas continue et passe par une alternance de phases de minéralisation/déménéralisation. Les cristaux de calcite présents dans les parties calcifiées sont plus petits chez les balanes que ceux des mollusques (Rodríguez-Navarro et al. 2006). Ces différences dans la formation et dans la composition des parties calcifiées peuvent expliquer les différents taux de décalcification constatés entre les deux groupes.

Le métabolisme des balanes (Clavier et al. 2009) et des huîtres (Lejart et al. 2012) étant connus, nos travaux en laboratoire se sont focalisés sur les mollusques intertiaux, en raison de leur facilité de prélèvement et de manipulation. Des mesures complémentaires sur d'autres espèces macrozoobenthiques (crabes, ligies, chitons, actinies...) pourraient aider à mieux comprendre comment les différents groupes phylogénétiques sont capables de s'adapter à la vie intertidale.

Contribution de la faune benthique aux flux de carbone en milieu rocheux intertidal

L'utilisation de chambres benthiques pour l'étude des flux de carbone en immersion et en émersion, nous a permis de prendre en compte l'ensemble de la biocénose présente sur un estran rocheux semi-exposé. Elle est caractérisée par la prédominance du zoobenthos, avec une forte abondance des balanes. Le bilan de carbone calculé à partir des mesures *in situ* nous montre que cette communauté est hétérotrophe à l'échelle annuelle.

L'activité photosynthétique est fortement influencée par l'irradiance et présente un cycle saisonnier. Même si la composition en espèces animales varie, comme celle des pigments, en fonction de la hauteur sur l'estran, les flux nets de carbone dus à la respiration et à la photosynthèse sont relativement constants. Les adaptations des différentes populations aux contraintes imposées sur les plus hauts niveaux de l'estran leur permettent de maintenir des niveaux métaboliques aussi élevé que sur les niveaux les plus bas.

Notre étude a permis de souligner l'importance de la dessiccation sur les flux de carbone en émersion. La grande variabilité des résultats obtenus pendant la marée basse indique que les communautés subissent l'influence de différents paramètres (température, irradiance, humidité de l'air). L'intégration des mesures de fluorimétrie *in situ* par PAM (Pulse Amplitude Modulation), à la fois en immersion et en émersion pourrait donner des informations complémentaires sur l'état physiologique et la régulation de la photosynthèse (Martínez et al. 2012). De plus, des méthodes de quantification du processus de dessiccation pourraient compléter nos résultats et expliquer la variabilité des réponses métaboliques des organismes pendant la marée basse.

En raison de la complexité des interactions entre le métabolisme et les paramètres physiques, un modèle d'arbre de régression a été appliqué aux données obtenues en émersion. Cette méthode d'exploration de données (data mining) constitue une aide à la décision et à la prévision qui met en œuvre des techniques statistiques et d'apprentissage machine sur de grandes quantités de données. Originiquement conçu pour l'économie, la finance et le commerce, cette technique est de plus en plus utilisée en biologie et écologie (Dalaka et al. 2000, Hirschman et al. 2002, Rochelle-Newall et al. 2007, Irwin & Finkel 2008, Tang et al. 2008). Les limites à l'utilisation de cette méthode sont la convivialité des logiciels, dont l'utilisation est parfois fort complexe, et les connaissances de base requises pour l'utilisation des différents algorithmes (Olden et al. 2008).

Dans notre étude, la technique des arbres de régression s'est avérée concluante et facilement interprétable, mais la faible précision dans les prédictions demandera le recours à d'autres méthodes de « data mining », comme les forêts d'arbres ou les réseaux des neurones (Cutler et al. 2007, Langman et al. 2010, Liu et al. 2010). Si elles ont un pouvoir explicatif plus faible que les arbres de régression, elles pourraient donner des prévisions plus précises. La complexité et la grande diversité des algorithmes disponibles pour ces méthodes de « data mining » impliquent un long travail d'analyse pour aboutir à des résultats fiables. Des études complémentaires sont donc, ici aussi, nécessaires pour pouvoir établir des prévisions à partir de nos résultats de flux de carbone pendant l'émergence.

L'utilisation des données REBENT sur les communautés des estrans rocheux exposés nous a permis d'évaluer la contribution de la macrofaune benthique aux flux de carbone. Nos résultats suggèrent que les espèces animales sont les principaux contributeurs à la respiration des biocénoses. Pour tester cette hypothèse, nous avons comparé les résultats globaux obtenus grâce à la méthode des cloches benthiques, à ceux calculé à partir des mesures réalisées au laboratoire sur les différentes espèces macrozoobenthiques (Tab. 12).

Les résultats des deux méthodes ont été comparés avec un test non paramétrique pour des échantillons appariés car les valeurs ont été calculées pour les mêmes conditions de température en fonction de la saison et du niveau de l'estran. La respiration à l'air et la calcification ne sont pas significativement différentes entre les deux méthodes (Wilcoxon's signed ranks, $p>0.05$), contrairement aux flux en immersion qui sont significativement plus élevés sur le terrain (Wilcoxon's signed ranks, $p<0.05$).

Les flux de carbone à l'air sont très variables et la méthode au laboratoire semble légèrement surestimer les respirations. Au contraire, les valeurs mesurées en immersion au laboratoire sont inférieures à celles obtenues *in situ*, dont elles représentent en moyenne 78%. Cette estimation suggère que la part de carbone produite par la respiration de la composante végétale et les microorganismes présents dans le biofilm qui tapisse les rochers, est faible en immersion, de l'ordre du quart de la respiration totale de la biocénose. Cette contribution est réduite ou nulle en émergence, où la respiration totale de la macrofaune semble suffisante pour expliquer les résultats mesurés *in situ*. Cette différence est vraisemblablement due à la dessiccation qui limite le métabolisme des algues (Ji & Tanaka 2002) et des microorganismes du biofilm. Quoi qu'il en soit, ces résultats valident les méthodes employées. Le calcul

indirect des respirations, à partir des mesures au laboratoire et des données d'abondance des espèces, semble ainsi pertinent et applicable pour l'estimation de la respiration des communautés intertidales, au moins pour les espèces étudiées.

Tab. 12. Comparaison entre les flux respiratoires à l'air et sous l'eau mesurés globalement *in situ* avec les cloches benthiques (CR), et les flux calculés en additionnant la respiration de chaque population macrozoobenthique (MR) ($\text{mmol C m}^{-2} \text{ h}^{-1}$).

Season	Shore level	Air		Underwater		Calcification	
		MR	CR	MR	CR	MG	CG
Winter	High	1.09	0.62	1.19	1.79	0.46	0.37
	Middle	0.43	0.37	0.46	2.17	0.13	0.45
	Low	0.70	0.97	0.74	0.76	0.38	0.27
Spring	High	3.26	2.04	1.68	1.88	0.74	0.59
	Middle	1.22	0.81	0.70	1.17	0.17	0.20
	Low	1.18	2.13	0.81	1.41	0.34	0.32
Summer	High	3.78	1.65	2.04	2.00	0.51	0.42
	Middle	1.37	1.55	0.80	0.75	0.12	0.42
	Low	4.54	2.69	1.65	1.90	0.60	0.57
Autumn	High	2.53	2.27	1.92	1.52	0.61	0.74
	Middle	1.13	2.01	0.80	2.78	0.09	0.88
	Low	1.00	2.46	0.79	2.79	0.17	0.13

Différents types d'organismes comme les macroalgues calcifiantes, les foraminifères, les coraux, les mollusques et les crustacées sont capables de précipiter du CaCO_3 pour la construction de leurs structures de soutien (Gattuso et al. 1997, Martin et al. 2007). La comparaison des nos résultats sur la calcification *in situ* avec les estimations faites à partir des études en laboratoire suggèrent que les flux de CaCO_3 sont exclusivement dus à la présence des espèces macrozoobenthiques. Les mesures d'alcalinité totale pendant des incubations *in situ* peuvent être influencées par des processus de reminéralisation de la matière organique et par des réactions biogéochimiques dans les milieux sédimentaires. Par exemple, l'eau interstitielle peut facilement devenir anoxique et des réactions autres que la calcification (réduction des sulfates, nitrification) peuvent intervenir (Boucher et al. 1994, Martin et al. 2007). Nous avons considéré que ces processus complémentaires étaient négligeables lors de nos mesures *in situ* car la présence d'un substrat rocheux ne permet pas le développement des

réactions observées en milieu sédimentaire. Seuls les flux d'excrétion et d'assimilation peuvent influencer de manière significative les mesures d'ammonium. Les mesures effectuées en laboratoire confirment que les variations d'alcalinité totale dues au processus d'excrétion de la macrofaune benthique ont une influence minime sur les flux des carbonates.

Les données d'abondance des espèces de macrofaune disponibles sur la région Bretagne nous ont permis d'estimer l'influence de la variation de la température sur la respiration. Les résultats obtenus sur la communauté macrozoobenthique intertidale de substrat rocheux montrent que l'augmentation de la température peut amener une augmentation significative des émissions de carbone. L'effet du changement climatique sur le métabolisme respiratoire des communautés côtières peut être complexe et particulier à chacune, en fonction de sa

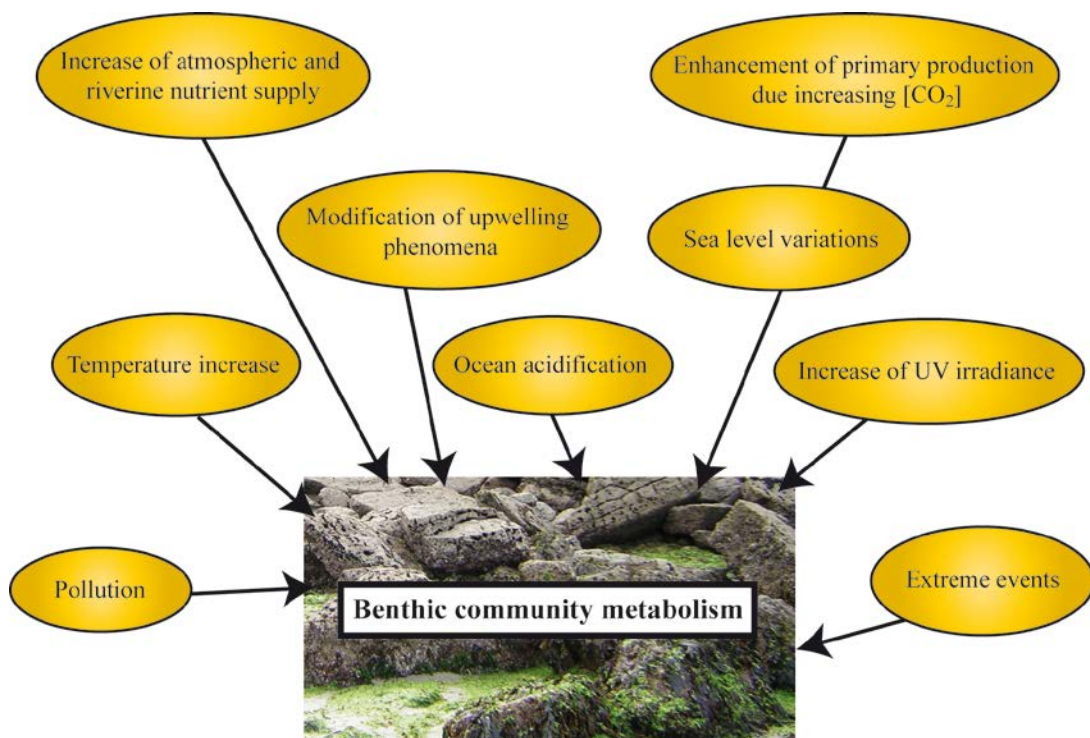


Fig. 54. Diagramme conceptuel illustrant les différents contraintes liées au changement global qui peuvent influencer le métabolisme des communautés benthiques intertidales (d'après Harley et al. 2006, Borges 2011).

composition et de sa localisation (Harley et al. 2006). L'influence du changement climatique sur de nombreux facteurs (température, pH des océans, courants, apports des nutriments, etc.), peut amener des augmentations significatives des flux de CO_2 vers l'atmosphère (Borges 2011) depuis la zone côtière (Fig. 54). Mais, à cause du peu de données disponibles, ces mécanismes de « feedback » restent encore difficilement quantifiables. Des travaux

complémentaires sont donc nécessaires pour préciser nos premiers résultats et statuer sur les effets des changements climatiques sur le fonctionnement des écosystèmes benthiques côtiers.

Dans les estimations globales, la contribution de la zone côtière est généralement calculée par une simple multiplication des flux de carbone par des superficies. De nouveaux modèles intégrant des données temporelles et spatiales de l'évolution des processus côtiers (production et dégradation de la matière organique, excrétion, respiration, calcification) pourraient mieux permettre d'évaluer la réelle contribution de ces écosystèmes aux bilans de carbone globaux (Siefert & Plattner 2004). L'hétérogénéité de cette zone nécessite des études approfondies et pour cette raison, différents programmes ont été entrepris ces dernières années pour répondre à la question «Est-ce que la zone côtière est une source ou un puits de CO₂ pour l'atmosphère ? » (Chen & Borges 2009). Plusieurs études ont fourni des informations sur les émissions de carbone dans les estuaires (Frankignoulle et al. 1998, Gattuso et al. 1998, Spilmont et al. 2007, Koné et al. 2009), les mangroves (Borges et al. 2003, Biswas et al. 2004), les herbiers (Clavier et al. 2011, Ouisse et al. 2011), les marais (Cai et al. 2003, Ferrón et al. 2007), les plaines tidales (Davoult et al. 2009, Migne et al. 2009), les fonds dominés par des macroalgues calcaires (Bensoussan & Gattuso 2007, Martin et al. 2007), les lagons coralliens (Boucher et al. 1998, Clavier & Garrigue 1999), mais la zone intertidale rocheuse reste encore peu connue (Golley et al. 2008). Dans ce milieu, l'alternance des marées implique l'utilisation de méthodes adaptées à l'étude des flux de carbone à la fois à l'air et sous l'eau. Dans cette étude, nous avons testé une méthode adaptée aux mesures *in situ* qui nous a permis de quantifier les flux de carbone de la communauté benthique présente sur un estran rocheux semi-exposé. À travers les mesures en laboratoire, nous avons aussi pu évaluer la contribution de la composante animale et comprendre les différentes adaptations respiratoires des espèces macrozoobenthiques. Cette étude peut donc être considérée comme une contribution à la connaissance du fonctionnement de la zone intertidale et les données obtenues pourront aider à la construction des nouveaux modèles côtiers sur le cycle du carbone.

References

- Abele D, Kruppe M, Philipp E, Brey T (2010) Mantle cavity water oxygen partial pressure (PO_2) in marine molluscs aligns with lifestyle. *Can J Fish Aquat Sci* 67:977-986
- Aldridge DW, Russell-Hunter W, McMahon RF (1995) Effects of ambient temperature and of temperature acclimation on nitrogen excretion and differential catabolism of protein and nonprotein resources in the intertidal snails, *Littorina saxatilis* (Olivi) and *L. obtusata* (L.). *Hydrobiologia* 309:101-109
- Alistair H (1995) Body-size variation exhibited by an intertidal limpet: Influence of wave exposure, tidal height and migratory behavior. *J Exp Mar Biol Ecol* 189:29-45
- Alyakrinskaya I (2005) Functional significance and weight properties of the shell in some mollusks. *Biol Bull* 32:397-418
- Alyakrinskaya IO (2002) Morphobiochemical adaptations to life on littoral in some sedentary gastropods. *Biol Bull* 29:394-403
- Alyakrinskaya IO (2004) Resistance to drying in aquatic mollusks. *Biol Bull* 31:299-309
- Amat JP, Coeur CL, Dorize L (2008) *Eléments de géographie physique*, In, Bréal
- Anderson M (1995) Variations in biofilms colonizing artificial surfaces: seasonal effects and effects of grazers. *J Mar Biol Assoc UK* 75:705-714
- Babarro JMF, Fernández-Reiriz MJ, Labarta U (2000) Metabolism of the mussel *Mytilus galloprovincialis* from two origins in the Ría de Arousa (north-west Spain). *J Mar Biol Assoc UK* 80:865-872
- Babarro JMF, Labarta U, Reiriz MJF (2007) Energy metabolism and performance of *Mytilus galloprovincialis* under anaerobiosis. *J Mar Biol Assoc UK* 87:941-946
- Banavar JR, Moses ME, Brown JH, Damuth J, Rinaldo A, Sibly RM, Maritan A (2010) A general basis for quarter-power scaling in animals. *Proc Natl Acad Sci* 107:15816-15820
- Bayne BL (1976) Marine mussels, their ecology and physiology, In: Bayne BL (ed), Cambridge University Press, Cambridge
- Bayne BL, Bayne C, Carefoot T, Thompson R (1976) The physiological ecology of *Mytilus californianus* Conrad. *Oecologia* 22:229-250
- Bayne BL, Scullard C (1977) Rates of nitrogen excretion by species of *Mytilus* (Bivalvia: Mollusca). *J Mar Biol Assoc UK* 57:355-369
- Bayne BL, Scullard C (1978) Rates of oxygen consumption by *Thais (Nucella) Lapillus* (L.). *J Exp Mar Biol Ecol* 32:97-111
- Belkin IM (2009) Rapid warming of large marine ecosystems. *Prog Oceanogr* 81:207-213

- Bensoussan N, Gattuso JP (2007) Community primary production and calcification in a NW Mediterranean ecosystem dominated by calcareous macroalgae. *Mar Ecol Prog Ser* 334:37-45
- Bierne N, Borsa P, Daguen C, Jollivet D, Viard F, Bonhomme F, David P (2003) Introgression patterns in the mosaic hybrid zone between *Mytilus edulis* and *M. galloprovincialis*. *Mol Ecol* 12:447-461
- Bierne N, David P, Boudry P, Bonhomme F (2002) Assortative fertilization and selection at larval stage in the mussels *Mytilus edulis* and *M. galloprovincialis*. *Evolution* 56:292-298
- Bishop SH, Ellis LL, Burcham JM (1983) Metabolic biochemistry and molecular biomechanics. In: *The mollusca*, Book 1. Academic Press, New York
- Biswas H, Mukhopadhyay S, De T, Sen S, Jana T (2004) Biogenic controls on the air-water carbon dioxide exchange in the Sundarban mangrove environment, northeast coast of Bay of Bengal, India. *Limnol Oceanogr* 49:95-101
- Blackmore D (1969) Studies of *Patella vulgata* L. I. Growth, reproduction and zonal distribution. *J Exp Mar Biol Ecol* 3:200-213
- Boaventura D, Cancela da Fonseca L, Hawkins SJ (2002) Analysis of competitive interactions between the limpets *Patella depressa* Pennant and *Patella vulgata* L. on the northern coast of Portugal. *J Exp Mar Biol Ecol* 271:171-188
- Boaventura D, Da Fonseca LC, Hawkins SJ (2003) Size matters: competition within populations of the limpet *Patella depressa*. *J Anim Ecol* 72:435-446
- Borges A (2011) Present day carbon dioxide fluxes in the coastal ocean and possible feedbacks under global change. In: Duarte P, Santana-Casiano JM (eds) *Oceans and the Atmospheric Carbon Content*. Springer Netherlands
- Borges A, Djenidi S, Lacroix G, Théate J, Delille B, Frankignoulle M (2003) Atmospheric CO₂ flux from mangrove surrounding waters. *Geophys Res Lett* 30:1558
- Boucher G, Clavier J, Garrigue C (1994) Oxygen and carbon dioxide fluxes at the water-sediment interface of a tropical lagoon. *Mar Ecol Prog Ser* 107:185-185
- Boucher G, Clavier J, Hily C, Gattuso JP (1998) Contribution of soft-bottoms to the community metabolism (primary production and calcification) of a barrier reef flat (Moorea, French Polynesia). *J Exp Mar Biol Ecol* 225:269-283
- Bourget E (1983) Seasonal variations of cold tolerance in intertidal mollusks and relation to environmental conditions in the St. Lawrence Estuary. *Can J Zool* 61:1193-1201
- Bourget E, Crisp DJ (1975) Factors affecting deposition of the shell in *Balanus balanoides* (L.). *J Mar Biol Assoc UK* 55:231-249
- Branch G, Newell R (1978) A comparative study of metabolic energy expenditure in the limpets *Patella cochlear*, *P. oculus* and *P. granularis*. *Mar Biol* 49:351-361
- Branch GM (1978) Respiratory adaptations in the limpet *Patella granatina*: a comparison with other limpets. *Compendium of Biochemistry and Physiology* 62 A:641-647
- Branch GM (1981) The biology of limpets: physical factors, energy flow, and ecological interactions. *Oceanogr Mar Biol Annu Rev* 19:235-380

Breiman L, Friedman J, Stone CJ, Olshen RA (1984) Classification and regression trees, In, Chapman & Hall/CRC

Brinkhoff W, Stöckmann K, Grieshaber M (1983) Natural occurrence of anaerobiosis in molluscs from intertidal habitats. *Oecologia* 57:151-155

Brown M (2009) Effects of desiccation on photosynthesis of intertidal algae from a southern New Zealand shore. *Botanica marina* 30:121-128

Brown MR, Jeffrey S (1992) Biochemical composition of microalgae from the green algal classes *Chlorophyceae* and *Prasinophyceae*. 1. Amino acids, sugars and pigments. *J Exp Mar Biol Ecol* 161:91-113

Bukhov N, Govindachary S, Egorova E, Carpentier R (2004) Recovery of photosystem I and II activities during re-hydration of lichen *Hypogymnia physodes*; thalli. *Planta* 219:110-120

Burnett LE (1988) Physiological responses to air exposure: acid-base balance and the role of branchial water stores. *Am Zool* 28:125-135

Buschbaum C, Saier B (2001) Growth of the mussel *Mytilus edulis* L. in the Wadden Sea affected by tidal emergence and barnacle epibionts. *J Sea Res* 45:27-36

Byrne M (2011) Impact of ocean warming and ocean acidification on marine invertebrate life history stages: vulnerabilities and potential for persistence in a changing ocean. In: *Oceanogr Mar Biol Annu Rev*, Book 49. CRC Press

Cai WJ, Wang ZA, Wang Y (2003) The role of marsh-dominated heterotrophic continental margins in transport of CO₂ between the atmosphere, the land-sea interface and the ocean. *Geophys Res Lett* 30:1849

Catanzano J, Thébaud O (1995) Le littoral: pour une approche de la régulation des conflits d'usage, In, Institut océanographique

Chauvaud L, Thompson JK, Cloern JE, Thouzeau G (2003) Clams as CO₂ generators: the *Potamocorbula amurensis* example in San Francisco Bay. *Limnol Oceanogr* 48:2086-2092

Chave KE (1984) Physics and chemistry of biomineralization. *Annu Rev Earth Planet Sci* 12:293

Chelazzi G, Focardi S, Deneubourg JL (1988) Analysis of movement patterns and orientation mechanisms in intertidal chitons and gastropods, In, Plenum Press New York

Chen CTA, Borges AV (2009) Reconciling opposing views on carbon cycling in the coastal ocean: Continental shelves as sinks and near-shore ecosystems as sources of atmospheric CO₂. *Deep Sea Res (II Top Stud Oceanogr)* 56:578-590

Chen Q, Mynett AE (2004) Predicting *Phaeocystis globosa* bloom in Dutch coastal waters by decision trees and nonlinear piecewise regression. *Ecol Model* 176:277-290

Chisholm JRM, Gattuso JP (1991) Validation of the alkalinity anomaly technique for investigating calcification and photosynthesis in coral reef communities. *Limnol Oceanogr* 36:1232-1239

Christensen JH, Hewitson B, Busuioc A, Chen A, Gao X, Held R, Jones R, Kolli RK, Kwon W, Laprise R (2007) Regional climate projections. In. University Press Cambridge, Cambridge

Cicin-Sain B, Bernal P, Vandeweerd V, Belfiore S, Goldstein K (2002) A guide to oceans, coasts, and islands at the world summit on sustainable development. In: Center for the Study of Marine Policy, Newark, Delaware

Clarke A (1990) Faecal egestion and ammonia excretion in the Antarctic limpet *Nacella continua* (Strebel, 1908). J Exp Mar Biol Ecol 138:227-246

Clavier J, Castets MD, Bastian T, Hily C, Boucher G, Chauvaud L (2009) An amphibious mode of life in the intertidal zone: aerial and underwater contribution of *Chthamalus montagui* to CO₂ fluxes. Mar Ecol Prog Ser 375:185-194

Clavier J, Chauvaud L, Carlier A, Amice E, Van der Geest M, Labrosse P, Diagne A, Hily C (2011) Aerial and underwater carbon metabolism of a *Zostera noltii* seagrass bed in the Banc d'Arguan, Mauritania. Aquat Bot

Clavier J, Garrigue C (1999) Annual sediment primary production and respiration in a large coral reef lagoon (SW New Caledonia). Mar Ecol Prog Ser 191:79-89

Conde-Padín P, Carballo M, Caballero A, Rolán-Alvarez E (2008) The relationship between hatching rate and number of embryos of the brood pouch in *Littorina saxatilis*. J Sea Res 60:223-225

Connell JH (1972) Community interactions on marine rocky intertidal shores. Annu Rev Ecol Syst 3:169-192

Connor K, Gracey AY (2011) High resolution analysis of metabolic cycles in the intertidal mussel *Mytilus californianus*. In: Am J Physiol Regul Integr Comp Physiol, Book 302. Am Physiological Soc

Cornelius PFS (1972) Thermal acclimation of some intertidal invertebrates. J Exp Mar Biol Ecol 9:43-53

Cruz-Motta JJ, Miloslavich P, Palomo G, Iken K, Konar B, Pohle G, Trott T, Benedetti-Cecchi L, Herrera C, Hernández A (2010) Patterns of spatial variation of assemblages associated with intertidal rocky shores: a global perspective. PloS one 5:e14354

Cubit JD (1984) Herbivory and the seasonal abundance of algae on a high intertidal rocky shore. Ecology:1904-1917

Cutler DR, Edwards TC, Jr., Beard KH, Cutler A, Hess KT, Gibson J, Lawler JJ (2007) Random forests for classification in ecology. Ecology 88:2783-2792

Daguin C, Bonhomme F, Borsig P (2001) The zone of sympatry and hybridization of *Mytilus edulis* and *M. galloprovincialis*, as described by intron length polymorphism at locus mac-1. Heredity 86:342-354

Dalaka A, Kompare B, Robnik-Šikonja M, Sgardelis SP (2000) Modelling the effects of environmental conditions on apparent photosynthesis of *Stipa bromoides* by machine learning tools. Ecol Model 129:245-257

Daniel MJ (1982) A comparative study of the pattern of ventilation movements in Hong Kong limpets, In: B. M, C.K. T (eds), Hong Kong University Press, Hong Kong

Das S, Seshappa G (1948) A contribution to the biology of *Patella*: on population distribution and sex-proportions in *Patella vulgata* Linnaeus at Cullercoats, England, In, John Wiley & Sons

- Davies PS (1967a) Physiological ecology of *Patella*. I. The effect of environmental accumulation on metabolic rate. J Mar Biol Assoc UK 46:647-658
- Davies PS (1967b) Physiological ecology of *Patella*. II. Effect of environmental acclimation on the metabolic rate. J Mar Biol Assoc UK 47:61-74
- Davies PS (1969) Physiological ecology of *Patella*. III. Desiccation effects. J Mar Biol Assoc UK 49:291-304
- Davoult D, Migné A, Créach A, Gévaert F, Hubas C, Spilmont N, Boucher G (2009) Spatio-temporal variability of intertidal benthic primary production and respiration in the western part of the Mont Saint-Michel Bay (Western English Channel, France). Hydrobiologia 620:163-172
- Dawes CJ, Moon RE, Davis MA (1978) The photosynthetic and respiratory rates and tolerances of benthic algae from a mangrove and salt marsh estuary: a comparative study. Estuar Coast Mar Sci 6:175-185
- de la Coba F, Aguilera J, Figueroa F, de Gálvez M, Herrera E (2009) Antioxidant activity of mycosporine-like amino acids isolated from three red macroalgae and one marine lichen. J Appl Phycol 21:161-169
- Della Santina P, Santini G, Chelazzi G (1995) Factors affecting variability of foraging excursions in a population of the limpet *Patella vulgata* (Mollusca, Gastropoda). Mar Biol 122:265-270
- Demers A, Guderley H (1994) Acclimatization to intertidal conditions modifies the physiological response to prolonged air exposure in *Mytilus edulis*. Mar Biol 118:115-122
- Denny MW, Gaines SD (2007) Encyclopedia of tidepools and rocky shores, In, University of California Press
- Dreiseitl S, Ohno-Machado L (2002) Logistic regression and artificial neural network classification models: a methodology review. J Biomed Inf 35:352-359
- Duarte CM, Marbà N, Gacia E, Fourqurean JW, Beggins J, Barrón C, Apostolaki ET (2010) Seagrass community metabolism: Assessing the carbon sink capacity of seagrass meadows.
- Duarte CM, Middelburg J, Caraco N (2005) Major role of marine vegetation on the oceanic carbon cycle. Biogeosciences 2:1-8
- Duarte P, Ferreira J (1997) Dynamic modelling of photosynthesis in marine and estuarine ecosystems. Environ Model Assess 2:83-93
- Dunkin DB, Hughes R (1984) Behavioural components of prey-selection by dogwhelks, *Nucella lapillus* (L.), feeding on barnacles, *Semibalanus balanoides* (L.), in the laboratory. J Exp Mar Biol Ecol 79:91-103
- Edwards DC, Conover DO, Iii FS (1982) Mobile predators and the structure of marine intertidal communities. Ecology 63:1175-1180
- Ehrhold A, Hamon D, Guillaumont B (2006) The REBENT monitoring network, a spatially integrated, acoustic approach to surveying nearshore macrobenthic habitats: application to the Bay of Concarneau (South Brittany, France). ICES J Mar Sci 63:1604-1615

- Espinosa F, Guerra-García JM, Fa D, García-Gómez JC (2006) Effects of competition on an endangered limpet *Patella ferruginea* (Gastropoda: Patellidae): Implications for conservation. *J Exp Mar Biol Ecol* 330:482-492
- Evans RG (1948) The lethal temperatures of some common British littoral molluscs. *J Anim Ecol* 17:165-173
- FAO (2010) The state of world fisheries and aquaculture - 2010. In: State World Fish Aquac, Rome
- Fenger T, Surge D, Schöne B, Milner N (2007) Sclerochronology and geochemical variation in limpet shells (*Patella vulgata*): A new archive to reconstruct coastal sea surface temperature. *Geochem Geophys Geosyst* 8:Q07001
- Ferrón S, Ortega T, Gómez-Parra A, Forja JM (2007) Seasonal study of dissolved CH₄, CO₂ and N₂O in a shallow tidal system of the bay of Cádiz (SW Spain). *J Mar Syst* 66:244-257
- Fraenkel G (1961) Resistance to high temperatures in a Mediterranean snail, *Littoria neritoides*. *Ecology* 42:604-606
- Franke HD, Gutow L (2004) Long-term changes in the macrozoobenthos around the rocky island of Helgoland (German Bight, North Sea). *Helgol Mar Res* 58:303-310
- Frankignoulle M, Abril G, Borges A, Bourge I, Canon C, Delille B, Libert E, Théate JM (1998) Carbon dioxide emission from European estuaries. *Science* 282:434-436
- Frankignoulle M, Canon C, Gattuso JP (1994) Marine calcification as a source of carbon dioxide: Positive feedback of increasing atmospheric CO₂. *Limnol Oceanogr* 39:458-462
- Frankignoulle M, Pinchon M, Gattuso JP (1995) Aquatic calcification as a source of carbon dioxide. *NATO ASI Ser, Ser I* 33:265-272
- Fretter V, Graham A (1962) British prosobranch molluscs: their functional anatomy and ecology, In, Ray Society, London
- Gabbott P, Bayne B (1973) Biochemical effects of temperature and nutritive stress on *Mytilus edulis* L. *J Mar Biol Assoc UK* 53:269-286
- Gattuso J-P, Frankignoulle M, Wollast R (1998) Carbon and carbonate metabolism in coastal aquatic ecosystems. *Annu Rev Ecol Syst* 29:405-434
- Gattuso J-P, Payri CE, Pichon M, Delesalle B, Frankignoulle M (1997) Primary production, calcification, and air-sea CO₂ fluxes of a macroalgal-dominated coral reef community (Moorea, French Polynesia). *J Phycol* 33:729-738
- Gazeau F, Quiblier C, Jansen J, Gattuso JP, Middelburg JJ, Heip CHR (2007) Impact of elevated CO₂ on shellfish calcification. *Geophys Res Lett* 34:L07603
- Gazeau F, Smith SV, Gentili B, Frankignoulle M, Gattuso J-P (2004) The European coastal zone: characterization and first assessment of ecosystem metabolism. *Estuar Coast Shelf Sci* 60:673-694
- Gibbs P, Pascoe P, Burt G (1988) Sex change in the female dogwhelk, *Nucella lapillus*, induced by tributyltin from antifouling paints. *J Mar Biol Assoc UK* 68:715-731
- Gibson R (2003) Go with the flow: tidal migration in marine animals. *Hydrobiologia* 503:153-161

- Glazier DS (2007) Beyond the ‘3/4-power law’: variation in the intra- and interspecific scaling of metabolic rate in animals. *Biol Rev* 80:611-662
- Golley C, Migne A, Davout D (2008) Benthic metabolism on a sheltered rocky shore: role of the canopy in the carbon budget. *J Phycol* 44:1146-1153
- Gosling E (1992) The Mussel *Mytilus*: ecology, physiology, genetics, and culture, In, Elsevier, Amsterdam
- Gosling E, Doherty S, Howley N (2008) Genetic characterization of hybrid mussel (*Mytilus*) populations on Irish coasts. *J Mar Biol Assoc UK* 88:341-346
- Gosling E, McGrath D (1990) Genetic variability in exposed-shore mussels, *Mytilus* spp., along an environmental gradient. *Mar Biol* 104:413-418
- Gosling E, Wilkins N (1981) Ecological genetics of the mussels *Mytilus edulis* and *M. galloprovincialis* on Irish coasts. *Mar Ecol Prog Ser* 4:221-227
- Graham A (1988) Molluscs: prosobranch and pyramidelid gastropods: keys and notes for the identification of the species, In, Brill Academic Pub
- Gray D, Naylor E (1996) Foraging and homing behaviour of the limpet, *Patella vulgata*: a geographical comparison. *J Molluscan Stud* 62:121-124
- Griffiths RJ (1981) Aerial exposure and energy balance in littoral and sublittoral *Choromytilus meridionalis* (Kr.) (Bivalvia). *J Exp Mar Biol Ecol* 52:231-241
- Grube M, Blaha J (2005) Halotolerance and lichen symbioses:adaptation to life at high salt concentrations in archaea, bacteria, and eukarya. In: Gunde-Cimerman N, Oren A, Plemenitaš A (eds), Book 9. Springer Netherlands
- Haris V (1990) Sessile animals of the sea shore, In, Springer
- Harley CDG, Denny MW, Mach KJ, Miller LP (2009) Thermal stress and morphological adaptations in limpets. *Funct Ecol* 23:292-301
- Harley CDG, Randall Hughes A, Hultgren KM, Miner BG, Sorte CJB, Thornber CS, Rodriguez LF, Tomanek L, Williams SL (2006) The impacts of climate change in coastal marine systems. *Ecol Lett* 9:228-241
- Hartnoll R, Wright J (1977) Foraging movements and homing in the limpet *Patella vulgata* L. *Anim Behav* 25:806-810
- Hawkins S, Hartnoll R (1982) The influence of barnacle cover on the numbers, growth and behaviour of *Patella vulgata* on a vertical pier. *J Mar Biol Assoc UK* 62:855-867
- Hawkins SJ, Hartnoll R (1983) Grazing of intertidal algae by marine invertebrates. *Oceanogr Mar Biol Annu Rev* 21:195-282
- Helmuth B, Harley CDG, Halpin PM, O'Donnell M, Hofmann GE, Blanchette CA (2002) Climate change and latitudinal patterns of intertidal thermal stress. *Science* 298:1015-1017
- Helmuth B, Mieszkowska N, Moore P, Hawkins SJ (2006) Living on the edge of two changing worlds: forecasting the responses of rocky intertidal ecosystems to climate change. *Annual Review of Ecology, Evolution, and Systematics* 37:373-404

Helmuth BST (1998) Intertidal mussel microclimates: predicting the body temperature of a sessile invertebrate. *Ecol Monogr* 68:51-74

Helmuth BST, Hofmann GE (2001) Microhabitats, thermal heterogeneity, and patterns of physiological stress in the rocky intertidal zone. *Biol Bull* 201:374-384

Hickman R, Illingworth J (1980) Condition cycle of the green-lipped mussel *Perna canaliculus* in New Zealand. *Mar Biol* 60:27-38

Hill A, Hawkins S (1991) Seasonal and spatial variation of epilithic microalgal distribution and abundance and its ingestion by *Patella vulgata* on a moderately exposed rocky shore. *J Mar Biol Assoc UK* 71:403-423

Hily C, Grall J, Chauvaud L, Lejart M, Clavier J (in press) CO₂ Generation by calcified invertebrates along rocky shores of Brittany, France. *Mar Freshwat Res*

Hirschman L, Park JC, Tsujii J, Wong L, Wu CH (2002) Accomplishments and challenges in literature data mining for biology. *Bioinformatics* 18:1553-1561

Hochachka PW, Mustafa T (1972) Invertebrate facultative anaerobiosis: A reinterpretation of invertebrate enzyme pathways suggests new approaches to helminth chemotherapy. *Science* 178:1056-1060

Hooker SB, Van Heukelem L, Thomas CS, Claustre H, Ras J, Schlüter L, Perl J, Trees C, Stuart V, Head E (2009) The third sea-wifs HPLC analysis Round-Robin experiment (SeaHARRE-3). *NASA Tech Memo* 215849:2009

Houlihan D (1979) Respiration in air and water of three mangrove snails. *J Exp Mar Biol Ecol* 41:143-161

Houlihan D, Innes A (1982) Respiration in air and water of four Mediterranean trochids. *J Exp Mar Biol Ecol* 57:35-54

Houlihan D, Newton J (1978) Respiration of *Patella vulgata* on the shore, In: McLusky DS, Berry AJ (eds), Scotland

Hoyaux J, Gilles R, Jeuniaux C (1976) Osmoregulation in molluscs of the intertidal zone. *Comp Biochem Physiol A: Physiol* 53:361-365

Huang SC, Newell R (2002) Seasonal variations in the rates of aquatic and aerial respiration and ammonium excretion of the ribbed mussel, *Geukensia demissa* (Dillwyn). *J Exp Mar Biol Ecol* 270:241-255

Hulseman J (1966) On the routine analysis of carbonates in unconsolidated sediments. *J Sediment Petrol* 36:622-625

Inoue K, Waite JH, Matsuoka M, Odo S, Harayama S (1995) Interspecific variations in adhesive protein sequences of *Mytilus edulis*, *M. galloprovincialis*, and *M. trossulus*. *Biol Bull* 189:370-375

Irwin AJ, Finkel ZV (2008) Mining a sea of data: Deducing the environmental controls of ocean chlorophyll. *PloS one* 3:e3836

Iwasaki K (1999) Short- and long-term movements of the patellid limpet *Patella flexuosa* within gaps in intertidal mussel beds. *J Molluscan Stud* 65:295-301

Jacques T, Pilson M (1980) Experimental ecology of the temperate scleractinian coral *Astrangia danae* I. Partition of respiration, photosynthesis and calcification between host and symbionts. Mar Biol 60:167-178

Jansen JM, Hummel H, Bonga SW (2009) The respiratory capacity of marine mussels (*Mytilus galloprovincialis*) in relation to the high temperature threshold. Comp Biochem Physiol, A: Mol Integr Physiol 153:399-402

Jenkins SR, Hartnoll RG (2001) Food supply, grazing activity and growth rate in the limpet *Patella vulgata* L.: a comparison between exposed and sheltered shores. J Exp Mar Biol Ecol 258:123-139

Ji Y, Tanaka J (2002) Effect of desiccation on the photosynthesis of seaweeds from the intertidal zone in Honshu, Japan. Phycol Res 50:145-153

Kashiyama Y, Miyashita H, Ohkubo S, Ogawa N, Chikaraishi Y, Takano Y, Suga H, Toyofuku T, Nomaki H, Kitazato H (2008) Evidence of global chlorophyll *d*. Science 321:658-658

Kautsky N (1982) Growth and size structure in a baltic *Mytilus edulis* population. Mar Biol 68:117-133

Koné YJM, Abril G, Kouadio K, Delille B, Borges A (2009) Seasonal variability of carbon dioxide in the rivers and lagoons of Ivory Coast (West Africa). Estuar Coast 32:246-260

Koroleff F (1969) Direct determination of ammonia in natural waters as indophenol blue. International council for the exploration of the sea, CM C 9

Koroleff F (1970) Direct determination of ammonia in natural waters as indophenol blue. In: International council for the exploration of the sea, Book 3, Copenhagen

Kostylev VE, Erlandsson J, Ming MY, Williams GA (2005) The relative importance of habitat complexity and surface area in assessing biodiversity: fractal application on rocky shores. Ecol Complex 2:272-286

Kronberg I (1990) Heat production in *Littorina saxatilis* Olivi and *Littorina neritoides* L. (gastropoda: Prosobranchia) during an experimental exposure to air. Helgol Mar Res 44:125-134

Labarta U, Fernández-Reiriz MJ, Babarro JMF (1997) Differences in physiological energetics between intertidal and raft cultivated mussels *Mytilus galloprovincialis*.

Laing I, Spencer B (2006) Bivalve cultivation: criteria for selecting a site, In, CEFAS

Lamote M, Johnson LE, Lemoine Y (2012) Photosynthetic responses of an intertidal alga to emersion: The interplay of intertidal height and meteorological conditions. J Exp Mar Biol Ecol 428:16-23

Langman O, Hanson P, Carpenter S, Hu Y (2010) Control of dissolved oxygen in northern temperate lakes over scales ranging from minutes to days. Aquatic Biol 9:193-202

Laruelle GG, Dürr HH, Slomp CP, Borges AV (2010) Evaluation of sinks and sources of CO₂ in the global coastal ocean using a spatially-explicit typology of estuaries and continental shelves. Geophys Res Lett 37:L15607

Lean JL, Rind DH (2009) How will Earth's surface temperature change in future decades. Geophys Res Lett 36:L15708

- Lee LH, Hsieh LY, Lin HJ (2011) *In situ* production and respiration of the benthic community during emersion on subtropical intertidal sandflats. Mar Ecol Prog Ser 441:33-47
- Leite LG, Ciotti ÁM, Christoforetti RA (2012) Abundance of biofilm on intertidal rocky shores: Can trampling by humans be a negative influence? Mar Environ Res 79:111-115
- Lejart M (2009) Etude du processus invasif de *Crassostrea gigas* en Bretagne: Etat des lieux, dynamique et conséquences écologiques. Université de Bretagne Occidentale,
- Lejart M, Clavier J, Chauvaud L, Hily C (2012) Respiration and calcification of *Crassostrea gigas*: contribution of an intertidal invasive species to coastal ecosystem CO₂ fluxes. Estuar Coast 35:622-632
- Lewis JR (1964) The ecology of rocky shores, In, English Universities Press
- Lewis JR, Seed R (1969) Morphological variation in *Mytilus* from south-west England in relation to the occurrence of *Mytilus galloprovincialis*. Cah Biol Mar 10:231-253
- Lighton J, Halsey L (2011) Flow-through respirometry applied to chamber systems: Pros and cons, hints and tips. Comp Biochem Physiol, A: Mol Integr Physiol 158:265-275
- Little C (1981) Osmoregulation and excretion in prosobranch gastropods Part I: physiology and biochemistry. J Molluscan Stud 47:221-247
- Little C (1983) The colonisation of land: origins and adaptations of terrestrial animals, In, Cambridge University Press, New York
- Little C (1989) Factors governing patterns of foraging activity in littoral marine herbivorous molluscs. J Molluscan Stud 55:273-284
- Little C (1990) The terrestrial invasion: an ecophysiological approach to the origins of land animals, In, Cambridge Univ Pr, New York
- Little C, Kitching J (1996) The biology of rocky shores., In, Oxford University Press, Oxford
- Little C, Williams GA, Trowbridge CD (2009) The biology of rocky shores. , In: press Ou (ed), New York
- Liu ZL, Peng CH, Xiang WH, Tian DL, Deng XW, Zhao MF (2010) Application of artificial neural networks in global climate change and ecological research: An overview. Chin Sci Bull 55:3853-3863
- Loh WY (2011) Classification and regression trees. WIREs Data Mining Knowl Discov 1:14-23
- Lombard F, da Rocha RE, Bijma J, Gattuso JP (2010) Effect of carbonate ion concentration and irradiance on calcification in planktonic foraminifera. Biogeosciences 7:247-255
- Lüning K (1980) Control of algal life-history by daylength and temperature. Systematics Association Special Volume 17
- Luttikhuijsen PC, Koolhaas A, Bol A, Piersma T (2002) *Mytilus galloprovincialis*-type foot-protein-1 alleles occur at low frequency among mussels in the Dutch Wadden Sea. J Sea Res 48:241-245

- Lutz RA, Clark GR (1984) Seasonal and geographic variation in the shell microstructure of a salt-marsh bivalve (*Geukensia demissa* (Dillwyn)). J Mar Res 42:943-956
- Mackenzie FT, Ver LM, Lerman A (2000) Coastal-zone biogeochemical dynamics under global warming. Int Geol Rev 42:193-206
- Makarieva AM, Gorshkov VG, Li B-L (2005) Temperature-associated upper limits to body size in terrestrial poikilotherms. Oikos 111:425-436
- Makarieva AM, Gorshkov VG, Li BL, Chown SL, Reich PB, Gavrilov VM (2008) Mean mass-specific metabolic rates are strikingly similar across life's major domains: evidence for life's metabolic optimum. Proc Natl Acad Sci 105:16994
- Malone PG, Dodd JR (1967) Temperature and salinity effects on calcification rate in *Mytilus edulis* and its paleoecological implications. Limnol Oceanogr 12:432-436
- Marsden ID, Weatherhead MA (1998) Effects of aerial exposure on oxygen consumption by the New Zealand mussel *Perna canaliculus* (Gmelin, 1791) from an intertidal habitat. J Exp Mar Biol Ecol 230:15-29
- Marsh CP (1986) Rocky intertidal community organization: the impact of avian predators on mussel recruitment. Ecology 67:771-786
- Marshall DJ, Dong Y, McQuaid CD, Williams GA (2011) Thermal adaptation in the intertidal snail *Echinolittorina malaccana* contradicts current theory by revealing the crucial roles of resting metabolism. J Exp Biol 214:3649-3657
- Marshall DJ, McQuaid CD (1991) Metabolic rate depression in a marine pulmonate snail: pre-adaptation for a terrestrial existence? Oecologia 88:274-276
- Marshall DJ, McQuaid CD (1992) Comparative aerial metabolism and water relations of the intertidal limpets *Patella granularis* L. (Mollusca: Prosobranchia) and *Siphonaria oculus* Kr. (Mollusca: Pulmonata). Physiol Zool 65:1040-1056
- Martin S, Clavier J, Chauvaud L, Thouzeau G (2007) Community metabolism in temperate maerl beds. I. Carbon and carbonate fluxes. Mar Ecol Prog Ser 335:19-29
- Martin S, Thouzeau G, Chauvaud L, Jean F, Guérin L, Clavier J (2006) Respiration, calcification, and excretion of the invasive slipper limpet, *Crepidula fornicata* L.: Implications for carbon, carbonate, and nitrogen fluxes in affected areas. Limnol Oceanogr 51:1996-2007
- Martínez B, Arenas F, Rubal M, Burgués S, Esteban R, García-Plazaola I, Figueroa F, Pereira R, Saldaña L, Sousa-Pinto I (2012) Physical factors driving intertidal macroalgae distribution: physiological stress of a dominant fucoid at its southern limit. Oecologia:1-13
- McConaughey TA, Gillikin DP (2008) Carbon isotopes in mollusk shell carbonates. Geo-Mar Lett 28:287-299
- McGranahan G, Balk D, Anderson B (2007) The rising tide: assessing the risks of climate change and human settlements in low elevation coastal zones. Environment and Urbanization 19:17-37
- McMahon R, Russell-Hunter W, Aldridge D (1995) Lack of metabolic temperature compensation in the intertidal gastropods, *Littorina saxatilis* (Olivii) and *L. obtusata* (L.). Hydrobiologia 309:89-100

McMahon RF (1988) Respiratory response to periodic emergence in intertidal molluscs. *Integr Comp Biol* 28:97-114

McMahon RF (1990) Thermal tolerance, evaporative water loss, air-water oxygen consumption and zonation of intertidal prosobranchs: a new synthesis. *Hydrobiologia* 193:241-260

McMahon RF, Russel-Hunter WD (1977) Temperature relation of aerial and aquatic respiration in six littoral snails in relation to their vertical zonation *Biol Bull* 152:182-198

McQuaid C, Branch G (1984) Influence of sea temperature, substratum and wave exposure on rocky intertidal communities: An analysis of faunal and floral biomass. *Mar Ecol Prog Ser* 19:145-151

Meeht GA, Stocker FT (2007) Global climate projections. In: Contribution of Working Group I to the Fourth Assessment Report of the Intergovernmental Panel on Climate Change, 2007 Cambridge University Press, Cambridge

Menge BA, Lubchenco J (1981) Community organization in temperate and tropical rocky intertidal habitats: Prey refuges in relation to consumer pressure gradients. *Ecol Monogr* 51:429-450

Micallef H, Bannister W (1967) Aerial and aquatic oxygen consumption of *Monodonta turbinata* (Mollusca: Gastropoda). *J Zool* 151:479-482

Middelburg JJ, Duarte CM, Gattuso JP (2005) Respiration in coastal benthic communities. In: Respiration in aquatic ecosystems Oxford, New York

Migné A, Davoult D, Spilmont N, Menu D, Boucher G, Gattuso JP, Rybarczyk H (2002) A closed-chamber CO₂-flux method for estimating intertidal primary production and respiration under emersed conditions. *Mar Biol* 140:865-869

Migne A, Spilmont N, Boucher G, Denis L, Hubas C, Janquin MA, Rauch M, Davoult D (2009) Annual budget of benthic production in Mont Saint-Michel Bay considering cloudiness, microphytobenthos migration, and variability of respiration rates with tidal conditions. *Cont Shelf Res* 29:2280-2285

Miller LP, Denny MW (2011) Importance of behavior and morphological traits for controlling body temperature in Littorinid snails. *Biol Bull* 220:209-223

Millie DF, Paerl HW, Hurley JP (1993) Microalgal pigment assessments using high-performance liquid chromatography: a synopsis of organismal and ecological applications. *Can J Fish Aquat Sci* 50:2513-2527

Millstein J, O'Clair C (2001) Comparison of age-length and growth-increment general growth models of the Schnute type in the Pacific Blue Mussel, *Mytilus trossulus* Gould. *J Exp Mar Biol Ecol* 262:155-176

Mueller DR, Vincent WF, Bonilla S, Laurion I (2005) Extremotrophs, extremophiles and broadband pigmentation strategies in a high arctic ice shelf ecosystem. *FEMS Microbiol Ecol* 53:73-87

Murphy R, Underwood A, Pinkerton M, Range P (2005) Field spectrometry: new methods to investigate epilithic micro-algae on rocky shores. *J Exp Mar Biol Ecol* 325:111-124

Navarrete SA, Castilla JC (1990) Barnacle walls as mediators of intertidal mussel recruitment: effects of patch size on the utilization of space. *Mar Ecol Prog Ser* 68:113-119

- Needham J (1935) Problems of nitrogen catabolism in invertebrates: Correlation between uricotelic metabolism and habitat in the phylum Mollusca. *Biochem J* 29:238-251
- Newell R (1973) Factors affecting the respiration of intertidal invertebrates. *Integr Comp Biol* 13:513-528
- Newell RC (1979) Biology of intertidal animals, In, *Marine ecological surveys*, Faversham, Kent
- Niall H (2012) Physiological ecology of lichens: Factors influencing the distribution and diversity of maritime communities.
- Nicastro K, Zardi G, McQuaid C, Stephens L, Radloff S, Blatch G (2010) The role of gaping behaviour in habitat partitioning between coexisting intertidal mussels. *BMC Ecol* 10:1-11
- Nuwayhid M, Davies PS, Elder H (1978) Gill structure in the common limpet *Patella vulgata*. *J Mar Biol Assoc UK* 58:817-823
- Obermüller BE, Morley SA, Clark MS, Barnes DKA, Peck LS (2011) Antarctic intertidal limpet ecophysiology: A winter–summer comparison. *J Exp Mar Biol Ecol* 403:39-45
- Olden JD, Lawler JJ, Poff NLR (2008) Machine learning methods without tears: a primer for ecologists. *The Quarterly review of biology* 83:171-193
- Ouisse V, Migné A, Davoult D (2010) Seasonal variations of community production, respiration and biomass of different primary producers in an intertidal *Zostera noltii* bed (Western English Channel, France). *Hydrobiologia* 649:3-11
- Ouisse V, Migné A, Davoult D (2011) Community-level carbon flux variability over a tidal cycle in *Zostera marina* and *Z. noltii* beds. *Mar Ecol Prog Ser* 437:79-87
- Paerl HW, Valdes LM, Pinckney JL, Piehler MF, Dyble J, Moisander PH (2003) Phytoplankton photopigments as indicators of estuarine and coastal eutrophication. *Bioscience* 53:953-964
- Pannella G (1976) Tidal growth patterns in recent and fossil mollusc bivalve shells: a tool for the reconstruction of paleotides. *Naturwissenschaften* 63:539-543
- Pannella G, MacClintock C (1968) Biological and environmental rhythms reflected in molluscan shell growth. *J Paleontol* 42:64-80
- Petersen J, Fyhn H, Johansen K (1974) Eco-physiological studies of an intertidal crustacean, *Pollicipes polymerus* (Cirripedia, Lepadomorpha): aquatic and aerial respiration. *J Exp Biol* 61:309-320
- Petersen JA, Johansen K (1973) Gas exchange in the giant sea cradle *Cryptochiton stelleri* (Middendorff). *J Exp Mar Biol Ecol* 12:27-43
- Pierrot D, Lewis E, Wallace D (2006) MS Excel program developed for CO₂ system calculations. In: ORNL/CDIAC-105, US Department of Energy. Carbon Dioxide Information Analysis Center, Oak Ridge National Laboratory, Oak Ridge, Tennessee
- Plagányi E, Branch GM (2000) Does the limpet *Patella cochlear* fertilize its own algal garden? *Mar Ecol Prog Ser* 194:113-122
- Prou J, Gouletquer P (2002) The French mussel industry: Present status and perspectives. *Bull Aquacult Assoc Can* 102:17-23

- Raffaelli D, Hawkins S (1999) Intertidal ecology, In, Kluwer Academic Pub
- Reid D (1996) Systematics and evolution of *Littorina*, In, Ray Society
- Ribeiro PA, Xavier R, Santos AM, Hawkins SJ (2009) Reproductive cycles of four species of *Patella* (Mollusca: Gastropoda) on the northern and central Portuguese coast. J Mar Biol Assoc UK 89:1215-1221
- Ritz C, Streibig JC (2008) Nonlinear regression with R, In, Springer
- Rochelle-Newall EJ, Winter C, Barrón C, Borges AV, Duarte CM, Elliott M, Frankignoulle M, Gazeau F, Middelburg JJ, Pizay MD (2007) Artificial neural network analysis of factors controlling ecosystem metabolism in coastal systems. Ecol Appl 17:185-196
- Rodríguez-Navarro AB, CabraldeMelo C, Batista N, Morimoto N, Alvarez-Lloret P, Ortega-Huertas M, Fuenzalida VM, Arias JI, Wiff JP, Arias JL (2006) Microstructure and crystallographic-texture of giant barnacle (*Austromegabalanus psittacus*) shell. J Struct Biol 156:355-362
- Roy RN, Roy LN, Vogel KM, Porter-Moore C, Pearson T, Good CE, Millero FJ, Campbell DM (1993) The dissociation constants of carbonic acid in seawater at salinities 5 to 45 and temperatures 0 to 45 C. Mar Chem 44:249-267
- Sabine CL, Feely RA, Gruber N, Key RM, Lee K, Bullister JL, Wanninkhof R, Wong CS, Wallace DWR, Tilbrook B, Millero FJ, Peng T-H, Kozyr A, Ono T, Rios AF (2004) The oceanic sink for anthropogenic CO₂. Science 305:367-371
- Sambrook J, Fritsch E, Maniatis T (1989) Molecular cloning: a laboratory manual, In, Cold Spring Harbor Laboratory Press, New York
- Sampath-Wiley P, Neefus CD, Jahnke LS (2008) Seasonal effects of sun exposure and emersion on intertidal seaweed physiology: Fluctuations in antioxidant contents, photosynthetic pigments and photosynthetic efficiency in the red alga *Porphyra umbilicalis* Kützing (Rhodophyta, Bangiales). J Exp Mar Biol Ecol 361:83-91
- Sanders CJ, Smoak JM, Naidu AS, Sanders LM, Patchineelam SR (2010) Organic carbon burial in a mangrove forest, margin and intertidal mud flat. Estuar Coast Shelf Sci 90:168-172
- Sandison EE (1966) The oxygen consumption of some intertidal gastropods in relation to zonation. J Zool 149:163-173
- Santini G, Thompson RC, Tendi C, Hawkins SJ, Hartnoll RG, Chelazzi G (2004) Intra-specific variability in the temporal organisation of foraging activity in the limpet *Patella vulgata*. Mar Biol 144:1165-1172
- Santini G, Williams GA, Chelazzi G (2000) Assessment of factors affecting heart rate of the limpet *Patella vulgata* on the natural shore. Mar Biol 137:291-296
- Santos R, Silva J, Alexandre A, Navarro N, Barron C, Duarte CM (2004) Ecosystem metabolism and carbon fluxes of a tidally-dominated coastal lagoon. Estuaries and Coasts 27:977-985
- Saulquin B, Gohin F (2010) Mean seasonal cycle and evolution of the sea surface temperature from satellite and in situ data in the English Channel for the period 1986–2006. Int J Remote Sens 31:4069-4093

- Schagerl M, Möstl M (2011) Drought stress, rain and recovery of the intertidal seaweed *Fucus spiralis*. Mar Biol 158:2471-2479
- Schöne BR, Rodland DL, Wehrmann A, Heidel B, Oschmann W, Zhang Z, Fiebig J, Beck L (2007) Combined sclerochronologic and oxygen isotope analysis of gastropod shells (*Gibbula cineraria*, North Sea): life-history traits and utility as a high-resolution environmental archive for kelp forests. Mar Biol 150:1237-1252
- Segal E (1956) Microgeographic variation as thermal acclimation in an intertidal mollusc. Biol Bull 111:129-152
- Seibel BA (2007) On the depth and scale of metabolic rate variation: scaling of oxygen consumption rates and enzymatic activity in the Class Cephalopoda (Mollusca). J Exp Biol 210:1-11
- Seibel BA, Drazen JC (2007) The rate of metabolism in marine animals: environmental constraints, ecological demands and energetic opportunities. Philos Trans R Soc Lond, Ser B: Biol Sci 362:2061-2078
- Siefert RL, Plattner GK (2004) The role of coastal zones in global biogeochemical cycles. Eos 85:470
- Silva ACF, Hawkins SJ, Boaventura DM, Thompson RC (2008) Predation by small mobile aquatic predators regulates populations of the intertidal limpet *Patella vulgata* (L.). J Exp Mar Biol Ecol 367:259-265
- Simpfendorfer RW, Vial MV, López DA, Verdala M, González ML (1995) Relationship between the aerobic and anaerobic metabolic capacities and the vertical distribution of three intertidal sessile invertebrates: *Jehlius cirratus* (Darwin) (Cirripedia), *Perumytilus purpuratus* (Lamarck) (Bivalvia) and *Mytilus chilensis* (Hupé) (Bivalvia). Comp Biochem Physiol B: Biochem Mol Biol 111:615-623
- Singh S, Kumari S, Rastogi R, Sinha R, Sinha R (2012) Photoprotective and biotechnological potentials of cyanobacterial sheath pigment, scytonemin. Afr J Biotec 9:580-588
- Skene KR (2004) Key differences in photosynthetic characteristics of nine species of intertidal macroalgae are related to their position on the shore. Can J Bot 82:177-184
- Smith S, Hollibaugh J (1993) Coastal metabolism and the oceanic organic carbon balance. Rev Geophys 31:75-89
- Smith S, Key G (1975) Carbon dioxide and metabolism in marine environments. Limnol Oceanogr 20:493-495
- Smith S, Mackenzie F (1987) The ocean as a net heterotrophic system: implications from the carbon biogeochemical cycle. Global Biogeochem Cy 1:187-198
- Soído C, Vasconcellos MC, Diniz AG, Pinheiro J (2009) An improvement of calcium determination technique in the shell of molluscs. Brazilian Archives of Biology and Technology 52:93-98
- Sokal RR, Rohlf FJ (1981) Biometry: the principles and practice of statistics in biological research, In, Freeman, New York
- Sokal RR, Rohlf FJ (1995) Biometry: the principles and practice of statistics in biological research, In, Freeman

- Sokolova IM, Granovitch AI, Berger VJ, Johannesson K (2000) Intraspecific physiological variability of the gastropod *Littorina saxatilis* related to the vertical shore gradient in the White and North Seas. Mar Biol 137:297-308
- Sokolova IM, Portner HO (2001) Physiological adaptations to high intertidal life involve improved water conservation abilities and metabolic rate depression in *Littorina saxatilis*. Mar Ecol Prog Ser 224:171-186
- Solomatine DP, Dulal KN (2003) Model trees as an alternative to neural networks in rainfall—runoff modelling. Hydrolog Sci J 48:399-411
- Solorzano L (1969) Determination of ammonia in natural waters by the phenolhypochlorite method. Limnol Oceanogr 14:799-801
- Somero GN (2002) Thermal physiology and vertical zonation of intertidal animals: optima, limits, and costs of living. Integr Comp Biol 42:780-789
- Southward A (1958) The zonation of plants and animals on rocky sea shores. Biol Rev 33:137-177
- Southward A, Southward EC (1978) Recolonization of rocky shores in Cornwall after use of toxic dispersants to clean up the Torrey Canyon spill. J Fish Res Board Can 35:682-706
- Spilmont N, Migné A, Seuront L, Davoult D (2007) Short-term variability of intertidal benthic community production during emersion and the implication in annual budget calculation. Mar Ecol Prog Ser 333:95-101
- Stillman JH, Somero GN (2000) A comparative analysis of the upper thermal tolerance limits of eastern Pacific porcelain crabs, genus *Petrolisthes*: influences of latitude, vertical zonation, acclimation, and phylogeny. Physiol Biochem Zool 73:200-208
- Sukhotin A, Pörtner HO (1999) Habitat as a factor involved in the physiological response to environmental anaerobiosis of White Sea *Mytilus edulis*. Mar Ecol Prog Ser 184:149-160
- Sukhotin AA, Flyachinskaya LP (2009) Aging reduces reproductive success in mussels *Mytilus edulis*. Mech Ageing Dev 130:754-761
- Sukhotin AA, Lajus DL, Lesin PA (2003) Influence of age and size on pumping activity and stress resistance in the marine bivalve *Mytilus edulis* L. J Exp Mar Biol 284:129-144
- Sukhotin AA, Pörtner HO (2001) Age-dependence of metabolism in mussels *Mytilus edulis* (L.) from the White Sea. J Exp Mar Biol Ecol 257:53-72
- Suzuki Y, Tanoue E (1991) Dissolved organic carbon enigma: implication for ocean margin. In: Mantoura RFC, Martin JM, Wollast R (eds) Ocean Margin Processes in Global Change, Berlin
- Tagliarolo M, Clavier J, Chauvaud L, Grall J (2012a) Calcification and respiratory rates of nine gastropod species from the intertidal rocky shore of Western Europe. Journal of Experimental Marine Biology and Ecology Submitted
- Tagliarolo M, Clavier J, Chauvaud L, Koken M, Grall J (2012b) Metabolism in blue mussel: Intertidal and subtidal beds compared. Aquatic Biology In press

Tagliarolo M, Clavier J, Grall J, Amice E, Maguer M, Donval A, Leynaert A, Moga S, Lenca P, Chauvaud L (in preparation) Aerial and underwater metabolism in an intertidal rocky shore community. .

Tagliarolo M, Grall J, Chauvaud L, Clavier J (2012c) Aerial and underwater metabolism of *Patella vulgata* L.: comparison of three intertidal levels. *Hydrobiologia* In print

Tang S, Chen C, Zhan H, Zhang T (2008) Determination of ocean primary productivity using support vector machines. *Int J Remote Sens* 29:6227-6236

Taylor JD, Kennedy WJ, Hall A (1973) The shell structure and mineralogy of the Bivalvia, In, British Museum (Natural History)

Taylor PM, Andrews EB (1988) Osmoregulation in the intertidal gastropod *Littorina littorea*. *J Exp Mar Biol Ecol* 122:35-46

Thompson RC, Norton TA, Hawkins SJ (2004) Physical stress and biological control regulate the producer-consumer balance in intertidal biofilms. *Ecology* 85:1372-1382

Thomsen J, Melzner F (2010) Moderate seawater acidification does not elicit long-term metabolic depression in the blue mussel *Mytilus edulis*. *Mar Biol* 157:2667-2676

Trenberth KE, Josey S (2007) Observations: surface and atmospheric climate change. In: Climate Change 2007: The Physical Science Basis: Contribution of Working Group I to the Fourth Assessment Report of the Intergovernmental Panel on Climate Change. Cambridge University Press, Cambridge

Truchot JP (1990) Respiratory and ionic regulation in invertebrates exposed to both water and air. *Annu Rev Physiol* 52:61-74

Underwood A (1984) The vertical distribution and seasonal abundance of intertidal microalgae on a rocky shore in New South Wales. *J Exp Mar Biol Ecol* 78:199-220

Underwood AJ (1973) Studies on zonation of intertidal prosobranch molluscs in the Plymouth Region. *J Anim Ecol* 42:353-372

Underwood AJ, Jernakoff P (1984) The effects of tidal height, wave-exposure, seasonality and rock-pools on grazing and the distribution of intertidal macroalgae in New South Wales. *Journal of Experimental Marine Biology and Ecology* 75:71-96

Van Heukelem L, Thomas CS (2001) Computer-assisted high-performance liquid chromatography method development with applications to the isolation and analysis of phytoplankton pigments. *J Chromatogr* 910:31-49

Vaughn CC, Hakenkamp CC (2001) The functional role of burrowing bivalves in freshwater ecosystems. *Freshwat Biol* 46:1431-1446

Vermaat JE, Verhagen FCA (1996) Seasonal variation in the intertidal seagrass *Zostera noltii* Hornem.: coupling demographic and physiological patterns. *Aquat Bot* 52:259-281

Vermeij GJ (1972) Intraspecific shore-level size gradients in intertidal molluscs. *Ecology* 53:693-700

Vermeij GJ (1973) Morphological patterns in high-intertidal gastropods: Adaptive strategies and their limitations. *Mar Biol* 20:319-346

- Wallis RL (1975) Thermal tolerance of *Mytilus edulis* of Eastern Australia. Mar Biol 30:183-191
- Warman CG, Reid DG, Naylor E (1993) Variation in the tidal migratory behaviour and rhythmic light-responsiveness in the shore crab, *Carcinus maenas*. J Mar Biol Assoc UK 73:355-364
- Watson D, Foster P, Walker G (1995) Barnacle shells as biomonitoring material. Mar Pollut Bull 31:111-115
- West L (1986) Interindividual variation in prey selection by the snail *Nucella* (= *Thais*) *emarginata*. Ecology 67:798-809
- White TJ (1968) Metabolic activity and glycogen stores of two distinct populations of *Acmaea scabra*. Veliger 11:102-104
- Widdows J (1973) The effects of temperature on the metabolism and activity of *Mytilus edulis*. Neth J Sea Res 7:387-398
- Widdows J, Bayne BL, Livingstone DR, Newell RIE, Donkin P (1979) Physiological and biochemical responses of bivalve molluscs to exposure to air. Compendium of Biochemistry and Physiology 62:301-308
- Widdows J, Shick J (1985) Physiological responses of *Mytilus edulis* and *Cardium edule* to aerial exposure. Mar Biol 85:217-232
- Williams SL, Dethier MN (2005) High and dry: variation in net photosynthesis of the intertidal seaweed *Fucus gardneri*. Ecology 86:2373-2379
- Witten IH, Frank E (2005) Data Mining: Practical machine learning tools and techniques, In, Morgan Kaufmann
- Wollast R (1991) The coastal organic carbon cycle: fluxes, sources and sinks. In: Mantoura RFC, Martin JM, Wollast R (eds) Ocean Margin Processes in Global Change. Wiley: London, Berlin
- Wood CM, Boutilier R, Randall D (1986) The physiology of dehydration stress in the land crab, *Cardisoma carnifex*: respiration, ionoregulation, acid-base balance and nitrogenous waste excretion. J Exp Biol 126:271-296
- Woodwell GM, Whittaker RH (1968) Primary production in terrestrial ecosystems. Am Zool 8:19-30
- Wright J, Hartnoll R (1981) An energy budget for a population of the limpet *Patella vulgata*. J Mar Biol Assoc UK 61:627-646
- Yonge CM (1947) The pallial organs in the aspidobranch Gastropoda and their evolution throughout the Mollusca. Philos Trans R Soc Lond, Ser B: Biol Sci:443-518
- Zacharias M (2012) Ecophysiological studies of selected macro and microalgae: production of organic compounds and climate change interactions. PhD, National University of Ireland,
- Zar JH (2010) Biostatistical analysis, In, Prentice hall, New Jersey

Liste des figures

Fig.1. Représentation schématique de l'influence relative des différents stress physiques et biologiques subis par les communautés intertidales en haut de l'estran (d'après Raffaelli & Hawkins 1999, Little et al. 2009).

Fig. 2. Exemples de producteurs primaires présents sur l'estran rocheux : A- *Fucus vesiculosus*, B- *Xanthoria* sp., C- *Laminaria digitata*.

Fig. 3. Exemples de consommateurs primaires : A- *Patella* sp., B- *Osilinus lineatus*, C- *Littorina saxatilis*.

Fig. 4. Exemples de filtreurs :A- *Mytilus* spp., B-balanes.

Fig. 5. Exemples de prédateurs : A- *Carcinus meanas*, B- *Haematopus ostralegus*, C- *Nucella lapillus*.

Fig. 6. Présentation schématique des phénomènes étudiés à trois échelles.

Fig. 7. Photo de la moulière intertidale étudiée (Plage des blancs sablons, Le Conquet).

Fig. 8. Sampling sites for intertidal and subtidal mussel respiration measurements in western Brittany (France).

Fig. 9. Monthly variation of mean sea surface (Marel Iroise Station) and air temperature (Météo France, Camaret station) from 2008 to 2011.

Fig. 10. Agarose gel of the PCR products of the “Foot protein 1” gene of mussels. Lanes 1 to 10, intertidal mussels; lanes 11 to 20, subtidal mussels.

Fig. 11. Variation in aerial respiration of mussels during the low-tide period at different temperatures (°C) and relative humidity levels (%), estimated from the variation of CO₂ concentration in incubation chambers. A: large intertidal, B: large subtidal, C: small intertidal, D: small subtidal mussels.

Fig. 12. Relationships between intertidal and subtidal hourly aerial respiration rates per g AFDW, and temperature (mean ± SD). A: large mussels, B: small mussels.

Fig. 13. Variation in ammonium excretion rates of mussels during summer and winter.

Fig. 14. Seasonal variation of net calcification rate (mean ± SD) estimated from total alkalinity variation during incubation. Positive values correspond to calcification. A: large mussels, B: small mussels.

Fig. 15. Relationship between intertidal and subtidal hourly underwater respiration (dissolved inorganic carbon, DIC) rates per g biomass (AFDW) and temperature (mean ± SD). A: large mussels, B: small mussels.

Fig. 16. Average hourly underwater and aerial carbon respiration of mussels per g AFDW (±SD).

Fig. 17. Photo des patelles sur les supports pendant les mesures de métabolisme au laboratoire.

Fig. 18. Sampling site (Grand Dellec, Plouzané) for *P. vulgata* respiration measurements in Western Brittany (France).

Fig. 19. Monthly variation in mean sea surface temperature (SST) (MAREL Iroise buoy) and air temperature (Air) (Météo France, Camaret station) in the study area from 2010 to 2012.

Fig. 20. *P. vulgata* ammonium excretion rates (mean \pm standard deviation, n=10) during summer and winter, at three tidal levels.

Fig. 21. Seasonal variation in *P. vulgata* net calcification rate (mean \pm standard deviation, n=10) at three tidal levels. Positive values correspond to calcification.

Fig. 22. Relationships between hourly underwater *P. vulgata* respiration (DIC) rates per g AFDW and temperature (mean \pm standard deviation, n=10), at three tidal levels.

Fig. 23. Variation in aerial respiration rates of *P. vulgata* during low tide at different temperatures ($^{\circ}$ C) and RH (%), as estimated from the variation in CO₂ concentration in incubation chambers at three tidal levels (a, high-shore; b, middle-shore; c, low-shore).

Fig. 24. Relationships between hourly aerial *P. vulgata* respiration rates per g AFDW, and temperature at three tidal levels (mean \pm standard deviation, n=10).

Fig. 25. Evolution of hourly underwater and aerial carbon respiration rates of *P. vulgata* per g AFDW (\pm standard deviation, n=10) at three tidal levels (a, high-shore; b, middle-shore; c, low-shore).

Fig. 26. Photos de quelques espèces de gastéropode étudié. (*O. lineatus* ; *L. littorea* ; *N. lapillus* ; *G. magus* ; *G. umbilicalis* ; *L. saxatilis*).

Fig. 27. Sampling sites for gastropods collection in Western Brittany (France) (A: *L. littorea*, *G. umbilicalis*; B: *M. neritoides*, *L. saxatilis*, *O. lineatus*, *G. cineraria*, *G. pennanti*, *N. lapillus*; C: *G. magus*).

Fig. 28. Average vertical distribution and percent immersion time of studied species (*M. n.*, *M. neritoides*; *L. s.*, *L. saxatilis*; *O. l.*, *O. lineatus*; *G.u.*, *G. umbilicalis*; *L. l.*, *L. littorea*; *N. l.*, *N. lapillus*; *G. p.*, *G. pennant*; *G. c.*, *G. cineraria*; *G. m.*, *G. magus*).

Fig. 29. Relationships between temperature and hourly underwater (white squares) and aerial (black circles) respiration rates per g AFDW (mean \pm standard deviation) for studied species (*M. n.*, *M. neritoides*; *L. s.*, *L. saxatilis*; *O. l.*, *O. lineatus*; *G.u.*, *G. umbilicalis*; *L. l.*, *L. littorea*; *N. l.*, *N. lapillus*; *G. p.*, *G. pennant*; *G. c.*, *G. cineraria*; *G. m.*, *G. magus*).

Fig. 30. Variation of hourly underwater and aerial carbon respiration rates at 13 $^{\circ}$ C, calculated per g AFDW as a function of the average individual biomass of the gastropod species (*M. n.*, *M. neritoides*; *L. s.*, *L. saxatilis*; *O. l.*, *O. lineatus*; *G.u.*, *G. umbilicalis*; *L. l.*, *L. littorea*; *N. l.*, *N. lapillus*; *G. p.*, *G. pennant*; *G. c.*, *G. cineraria*; *G. m.*, *G. magus*).

Fig. 31. Ammonium excretion rates (mean \pm standard deviation) during summer and winter as a function of the average individual biomass of the gastropod species (*M. n.*, *M. neritoides*; *L. s.*, *L. saxatilis*; *O. l.*, *O. lineatus*; *G.u.*, *G. umbilicalis*; *L. l.*, *L. littorea*; *N. l.*, *N. lapillus*; *G. p.*, *G. pennant*; *G. c.*, *G. cineraria*; *G. m.*, *G. magus*).

Fig. 32. Seasonal variation in net calcification rate (mean \pm standard deviation) for all studied species. Positive values correspond to calcification (*M. n.*, *M. neritoides*; *L. s.*, *L. saxatilis*; *O. l.*, *O. lineatus*; *G.u.*, *G. umbilicalis*; *L. l.*, *L. littorea*; *N. l.*, *N. lapillus*; *G. p.*, *G. pennant*; *G. c.*, *G. cineraria*; *G. m.*, *G. magus*).

Fig. 33. Average annual carbon emissions due to calcification, and aerial and underwater respiration as a function of the average individual biomass of the gastropod species (*M. n.*, *M. neritoides*; *L. s.*, *L. saxatilis*; *O. l.*, *O. lineatus*; *G.u.*, *G. umbilicalis*; *L. l.*, *L. littorea*; *N. l.*, *N. lapillus*; *G. p.*, *G. pennant*; *G. c.*, *G. cineraria*; *G. m.*, *G. magus*).

Fig. 34. Chambres benthiques disposées sur le niveau bas de l'estran, pendant la marée basse (photo du haut) et pendant la marée haute (photo du bas).

Fig. 35. Illustration schématique des processus étudiés.

Fig. 36. Schematic representation of the experimental apparatus. Multiparameter probe and water pump were used during underwater measurements.

Fig. 37. An example regression tree.

Fig. 38. Average seasonal variation of aerial and underwater PAR at the three sampling sites.

Fig. 39. Average monthly variation of mean sea surface (Marel Iroise Station) and air temperature (Météo France, Camaret station) from January 2011 to April 2012.

Fig. 40. Seasonal variation of community respiration ($\text{mmol Cm}^{-2} \text{h}^{-1}$) at the different shore-levels. White bars represent aerial respiration and black bars represent underwater respiration. (A, High-shore; B, Middle-shore; C, Low-shore).

Fig. 41. Linear relationship between net ΔO_2 and ΔDIC (dissolved inorganic carbon).

Fig. 42. Seasonal variation of average daily DIC and CaCO_3 fluxes at the different shore levels.

Fig. 43. Relationships between irradiance and underwater net community production (NCP) measured as O_2 emission (black dots) or CO_2 consumption (white dots). A, winter; B, spring; C, summer; D, autumn.

Fig. 44. Relationship between net community CaCO_3 fluxes and irradiance at the three shore levels. (A, winter; B, spring; C, summer; D, autumn).

Fig. 45. Relationships between net aerial CO_2 fluxes and the four parameters measured *in situ* (A, irradiance; B, temperature; C, air humidity; D, emersion time).

Fig. 46. Regression tree for aerial NCP fluxes produced using REPTree algorithm. Average NCP values ($\text{mmol m}^{-2} \text{h}^{-1}$) calculated for each terminal leaf are in green circles.

Fig. 47. Relationships between aerial carbon fluxes measured on natural drying, splashing and raining simulated conditions and emersion time (A, CR-dark incubations; B, NCP-light incubations).

Fig. 48. Chl α concentration measured through fluorimetric method at the three levels and for the four seasons.

Fig. 49. Positionnement représentant les deux niveaux de l'estran choisis pour le suivi de la faune benthique dans le cadre du programme REBENT.

Fig. 50. REBENT sites for intertidal rocky shore communities monitoring.

Fig. 51. Geographical variation of average annual carbon fluxes ($\text{mol C m}^{-2} \text{yr}^{-1}$) in high-shore (yellow point) and low-shore (red point).

Fig. 52. Estimated annual carbon fluxes ($\text{mol C m}^{-2} \text{yr}^{-1}$) for exposed rocky shore communities in function of temperature variation. 0 correspond to the average annual temperature calculated for the studied period.

Fig. 53. Rapport respiratoire air/eau en fonction de la position sur l'estran et de la température. Les rapports ont été calculés pour trois températures : 6°C, bleu ; 13°C, noir ; 18°C, rouge. (M. n., M. neritoides; L. s., L. saxatilis; C. m., Chthamalus montagui; O. l., O. lineatus; G.u., G. umbilicalis; P. sp., Patella sp.; L. l., L. littorea; N. l., N. lapillus; C. g., Crassostrea gigas; G. p., G. pennanti; M. spp., Mytilus spp.; G. c., G. cineraria; G. m., G. magus).

Fig. 54. Diagramme conceptuel illustrant les différents contraintes liées au changement global qui peuvent influencer le métabolisme des communautés benthiques intertidales (d'après Harley et al. 2006, Borges 2011).

Liste des tableaux

Tab. 1. Parameters of Arrhenius plots relating the logarithm of hourly underwater and aerial respiration per g AFDW to the inverse of absolute temperature.

Tab. 2. Parameters of Arrhenius plots relating the logarithm of hourly underwater and aerial respiration rates of *P. vulgata* per g AFDW to the inverse of absolute temperature, at three tidal levels. a, normalization constant; Ea, activation energy (Joules per mole); K, Boltzmann's constant (8.31 JK-1 mol-1); R², coefficient of determination.

Tab. 3. *P. vulgata* aerial, underwater, and calcification carbon contributions (%) to total annual carbon emissions, at three tidal levels.

Tab. 4. Parameters of Arrhenius plots relating the logarithms of the hourly underwater and aerial respiration rates of each studied species per g AFDW to the inverse of absolute temperature (°K), at three tidal levels.

Tab. 5. Percentage of calcium carbonate in the shell of each studied.

Tab. 6. Average macrozoobenthos biomass for each season and level (g AFDW m⁻²) at the three studied shore levels.

Tab. 7. Pigment concentration at the three shore-levels during winter (Win), summer (Sum) and autumn (Aut) (mg m⁻²). For violaxanthin, scytonemin and red scytonemin only presence/absence data are available (*=presence). Values for summer are not available at the high-shore.

Tab. 8. Mean calcification and parameters of Arrhenius plots relating the logarithm of hourly underwater and aerial respiration rates per g AFDW to the inverse of absolute temperature. a, normalization constant; Ea, activation energy (Joules per mole); K, Boltzmann's constant (8.31 JK-1 mol-1).

Tab. 9. Annual variation of average sea surface (above value) and air (below value) temperatures in °C from 2004 to 2010 (Météo-France and PREVIMER (IFREMER)). See Fig. 50 for location of sites.

Tab. 10. Carbon fluxes (mol C m⁻² yr⁻¹) calculated at high-shore level for each site and species group (aerial respiration-underwater respiration-calcification) and total values.

Tab. 11. Carbon fluxes (mol C m⁻² yr⁻¹) calculated at low-shore for each site and species group (aerial respiration-underwater respiration-calcification), and total values.

Tab. 12. Comparaison entre les flux respiratoires à l'air et sous l'eau mesurés globalement *in situ* avec les cloches benthiques, et les flux calculés en additionnant la respiration de chaque population macrozoobenthique (mmol C m⁻² h⁻¹).

Annexes

Annexe 1

Photos des instruments et chambres de mesure utilisée pour les mesures en laboratoire en immersion.



Fig. 55. Bouteilles utilisée pour les incubations d'une heure.



Fig. 56. Appareil pour les mesures d'alcalinité.



Fig. 57. pH-metre.

Annexe 2

Photos des instruments et chambres de mesure utilisée pour les mesures en laboratoire en émersion.



Fig. 57. Chambres d'incubation utilisées pour les moules.



Fig. 57. Chambres d'incubation utilisées pour les gastéropodes.

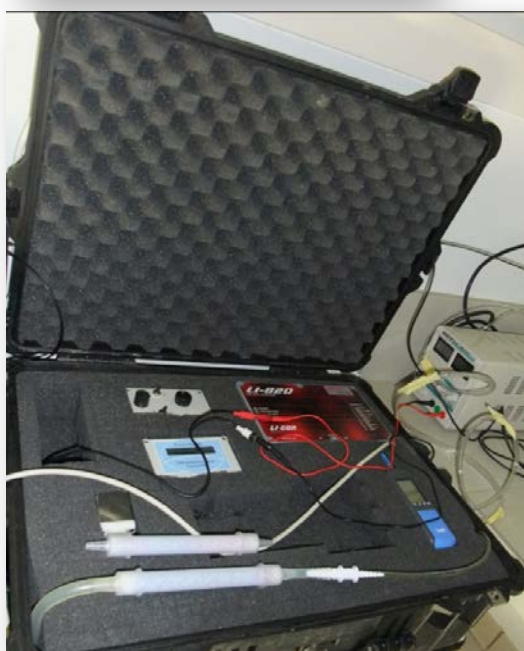


Fig. 57. Analyseur de CO₂ par infrarouge.

Annexe 3

Résumé des métabolismes annuels et des biomasses moyennes individuelles mesurés en laboratoire sur les principales espèces du macrozoobenthos vivant sur les estrans rocheux.

	Respiration en émersion (mmol CO ₂ g AFDW ⁻¹ y ⁻¹)	Respiration en immersion (mmol DIC g AFDW ⁻¹ y ⁻¹)	Calcification en immersion (mmol CaCO ₃ g AFDW ⁻¹ y ⁻¹)	Biomasse moyenne individuelle (g AFDW)
<i>Mytilus</i> spp. intertidal adulte	12	130	11	0.38
<i>Mytilus</i> spp. subtidal adulte	-	246	24	1.4
<i>Patella</i> sp. haut	112	4	3	0.45
<i>Patella</i> sp. milieu	85	31	14	0.47
<i>Patella</i> sp. bas	25	85	24	0.40
<i>Melarhaphe neritoides</i>	208	15	8	0.01
<i>Littorina saxatilis</i>	124	34	26	0.02
<i>Osilinus lineatus</i>	43	59	5	0.28
<i>Gibbula umbilicalis</i>	70	58	26	0.07
<i>Littorina littorea</i>	25	60	13	0.35
<i>Nucella lapillus</i>	18	82	16	0.23
<i>Gibbula pennanti</i>	16	103	36	0.08
<i>Gibbula cineraria</i>	2	134	57	0.03
<i>Gibbula magus</i>	-	93	31	0.18

Annexe 4

Flux de carbone ($\text{mol C m}^{-2} \text{ y}^{-1}$) calculé pour les groupes d'espèces présents sur le niveau haut de l'estran (moyenne des neuf sites du réseau REBENT). Les résultats sont exprimés en fonction des simulations de variation de température ($\pm 2^\circ\text{C}$) ; le 0 correspond à la moyenne annuelle des températures calculée pour la période d'étude.

	Barnacle	Mussel	Limpet	Oyster	Gastropod	Total
+0.5	4.3	0.0	0.9	0.0	5.5	10.8
+1	4.5	0.0	0.9	0.0	5.7	11.2
+1.5	4.7	0.0	1.0	0.0	6.0	11.7
+2	5.0	0.0	1.0	0.0	6.2	12.2
0	4.1	0.0	0.9	0.0	5.3	10.3
-0.5	4.0	0.0	0.9	0.0	5.1	10.0
-1	3.8	0.0	0.9	0.0	4.8	9.5
-1.5	3.6	0.0	0.9	0.0	4.6	9.1
-2	3.4	0.0	0.8	0.0	4.5	8.7

Flux de carbone ($\text{mol C m}^{-2} \text{ y}^{-1}$) calculé pour les groupes d'espèces présentes sur le niveau bas de l'estran (moyenne des neuf sites du réseau REBENT). Les résultats sont exprimés en fonction des simulations de variation de température ($\pm 2^\circ\text{C}$) ; le 0 correspond à la moyenne annuelle des températures calculée pour la période d'étude.

	Barnacle	Mussel	Limpet	Oyster	Gastropod	Total
+0.5	4.3	9.6	1.7	0.4	1.6	17.5
+1	4.5	9.7	1.8	0.5	1.6	18.0
+1.5	4.7	9.8	1.8	0.5	1.7	18.5
+2	4.9	10.0	1.8	0.6	1.7	19.0
0	4.1	9.4	1.7	0.4	1.5	17.1
-0.5	4.0	9.5	1.6	0.4	1.5	17.1
-1	3.7	9.2	1.6	0.4	1.4	16.3
-1.5	3.6	9.1	1.6	0.3	1.4	16.0
-2	3.4	9.0	1.5	0.3	1.4	15.6

Annexe 5

Biomasse moyenne (g AFDW m⁻²) calculée pour les groupes d'espèces présents sur le niveau haut de l'estran. Les résultats sont exprimés en fonction de l'année et du site de surveillance REBENT.

		Balanus	<i>G. pennanti</i>	<i>G. umbilicalis</i>	<i>L. littorea</i>	<i>L. obtusata</i>	<i>L. saxatilis</i>	<i>Mytilus</i> spp.	<i>N. lapillus</i>	<i>O. lineatus</i>	<i>Ostreidae</i> spp.	<i>Patella</i> spp.	<i>M. neritoides</i>
2004	Callot	48	0	0	0	0	0	0	0	0	0	2	0
	Doelan	92	0	0	0	0	0	0	0	0	0	6	74
	Ile de l'Aber	132	0	0	0	0	0	0	0	0	0	2	52
	l'Arcouest	10	0	0	0	0	0	0	0	0	0	4	0
	Locmariaquer	88	0	0	0	0	1	0	0	0	0	0	23
	Rade de Brest	94	0	0	0	0	0	0	0	0	0	0	4
	Saint Briac	68	0	0	0	0	0	2	0	0	6	5	12
	Sainte Marguerite	76	0	0	0	0	0	0	0	0	0	26	8
2005	Callot	48	0	0	0	0	1	0	0	0	0	3	0
	Doelan	65	0	0	0	0	0	0	0	0	0	2	77
	Ile de l'Aber	86	0	0	0	0	0	0	0	0	0	7	72
	l'Arcouest	7	0	0	0	0	0	0	0	1	0	3	0
	Locmariaquer	71	0	0	0	0	0	0	0	0	0	1	12
	Molene	3	0	0	0	0	0	0	0	0	0	0	3
	Saint Briac	58	0	1	0	0	0	7	0	0	0	2	0
	Sainte Marguerite	61	0	0	0	0	0	0	0	0	0	13	7
2006	Callot	47	0	0	0	0	0	0	0	0	0	2	4
	Doelan	43	0	0	0	0	0	0	0	0	0	1	40
	Ile de l'Aber	147	0	0	0	0	0	1	0	1	0	10	42
	l'Arcouest	6	0	0	1	0	0	0	0	2	0	5	0
	Locmariaquer	69	0	0	0	0	0	0	0	0	0	0	43
	Molene	3	0	0	0	0	0	0	0	0	0	0	0
	Rade de Brest	67	0	0	0	0	0	0	0	0	0	0	4
	Saint Briac	59	0	1	0	0	0	5	0	0	2	7	13
2007	Sainte Marguerite	75	0	0	0	0	0	0	0	0	0	27	6
	Doelan	90	0	0	0	0	0	0	0	0	0	2	76
	Ile de l'Aber	162	0	0	0	0	0	1	0	1	0	12	43
	l'Arcouest	7	0	0	0	0	0	0	0	0	0	5	0

	Locmariaquer	104	0	0	0	0	1	0	0	0	0	1	28
	Molene	4	0	0	0	0	1	0	0	0	0	0	2
	Rade de Brest	84	0	0	0	1	0	0	0	0	0	0	0
	Saint Briac	52	0	0	0	0	0	6	0	0	2	6	5
	Sainte Marguerite	66	0	0	0	0	0	0	0	0	0	22	21
2009	Callot	38	0	0	0	0	13	0	0	1	0	1	15
	Doelan	121	0	0	0	0	0	0	0	0	0	5	200
	Ile de l'Aber	111	0	0	0	0	0	1	0	0	0	65	47
	l'Arcouest	7	0	0	0	0	0	0	0	1	0	5	0
	Locmariaquer	112	0	0	0	0	0	0	0	2	0	0	51
	Molene	4	0	0	0	0	0	0	0	0	0	0	4
	Rade de Brest	94	0	0	0	0	0	0	0	2	0	0	13
	Saint Briac	71	0	0	0	0	0	3	0	0	4	7	10
	Sainte Marguerite	67	0	0	0	0	0	0	0	0	0	30	14
2010	Callot	43	0	0	0	0	11	0	0	0	0	3	13
	Doelan	117	0	0	0	0	0	0	0	0	0	3	130
	Ile de l'Aber	175	0	0	0	0	0	1	0	0	0	4	22
	l'Arcouest	7	0	0	0	0	0	0	0	1	0	7	0
	Locmariaquer	98	0	0	2	0	0	0	0	0	0	0	40
	Molene	6	0	0	0	0	0	0	0	0	0	0	1
	Rade de Brest	74	0	0	1	0	0	0	0	0	0	0	4
	Saint Briac	69	0	0	0	0	0	0	0	0	2	7	30

Biomasse moyenne (g AFDW m⁻²) calculée pour les groupes d'espèces présents sur le niveau bas de l'estran. Les résultats sont exprimés en fonction de l'année et du site de surveillance REBENT.

		<i>Balanus</i>	<i>G. pennanti</i>	<i>G. umbilicalis</i>	<i>L. littorea</i>	<i>L. obtusata</i>	<i>L. saxatilis</i>	<i>Mytilus</i> spp.	<i>N. lapillus</i>	<i>O. lineatus</i>	<i>Ostreidae</i> spp.	<i>Patella</i> spp.	<i>M. neritoïdes</i>
2004	Callot	60	0	0	0	0	0	0	0	15	0	21	0
	Doelan	109	0	0	0	0	0	46	0	0	0	10	29
	Ile de l'Aber	124	0	0	0	0	0	146	1	0	0	8	4
	l'Arcouest	54	0	0	0	0	0	2	0	2	17	14	0
	Locmariaquer	77	0	0	0	0	4	9	1	26	88	22	5
	Rade de Brest	95	0	0	0	0	0	0	0	0	28	18	0
	Saint Briac	33	0	0	0	0	0	0	0	0	0	39	19
	Sainte Marguerite	52	0	0	0	0	0	0	1	0	0	13	5
2005	Callot	32	0	0	0	0	0	0	0	8	0	9	0
	Doelan	91	0	0	0	0	0	29	0	0	0	3	12
	Ile de l'Aber	73	0	2	0	0	0	120	0	0	0	3	0
	l'Arcouest	46	0	0	0	0	0	2	0	4	18	1	0
	Locmariaquer	84	0	0	0	0	1	7	0	11	56	16	0
	Molene	0	0	0	0	0	0	0	0	0	0	4	0
	Saint Briac	41	0	2	0	0	0	0	3	0	0	4	0
	Sainte Marguerite	27	0	0	0	0	0	0	1	0	0	14	1
2006	Callot	45	0	0	0	0	0	0	0	10	0	13	0
	Doelan	46	0	1	0	0	0	289	1	0	0	5	12
	Ile de l'Aber	60	3	0	0	0	0	19	0	0	0	35	0
	l'Arcouest	46	0	0	0	0	0	2	0	4	9	24	0
	Locmariaquer	54	0	1	16	0	0	0	0	7	26	22	3
	Molene	0	0	0	0	0	0	0	0	0	0	5	0
	Rade de Brest	38	0	2	0	0	0	0	2	0	24	13	0
	Saint Briac	60	1	2	0	0	0	0	0	0	0	8	7
2007	Sainte Marguerite	29	0	0	0	0	0	0	0	0	0	18	0
	Doelan	113	0	0	0	0	0	126	5	0	0	46	22
	Ile de l'Aber	100	0	2	0	0	0	874	0	1	0	7	0
	l'Arcouest	26	0	0	0	0	0	0	1	2	6	12	0
	Locmariaquer	115	0	0	0	0	3	6	0	4	24	23	0
2008	Molene	0	0	0	0	1	0	0	0	0	0	6	0

	Rade de Brest	44	0	1	0	0	0	0	0	0	17	15	0
	Saint Briac	36	0	0	0	0	0	0	0	0	0	7	0
	Sainte Marguerite	23	0	0	0	0	0	0	1	0	0	15	0
2009	Callot	48	0	0	0	0	0	0	0	12	0	20	1
	Doelan	123	0	0	0	0	0	229	1	0	0	17	32
	Ile de l'Aber	62	0	1	0	0	0	429	4	0	0	7	1
	l'Arcouest	30	0	0	0	0	0	0	0	2	13	12	0
	Locmariaquer	70	0	0	0	0	2	1	0	0	4	26	4
	Molene	1	0	0	0	0	0	0	0	0	0	10	0
	Rade de Brest	93	0	3	0	0	0	0	0	1	28	9	0
	Saint Briac	44	0	0	0	0	0	0	0	0	0	6	7
	Sainte Marguerite	11	0	0	0	0	0	0	0	1	0	15	2
2010	Callot	51	0	0	0	0	0	0	0	14	0	17	0
	Doelan	150	0	0	0	0	2	389	0	0	0	13	22
	Ile de l'Aber	93	0	1	0	0	0	22	0	0	0	8	0
	l'Arcouest	66	0	0	0	0	0	0	0	3	11	12	0
	Locmariaquer	92	0	0	3	0	3	6	0	0	6	12	0
	Molene	0	0	0	0	0	0	0	0	0	0	12	0
	Rade de Brest	78	0	2	0	0	0	0	0	0	21	22	0
	Saint Briac	95	0	0	0	0	0	0	0	0	0	9	23

Annexe 6 : Liste des publications

Tagliarolo M, Grall J, Chauvaud L, Clavier J (2012) Aerial and underwater metabolism of *Patella vulgata* L.: comparison of three intertidal levels. *Hydrobiologia*:1-13

Tagliarolo M, Clavier J, Chauvaud L, Koken M, Grall J (2012) Metabolism in blue mussel: Intertidal and subtidal beds compared. *Aquatic Biology*, Sous presse.

Tagliarolo M, Clavier J, Chauvaud L, Grall J (2012) Calcification and respiratory rates of nine gastropod species from the intertidal rocky shore of Western Europe. *Marine Biology*, Soumis.

Tagliarolo M, Clavier J, Grall J, Amice E, Maguer M, Donval A, Leynaert A, Moga S, Lenca P, Chauvaud L (en préparation) Aerial and underwater metabolism in an intertidal rocky shore community.

Tagliarolo M, Grall J, Maguer M, Chauvaud L, Clavier J (en préparation) Carbon production of intertidal exposed rocky shore macrozoobenthic communities.

Annexe 7 : Liste des abréviations

ABT : « Arrhenius Breakpoint Temperature »

AFDW : Poids sec sans cendres

ANCOVA: Analyse de la covariance

ANOVA: Analyse de la variance

AT: Alcalinité Totale

CaCO₃ : Carbonate de calcium

Chl : Chlorophylle

CO₂ : Dioxyde de carbone

CR : Respiration de la communauté

DIC: Carbone inorganique dissout

DNA : Acide désoxyribonucléique

G : Calcification

GPP : Production primaire brute de la communauté

HCl : Acide chlorhydrique

HPLC : Chromatographie en phase liquide à haute performance

HSD: « Honestly Significant Difference »

MAREL: Mesures Automatisées en Réseau pour l'Environnement et le Littoral

MR : Respiration de la communauté macrozoobenthique

NCP : Production nette de la communauté

O₂ : Dioxygène

PAR : Rayonnement photosynthétiquement actif

PCR : Réaction en chaîne par polymérase

PI : Production en fonction de l'irradiance

PVC: Polyvinyle chlorite

R : Respiration

REBENT : REseau de surveillance BENTthique

RH : Humidité Relative

SHOM: Service Hydrographique et Océnographique de la Marine

SOMLIT: Service d'Observation en Milieu Littoral

SST : Température de surface de la mer

UV : Ultraviolets

Résumé

La zone côtière représente seulement une petite partie de la surface océanique, mais elle joue un rôle important dans le cycle du carbone. Pour contribuer à préciser ce rôle, l'objectif de cette thèse était d'étudier les flux de carbone, en immersion et en émersion, des communautés benthiques intertidales vivant sur les estrans rocheux. La respiration et la calcification des principales espèces macrozoobenthiques ont été mesurées en laboratoire pour d'estimer les différentes adaptations métaboliques liées à une vie en milieu intertidal. En complément, les flux globaux de carbone des communautés ont été quantifiés aux interfaces air-sédiment et eau-sédiment grâce à des mesures *in situ*. D'une manière générale, la respiration de la communauté prévaut sur la production primaire, en conséquence les estrans rocheux semi-battus peuvent être considérés comme hétérotrophes. Grâce aux mesures de respiration en laboratoire et aux comptages d'espèces effectués sur les côtes rocheuses bretonnes, nous avons pu estimer la contribution du macrozoobenthos aux flux de carbone à une échelle régionale. La comparaison entre les résultats *in situ* et les études en laboratoire a permis de valider nos méthodes.

Mots-clés : flux de carbone, respiration, calcification, production primaire, CO₂, intertidal, estran rocheux

Abstract

Coastal zone represents only a small part of ocean surface, but play a major role in carbon cycling. To help clarify this role; this thesis aimed to study carbon fluxes of intertidal benthic rocky shore communities during immersion and emersion. Respiration and calcification measurements of principal macrozoobenthic species were performed in the laboratory in order to evaluate their different metabolic adaptation to intertidal conditions. In addition, community carbon fluxes were quantified *in situ* at the air-sediment and water-sediment interfaces. Community respiration generally prevails on primary production indicating that semi-exposed intertidal rocky shore communities could be considered as heterotrophic. The contribution of macrozoobenthic organisms to carbon fluxes was estimated on a regional scale through respiration and calcification rates measured in the laboratory and species abundances recorded in Brittany (France) exposed rocky shores. The comparison between *in situ* and laboratory studies allowed our methods validation.

Keywords: carbon fluxes, respiration, calcification, primary production, CO₂, intertidal, rocky shore